



DISSERTATION

Model of spinal cord reflex circuits in humans: Stimulation frequency-dependence of segmental activities and their interactions

ausgeführt zum Zwecke der Erlangung des akademischen Grades eines
Doktors der technischen Wissenschaften unter der Leitung von

Ao. Univ. Prof. DDDr. Frank Rattay

E101

Institut für Analysis und Scientific Computing

eingereicht an der Technischen Universität Wien,

Fakultät für Mathematik und Geoinformation

von

DI Ursula Hofstätter

0025015

Alserbachstraße 11/12

A-1090 Wien

Wien, am 22.10.2009

Kurzfassung der Dissertation

Modellierung spinaler Netzwerke im Menschen: Stimulationsfrequenzabhängige segmentale Reflexe und deren gegenseitige Beeinflussung

Motivation und Ziele der Dissertation

Die elektrische Stimulation des unteren (lumbosakralen) Rückenmarks von Probanden mit kompletter Querschnittsläsion mittels rückenmarksnahen Implantaten kann Aktivitäten in der gelähmten Beinmuskulatur generieren. Niedrige Stimulationsfrequenzen (2.1 Hz) führen zu Muskelzuckungen, die als die einfachsten spinalen Reflexe identifiziert werden konnten und nur die Aktivität monosynaptischer Bahnen involvieren. Im Gegensatz dazu bewirken höhere Stimulationsfrequenzen (25-50 Hz) unwillkürliche, automatisierte schreitähnliche Bewegungen in den gelähmten Beinen der liegenden Probanden.

Das Ziel der vorliegenden Dissertation war eine Standardisierung der spinalen Reflexe der unteren Extremitäten bei Rückenmarkstimulation mit 2.1 Hz durch die eingehende Analyse elektrophysiologischer Messdaten. Ein weiteres Hauptaugenmerk lag auf der Erforschung der Effekte höherer Stimulationsfrequenzen auf die ausgelösten Reflexe, insbesondere ihrer Modifikation durch rhythmische Modulationen auf Grund der zusätzlichen Anregung interneuronaler Netzwerke. Die Generierung simpler periodischer Reflexmodulationen, die jeweils zwei aufeinander folgende Antworten umfassten, wurde als Hinweis für die Aktivität von interneuronalen Netzwerken betrachtet. Derart modifizierte Reflexe, abgeleitet von antagonistischen Muskelgruppen, wurden ausschließlich bei der Applikation von Stimulationsfrequenzen zwischen jenen, die zu den einfachen Muskelzuckungen führten, sowie jenen, die schreitähnlichen Bewegungen auslösen konnten, beobachtet.

Die Hypothese dieser Dissertation ist, dass höhere Stimulationsfrequenzen eine Ausweitung des Stimulationseffektes auf lumbale, interneuronale Netzwerke nach sich zieht, welche die ausgelöste Aktivität beeinflussen. Diese Annahme wurde durch ein biologisch realistisches mathematisches Modell getestet. Im Besonderen wurde der Einfluss von Netzwerken aus Interneuronen, die bekanntermaßen die Exzitabilität von Motoneuronen während spinaler Reflexe sowie Lokomotion adaptieren können (inhibitorische Ia-Interneurone und Renshaw-Zellen), auf die Generierung simpler periodischer Reflexmuster untersucht.

Methodik

Unabhängig voneinander wurden die Analyse elektrophysiologischer Messdaten sowie die neuromathematische Modellierung als Methoden zur Testung der Arbeitshypothese gewählt.

Zunächst wurde anhand elektromyographischer (EMG) Aufzeichnungen die Reflexaktivität von sechs Personen mit chronischer kompletter Querschnittslähmung evaluiert. Alle Probanden hatten Systeme zur epiduralen Rückenmarkstimulation auf Höhe des Lumbalmarks implantiert. Eine große Anzahl von Antworten bei Stimulation mit 2.1 Hz (der niedrigsten verfügbaren Frequenz) wurde auf ihre EMG Charakteristiken analysiert, insbesondere die Latenzzeiten, Amplituden sowie Potentialformen. Des Weiteren wurde der Effekt einer Erhöhung der Stimulationsfrequenz auf 5, 11, 16 und 22 Hz auf die EMG Aktivität untersucht. Die Generierung von Reflexen mit periodischen Modulationen wurde dokumentiert.

Anschließend wurde durch umfangreiche Computersimulationen ein biologisch realistisches Netzwerkmodell auf seine Fähigkeit, simple periodische Reflexmodulationen mit einer Periode von jeweils zwei aufeinander folgenden Antworten zu erzeugen, getestet. Zu diesem Zweck wurde ein neues mathematisches Modell entwickelt, das das häufig verwendete *Leaky Integrate-and-Fire* Modell durch detaillierte, auf experimentellen Daten basierende neurophysiologische Zeitverläufe von postsynaptischen Potentialen ergänzt. Das vorliegende mathematische Modell wurde als realistischer Integrator postsynaptischer Effekte von spezialisierten Rückenmarksneuronen konzipiert. Im Besonderen wurden monosynaptisch anregende sowie disynaptisch hemmende Einflüsse auf die Motoneurone durch Populationen von Ia-Afferenzen, Ia-Interneuronen und Renshaw-Zellen berücksichtigt. Dabei basierte das mathematische Modell auf einem nicht-linearen, rekursiven Algorithmus zur Simulation räumlich sowie zeitlich verteilter neuronaler Effekte. Um die jeweilige funktionelle Rolle eines Elements des Neuronennetzwerkes in der Generierung einfacher Reflexmuster zu untersuchen, wurden das Gesamtmodell durch das schrittweise Hinzufügen von interneuronalen Populationen und Verschaltungen entwickelt und die einzelnen Teilmodelle analysiert.

Resultate

Die neurophysiologische Studie lieferte drei wesentliche Ergebnisse. (i) Die epidurale Stimulation des lumbosakralen Rückenmarks in Personen mit kompletter Querschnittsverletzung bei 2.1 Hz löste monosynaptische, segmentale Reflexe in einer Vielzahl von Beinmuskeln aus. Diese Antworten wiesen kurze und konstante Latenzzeiten sowie relativ einfache Potentialformen auf. Während der kontinuierlich applizierten Stimulation kam es zu keinen Interaktionen zwischen den Antworten in antagonistischen Muskeln. (ii) Durch eine Erhöhung der Stimulationsfrequenz auf 11-22 Hz wurden in 20.8 % aller Datensätze einfachste rhythmische Aktivitäten evoziert, bei denen aufeinander folgende Reflexe alternierend variierten. In den antagonistischen Muskelgruppen des Oberschenkels, Quadrizeps und Hamstrings, war das bei 16 Hz-Stimulation am häufigsten beobachtete Muster durch die anti-phasische Alternierung der Reflexantworten der Antagonisten gekennzeichnet. (iii) Unabhängig von den Effekten höherer Stimulationsfrequenzen wurde ein bislang nicht beschriebener Reflex typ im Flexormuskel Tibialis anterior entdeckt. Diese Antworten, ausgelöst durch 2.1 Hz-Stimulation, hatten

sowohl Charakteristika monosynaptischer als auch komplexerer oligo- / polysynaptischer Reflexe.

Die Entstehung simpler Reflexmuster konnte mit dem mathematischen Netzwerkmodell reproduziert werden. Im Speziellen konnte gezeigt werden, dass vor allem die Aktivität der Renshaw-Zellen sowie deren gegenseitigen Interaktionen eine entscheidende Rolle in der Generierung stabiler Modulationen spielte. Demgegenüber übten die Ia Interneurone, verantwortlich für die reziproke Inhibition während verschiedenster Aktivitäten spinaler Netzwerke, einen geringeren Einfluss auf die Entstehung der einfachen rhythmischen Muster aus. Isoliert von der Aktivität des antagonistischen Netzwerkes konnten die segmentalen Netzwerke einer einzelnen Motoneuronpopulation alternierende Reflexreihen erzeugen. Indes erforderte die Generierung von anti-phasischen Modulationen Verschaltungen zwischen den beiden Netzwerken. Anti-phasische Modulationsmuster wurden vor allem in jenen Fällen hervorgerufen, in denen die beiden modellierten Reflexsysteme asymmetrisch mit „Flexor“- oder „Extensoreigenschaften“ ausgestattet wurden. Im kompletten Gesamtmodell, das die Aktivität von Ia-Interneuronen sowie Renshaw-Zellen berücksichtigte, war der Einfluss der letzteren größtenteils reduziert. Die Kapazität des Modells, stabile, rhythmische Reflexmodulationen zu generieren, ging unter diesen Umständen verloren.

Schlussfolgerungen

Die Reflexantworten auf 2.1 Hz-Stimulation waren eine Folge der Aktivierung von Gruppe Ia-Afferenzen mit großem Durchmesser innerhalb der lumbosakralen Hinterwurzeln L2-S2 und der daraufhin folgenden monosynaptischen Erregung von Motoneuronen. Die zusätzliche Rekrutierung von Gruppe II-Afferenzen führte zu den komplexeren Antworten in Tibialis anterior mit polyphasischen EMG-Potentialformen. Bei Stimulationsfrequenzen von 11-22 Hz wurde der zentrale Anregungszustand erhöht, sodass gleichzeitig zur Aktivierung monosynaptischer Pfade auch die Anregung von interneuronalen Netzwerken erfolgte. Deren Aktivität führte wiederum zur Generierung von simplen periodischen Reflexmodulationen.

Das Computermodell zeigte die zeitliche Summation von postsynaptischen Potentialen als zentralen Mechanismus für die Erhöhung des spinalen Anregungszustandes. Gleichzeitig war die Unabhängigkeit der Reflexantworten auf 2.1 Hz-Stimulation darauf zurückzuführen, dass selbst die am längsten andauernden interneuronalen Aktivitäten bei einer derart niedrigen Frequenz bereits abgeebbt waren, bevor der nächste Stimulus appliziert wurde. Das vorliegende Modell lieferte somit deutliche Hinweise auf die Frequenzabhängigkeit der Aktivierung von segmentalen Netzwerken. Die vom Computermodell generierten Reflexmuster ähnelten stark jenen, die in der neurophysiologischen Studie beobachtet wurden. Im Speziellen wurden die intersegmentalen Interaktionen bei einer Stimulationsfrequenz von 16 Hz demonstriert.

Die Signifikanz der vorliegenden Dissertation ist mannigfaltig. Elektrophysiologisch liefert sie eine Standardisierung von monosynaptischen Reflexen der Beinmuskulatur im Menschen, ausgelöst durch rückenmarksnahe Stimulation. Ein tieferes Verständnis für die Rolle der Signalfrequenz für die Konfiguration neuronaler Netzwerke ist ein wesentlicher Beitrag für den Bereich der Neurowissenschaften. Die mathematische Modellierung liefert zudem einen überraschenden Einblick in die Rolle spezialisierter Interneurone bei der Generierung rhythmischer Aktivitäten.

Summary

Model of spinal cord reflex circuits in humans: Stimulation frequency-dependence of segmental activities and their interactions

Motivation and objectives

Electrical stimulation delivered by electrodes close to the lower (lumbosacral) spinal cord of humans with complete spinal cord injury elicits muscle activities in the paralyzed lower limbs. With low repetition rates of stimulation (2.1 Hz), twitches are elicited in multiple lower limb muscles that have been suggested to be the simplest spinal reflexes transmitted via single synapses. By contrast, the same stimulation applied at higher rates (frequency range of 25-50 Hz) produces automatic stepping-like movements in the supine individuals with long-standing paraplegia.

The aim of the present study was to further elaborate the ‘standard’ spinal reflexes in response to 2.1 Hz-stimulation by analyzing a large size of human electrophysiological data. Furthermore, a main focus was on the effect of increased stimulation frequencies on the modification of these simple reflexes due to the integration of interneuronal circuit activities. The elicitation of simple periodic patterns covering only two successive responses was thereby regarded as an indication for interneuronal activity. Such patterns with interactions between antagonistic muscle groups were readily evoked when the stimulation frequencies were between the ones eliciting twitches and those resulting in stepping-like lower limb movements.

The hypothesis that at higher frequencies the stimulation effect expands to lumbar circuits that influence the activity between muscles shall be tested by a biologically realistic mathematical model. In particular, circuits including interneurons specialized in adjusting excitability of motoneurons during spinal reflexes as well as locomotion (Ia interneurons and Renshaw cells) were tested for their efficacy in generating simple periodic outputs.

Material and Methods

Analysis of electrophysiological data and neuromathematical modeling were chosen as two independent methods. First, electromyographic (EMG) recordings of reflex activities derived from six individuals with chronic complete spinal cord injury were evaluated. The subjects had epidural spinal cord stimulation systems implanted at lumbar cord levels. A large number of compound muscle action potentials (CMAPs) associated with the responses to 2.1 Hz-stimulation (the lowest available stimulation frequency) were analyzed for their EMG characteristics, i.e., latencies, peak-to-peak amplitudes, and waveforms. Furthermore, the effect of increasing the stimulation frequency to 5, 11, 16, and 22 Hz on the EMG activities was explored. The elicitation of responses with simple periodic patterns was documented.

Second, the capacity of biologically realistic network models to re-produce the simple periodic patterns covering two successive responses was tested by means of computer simulation. For this purpose, a novel mathematical model was developed that extends the widely used *Leaky Integrate-and-Fire* model by detailed neurophysiological time courses of postsynaptic potentials gained from experimental studies. The present model was designed as a biologically realistic mathematical integrator of postsynaptic effects of specialized spinal cord neurons. Particularly, it considered monosynaptic excitatory and disynaptic inhibitory actions exerted by populations of Ia fibers, Ia interneurons as well as Renshaw cells on the motor pools. Thereby, the mathematical model based on a non-linear recursive algorithm simulating spatially and temporally distributed neuronal effects. In order to test the functional roles of the network elements on the generation of particular motor outputs, the complexity of the complete model was approached by successively adding interneuronal populations and connectivities.

Results

The neurophysiological study produced three main findings. *(i)* Epidural stimulation of the human lumbosacral cord (deprived of brain influence by accidental lesion) at a low frequency of 2.1 Hz elicited monosynaptic, segmental reflexes in multiple lower limb muscles bilaterally. These responses had short and constant latencies and rather simple CMAP waveforms. There were no interactions between muscles during continuous stimulation. *(ii)* By increasing the stimulation frequency to 11-22 Hz, the independence of successively elicited reflexes was replaced by periodic modulations with cycle periods covering two responses in 20.8% of all data sets. In the thigh muscle groups quadriceps and hamstrings, the pattern most frequently detected at 16 Hz-stimulation was characterized by anti-phase alternations of responses in the antagonistic motor pools. *(iii)* Independently from the effects induced by higher stimulation frequencies, a not yet described type of reflex was detected in the flexor muscle tibialis anterior. These responses to 2.1 Hz-stimulation had both features of simple monosynaptic reflexes as well as characteristics of more complex oligo-/polysynaptic reflexes.

The generation of simple periodic patterns could be re-produced by the assumed network models. In particular, it was rather the activity of Renshaw cells and their mutual interactions that accounted for stable response modulations. On the other hand, the Ia interneurons, responsible for reciprocal inhibition during various spinal network activities, had less impact on the generation of simple periodic patterns. The segmental circuits associated with a single motoneuron population could produce alternating motor outputs independent from the activity in the antagonistic circuit. However, the generation of anti-phase alternations of antagonistic motoneuron pool firings required the incorporation of interconnections between the two circuits. Such type of patterned output was most readily produced when assuming two network circuits with asymmetric parameter settings corresponding to 'flexor' and 'extensor' connectivities. In the complete model network

considering Ia interneuron and Renshaw cell activity, the influence of the latter was largely reduced and the capacity of producing stable rhythmic patterns was lost.

Conclusions

The reflexes elicited by 2.1 Hz-stimulation were due to the activation of large-diameter group Ia afferent fibers within the posterior roots and the concomitant strong monosynaptic excitatory drive of the spinal motor cells. The additional recruitment of some group II fibers accounted of the elicitation of the more complex polyphasic responses detected in tibialis anterior. At stimulation frequencies of 11-22 Hz, the central state of excitability was increased, hence leading to the concomitant activation of spinal interneuronal circuits that led to a modification of the successive responses with simple periodic patterns.

The computer model revealed temporal summation of postsynaptic potentials elicited by stimulation pulses applied in close succession as leading mechanism elevating the central state of excitability. At the same time, the independence of segmental reflexes at 2.1 Hz was due to the cessation of even the longest lasting interneuronal activities induced by one stimulation pulse before the next stimulus was applied. The present model thus provided strong evidence for the frequency-dependence of the effective incorporation and activation of segmental circuits in the sensory-motor transmission. The motor outputs produced by the mathematical model closely resembled those derived from the neurophysiological recordings and particularly, inter-segmental coordination of segmental activities was demonstrated for stimulation frequencies of 16 Hz.

The significance of the present thesis is manifold. Electrophysiologically, it scrutinizes the standard human lower limb muscle reflexes in response to 2.1 Hz-epidural stimulation of the lumbosacral spinal cord isolated from supraspinal influence. In the field of neurosciences, it contributes to the understanding of the role of signal frequency in the configuration of neuronal circuits. Furthermore, it elaborates the functional roles of specialized interneurons of the lumbar spinal cord machinery in generating rhythmic activities.

Acknowledgements

I wish to acknowledge the outstanding mentorship of Professor Milan R. Dimitrijevic, MD, PhD, Department of Physical Medicine and Rehabilitation, Baylor College of Medicine, Houston, TX, USA, and Foundation for Movement Recovery, Oslo, Norway, throughout all my work. Thank you for introducing me to the field of human neurosciences.

Special thanks are due to Professor DDDr. Frank Rattay, Institute of Analysis and Scientific Computing, Vienna University of Technology, Vienna, Austria, for his scientific support. Prof. Rattay made my studies in the inter-disciplinary field of neuromathematics and 'Brain Modeling' possible. His supervision and mentorship accompanied me from the very beginning.

I am grateful for the invaluable support of my 'mentor-deputy' Dr. Karen Minassian, Institute of Analysis and Scientific Computing, Vienna University of Technology, Vienna, Austria. With his patient advice and supervision he steadily encouraged me to work to my full potential. Thank you, Karen, for being a marvelous teacher, colleague, and friend!

I am thankful to Professor Dr. Tatiana Deliagina, The Nobel Institute for Neurophysiology, Department of Neuroscience, Karolinska Institutet, Stockholm, Sweden, for her insightful comments of the present work.

My sincere gratitude is extended to Elisabeth Dallmer as well as Alice and Rudolf Hofstötter who inspired and supported me in so many ways throughout my studies.

This thesis bases on studies supported by the Austrian Science Fund (FWF), Proj. Nr. L512-N13, the Wings for Life Spinal Cord Research Foundation. Proj. Nr. WFL FR-001/06, the Medical-Scientific Fund of the Mayor of Vienna, Proj. Nr. 2516, and the Interreg IIIa Project 'Grenzenlos bewegen'.

Table of Contents

Kurzfassung der Dissertation	2
Summary	6
Acknowledgments	9
Table of Contents	10
Abbreviations	13
Posterior root-muscle reflexes of the human lumbar cord elicited by epidural stimulation	14
Summary	14
Introduction and Background	15
Material and Methods	17
Subjects	17
Spinal cord stimulation system	18
Electrode position and stimulation effect	19
Stimulation protocol	20
Surface-poly electromyography	20
Data analysis	21
Results	24
Simple segmental posterior root-muscle reflexes elicited by low-rate SCS	24
Modulated posterior root-muscle reflexes elicited by SCS at higher rates	27
Complex posterior root-muscle reflexes in tibialis anterior elicited by low-rate SCS	29
Discussion	36
Simple segmental posterior root-muscle reflexes elicited by SCS at 2.1 Hz	37
Posterior root-muscle reflexes elicited by SCS at higher rates	38
Complex posterior root-muscle reflexes elicited by SCS at 2.1 Hz	40
Conclusions	43

Simulation of reciprocal spinal segmental circuitries – A biologically realistic mathematical model	45
Summary	45
Introduction and Background	46
Posterior root-muscle reflexes and lumbar spinal locomotor circuits in humans	46
Posterior root-muscle reflexes modulated with simple periodic patterns	48
Material and Methods	56
Modeling a spiking neuron – General aspects and biological abstractions	56
The leaky Integrate-and-Fire Model and its refinement in the present work	58
<i>The Leaky Integrate-and-Fire Model</i>	58
<i>Excitatory and Inhibitory Postsynaptic Potentials</i>	61
The Alpha Function	61
Selection of neurons and interneurons involved in the present simplified reciprocal spinal network – Specification of model parameters	62
<i>Ia afferents and motoneurons</i>	65
<i>Ia inhibitory interneurons</i>	67
<i>Renshaw cells and recurrent inhibition</i>	69
Results	71
Model I: Ia afferent fibers monosynaptically projecting on homonymous motoneurons	71
Model II: The influence of tonic background activity exerted by Ia interneurons	73
Model III: The effect of recurrent inhibition of a single motoneuron pool	76
Model IV: The effect of recurrent inhibition including mutual inhibition between ‘opposite’ Renshaw cells populations on the output of two antagonistic motoneuron pools	84
Model V: The effect of recurrent facilitation	90
Model VI: The effect of mutual reciprocal Ia inhibition	96
Model VII: The complete network model	98
Conclusions	105
Appendix A - <i>Determination of parameter settings</i>	107
I. monosynaptic EPSP produced in motoneurons by Ia fibers	107
II. disynaptic IPSP mediated by Ia interneurons	107
III. Recurrent inhibition mediated by Renshaw cells	108
Appendix B – <i>Supplementary results</i>	109
ad Model I: Ia afferent fibers monosynaptically projecting on homonymous motoneurons	109
ad Model III: The effect of recurrent inhibition within a single motoneuron pool	110
Appendix C – <i>Matlab codes</i>	119

References	135
<i>Curriculum vitae</i>	143
<i>List of Scientific Publications</i>	145
<i>Contributions to International Conferences</i>	147

Abbreviations

AHP	afterhyperpolarization, afterhyperpolarizing
CMAP	compound muscle action potential
CPG	central pattern generator
EMG	electromyography, electromyographic
EPSP	excitatory postsynaptic potential
Ham	hamstrings
IPSP	inhibitory postsynaptic potential
LIF	leaky Integrate-and-Fire
LLPG	lumbar locomotor pattern generator
PRM reflex	posterior root-muscle reflex
PSP	postsynaptic potential
Q	quadriceps
SCI	spinal cord injury, spinal cord injured
SCS	spinal cord stimulation
TA	tibialis anterior
TS	triceps surae

Posterior root-muscle reflexes of the human lumbar cord elicited by epidural stimulation

Summary

Sustained epidural stimulation of the lumbar cord with frequencies of 25-50 Hz can activate spinal networks that generate locomotor-like movements in the lower limbs of chronic complete spinal cord injured individuals. These rhythmic activities are composed of a series of stimulus-triggered posterior root-muscle (PRM) reflexes, each initiated within the posterior roots, processed by the lumbar cord, and recorded from various lower limb muscles. At lower stimulation frequencies (2.1 Hz), PRM reflexes have previously been recognized as segmental muscle twitches and suggested to be monosynaptic in nature.

The aim of the present study was to further electrophysiologically characterize lumbar cord reflexes elicited by 2.1 Hz-epidural stimulation. A further aim was to document their behavior at transitional frequencies below the ones producing functional motor outputs.

Stimulation at 2.1 Hz resulted in simple segmental PRM reflexes, recorded from quadriceps, hamstrings, tibialis anterior, and triceps surae bilaterally. The results support the interpretation of their monosynaptic nature, even with intensities of 5 times the response thresholds. Only an increase of stimulation frequency to 11-22 Hz could lead to modifications of the simple PRM reflexes with patterns suggesting interactions between the segmental responses to successive stimuli or between antagonistic muscles. Occasionally, monosynaptic PRM reflexes with additional delayed electromyographic components were elicited in tibialis anterior at 2.1 Hz that suggested the contribution of group II muscle spindle afferents.

The conceptual novelty of this work is in elaborating characteristic short-latency reflexes of the human lumbar cord in response to low-rate electrical stimulation and the role of increased frequencies of afferent volleys on the configuration of spinal circuits.

Introduction and Background

Dorsal root-ventral root reflex studies in cats rapidly advanced the knowledge on reflex activity of the mammalian spinal cord in the 1940's. These electrophysiological in situ experiments based on single pulse stimulation of a dorsal root and the recording of the elicited reflex discharges from the ipsilateral ventral root of the same segment. By providing a controlled afferent input and an effective measure of the output, the method allowed for the analysis of specific spinal reflex pathways. The central sites of both stimulation and recording clarified the physiological features of spinal reflexes that were assumed from previous anatomical studies. The success in these early studies of segmental spinal reflexes was provided by the developments in experimental tools, allowing precise timing of events and accurate spatial localization of activity (Lloyd, 1944; Hultborn, 2006).

Short latency dorsal root-ventral root reflexes were discovered in cat by Eccles and Pritchard (1937). The central reflex time found was as short as to allow the assumption that the testing volley in the dorsal root fibers directly set up a discharge from the motoneurons via a single synapse. This was probably the first physiological demonstration of the anatomical, monosynaptic connection between primary afferent fibers and motoneurons (Eccles & Pritchard, 1937; Hunt & Perl, 1960). Thereafter, the characteristics of the monosynaptic reflex response were elucidated by Renshaw (1940). He found that dorsal root-ventral root reflexes showed temporal discontinuities in the populations of responding motoneurons. The early wave of the discharge was recognized as a two-neuron-arc reflex, initiated only by the fastest conducting dorsal root afferent fibers. The second portion of the reflex discharge followed the early wave at intervals corresponding to additional synaptic delays, and had an extended duration.

In a series of classical analyses, Lloyd (1943a, 1943b, 1944) described the correlation of dorsal root-ventral root reflexes with fiber size range of the stimulated afferents and their peripheral origin. He demonstrated that dorsal root-ventral root reflexes consisted of two-neuron-arc discharges, together with delayed, diffuse multineuron-arc discharges. The monosynaptic reflexes were initiated in large, low-threshold group I afferent fibers arising in muscle and could be demonstrated in extensor as well as flexor muscles. The polysynaptic discharges were found to be evoked by stimulation of group II muscle or cutaneous afferent fibers, distributed almost exclusively to flexor muscles. Thus the segmental reflex discharge initiated by dorsal root stimulation and recorded from a ventral root was demonstrated to contain three major elements, extensor two-neuron-arc, flexor two-neuron-arc and flexor multineuron-arc discharges.

Investigations of dorsal root-ventral root reflexes have not been carried out in humans since invasive stimulation as well as recording techniques would be required. On the other hand, minimally invasive methods have been described in humans that are effective to stimulate afferent structures at rather central sites close to the spinal cord. Posterior roots can be stimulated at localized sites p.e. by needle electrodes inserted epidurally, i.e., into the spinal canal but outside the outermost membrane covering the spinal cord (Ertekin et al., 1996). Also, a reflex discharge from the spinal cord can be not only recorded as the outflow through anterior roots, but also electromyographically from the surface of the respective muscle (Magladery et al., 1951; Jankowska, 1992) to which the discharge is directed.

Similarly, it has been shown that stimulation applied by electrodes placed in the lumbar epidural can similarly activate afferent fibers within the lumbar posterior roots in individuals with complete, long-standing spinal cord injury (SCI) (Murg et al., 2000; Minassian et al., 2004). In particular, it was demonstrated that non-patterned trains of stimuli delivered via such electrodes at 25-50 Hz can induce rhythmic locomotor-like activity in the paralyzed lower limbs with alternating extension and flexion phases (Dimitrijevic et al., 1998; Gerasimenko et al., 2002; Minassian et al., 2004). Electrical stimulation at 5-15 Hz applied at identical stimulation sites and intensities, on the other hand, can evoke bilateral extension of the lower limbs (Jilge et al., 2004).

Analysis of the stimulation-induced electromyographic (EMG) activities detected from the surface of several lower limb flexor and extensor muscles revealed that the EMGs associated with these functional motor outputs are composed of series of stimulus-triggered compound muscle action potentials (CMAPs) (Minassian et al., 2004). These responses were termed PRM reflexes (Minassian et al., 2007a, 2007b) in accordance with their initiation and recording sites. Hence, PRM reflexes described in these studies represented equivalents of the classical dorsal root-ventral root reflexes.

Functional motor outputs, i.e., locomotor-like activity or bilateral extension of the lower limbs, were produced by successively elicited PRM reflexes with organized modifications of amplitudes and latencies (Jilge et al., 2004; Minassian et al., 2004). These modifications indicated activation of functional lumbar networks by the sustained stimulation since the model under consideration was the human lumbar cord deprived of brain influence. Supportive evidence 'that a given sensory input can have either an excitatory or inhibitory effect on a given motoneuron as dependent on a CNS selection process related to the phase and intent of movement' (Stuart, 2002) has also been provided by animal experiments (Hultborn, 2001; McCrea, 2001).

The aim of the present study was to advance the knowledge about the sensory-motor mechanisms of spinal reflexes elicited by posterior root stimulation. Thereby, the focus on electrophysiological characteristics of monosynaptic segmental PRM reflexes evoked by low-rate epidural stimulation (2.1 Hz) and recorded from quadriceps (Q), hamstrings (Ham), tibialis anterior (TA), and triceps surae (TS) bilaterally. Additionally, the effect of increasing the stimulation frequency on the configuration of spinal networks will be

explored. The hypothesis is that at higher rates of incoming volleys the stimulation effect will expand to lumbar circuits that in turn will plurisegmentally influence the elicited PRM reflexes. Finally, a more complex and not yet described type of PRM reflex elicited at 2.1 Hz will be introduced that is distributed exclusively to the ankle flexor muscle TA. This PRM reflex-type has features of two-neuron-arc discharges, together with additional, delayed components.

The significance of the present study lies in the electrophysiological description of monosynaptic PRM reflexes of the human lumbar cord deprived of supraspinal influences. Expanding the knowledge about these simple, independent PRM reflexes will be essential for understanding the complex reorganization of reflex systems during rhythmic outputs of human lumbar spinal cord circuits activated by SCS at higher rates of stimulation (Dimitrijevic et al., 1998; Gilge et al., 2004; Minassian et al., 2004, 2007b). In the present work, information is provided on the conditions that secure the elicitation of these independent segmental reflexes and furthermore on the role of frequency in activating spinal circuits other than two-neuron reflex arcs, reflected by the divergence of the monosynaptic PRM reflex from its simple nature.

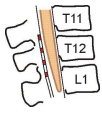
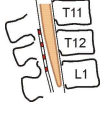
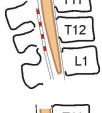
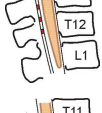
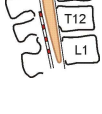
Material and Methods

Subjects

Six subjects with chronic traumatic motor complete SCI (5 ASIA A, 1 ASIA B¹) were selected for the present study. Subject demographic data are listed in Table 1. At the time of data collection, the subjects were otherwise healthy adults in a chronic condition (≥ 1 year post-injury) and met the following criteria: stretch and cutaneomuscular reflexes in the lower extremities were preserved; lumbosacral evoked potentials reflecting the spinal cord gray matter function below the level of the lesion were present (Lehmkuhl et al., 1984); the absence of supraspinal, trans-lesional activation of motor units was documented by brain motor control assessment (BMCA; Sherwood et al., 1996) using multichannel surface EMG recording; no antispastic medications were used. The subjects participated to a program of restorative neurology for the control of spasticity by spinal cord stimulation (SCS, Pinter et al., 2000) and had systems for epidural SCS implanted subcutaneously. The vertebral levels of the implanted electrode arrays ranged from the lower half of T11 to the lower third of L1 in the different subjects. Implantations as well as clinical stimulation protocols were approved by the local ethics committee, and all subjects gave their informed consent.

¹ ASIA classification: ASIA A, no sensory or motor function preserved below the level of the lesion; ASIA B, sensory but no motor function below the level of the lesion. For details see Maynard FM et al., 1997.

Table 1. Subject demographic information at the time of data collection

Subject No.	Sex	Age (years)	Time since SCI (years)	Level of SCI	ASIA Class.	Electrode position (vertebral level)	
1	m	22	5	C6	A	T12-L1	
2	m	18	3	C5	A	T12-L1	
3	m	25	1	C7	B	T12-L1	
4	f	25	4	T6	A	T12	
5	m	33	13	T5	A	T11-T12	
6	f	33	2	T5	A	T12-L1	

Spinal cord stimulation system

Spinal cord stimulation was delivered via a cylindrical electrode array (Pisces-Quad electrode, Model 3487A, Medtronic, Minneapolis, MN, USA) placed in the spinal canal, but outside the meninges covering the spinal cord in the dorsal epidural space (Fig. 1). The array consisted of four independent electrodes, each 3 mm long with an inter-electrode spacing of 6 mm. For their identification, the electrodes were labeled as 0 to 3, with 0 being the most rostral one. The electrode array was connected to a programmable pulse generator (Itrel 3, Model 7425, Medtronic), located subcutaneously in the abdominal wall. The pulse generator delivered quasi monophasic stimulus pulses. To avoid charge accumulation, a second long pulse was used with essentially smaller amplitudes. Following stimulation parameters were offered: pulse widths, 60-450 μ s; stimulus intensities, 0-10.5 V; and stimulation frequencies, 2.1 Hz -130 Hz. Each electrode of the array could be set at +, -, or 'off', allowing for various bipolar electrode combinations. Monopolar stimulation was carried out with one of the electrodes selected as cathode and the active area of the pulse generator case, labeled as 'c', as anode. Impedance was within a range of 300-1500 Ω , partially depending on the active electrode combinations.

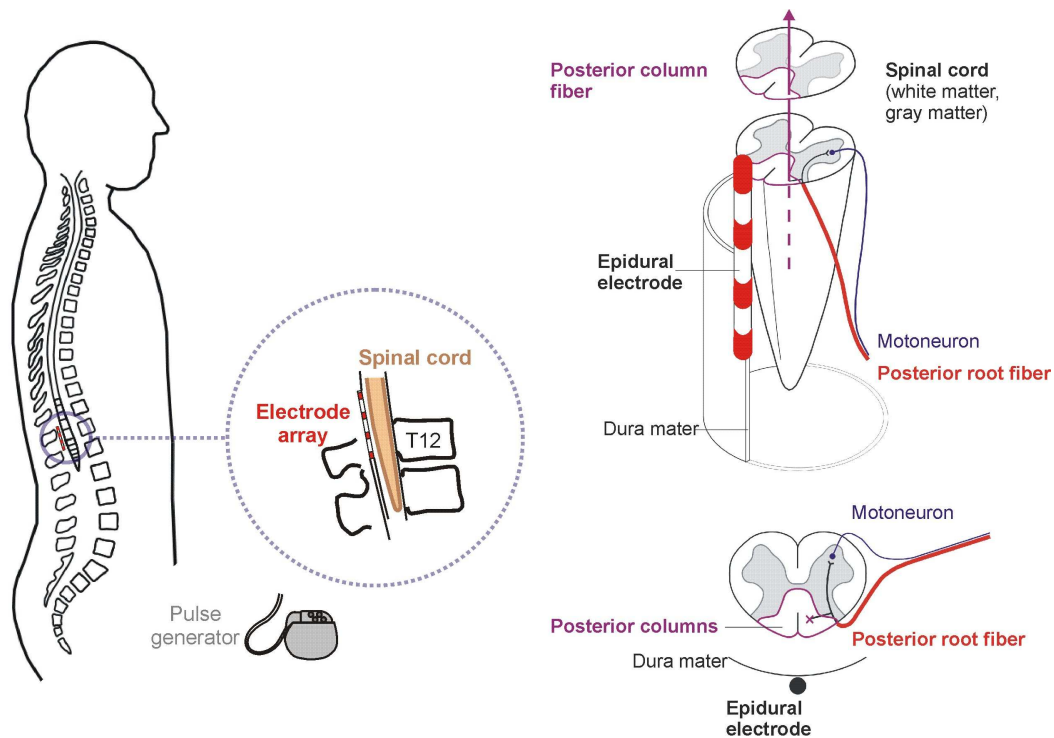


Figure 1. Schematic sketch demonstrating the location of the implanted epidural electrode array with respect to vertebral levels (left) and anatomical structures (right).

Electrode position and stimulation effect

The effect of SCS is determined by the rostro-caudal position of the active cathode (Struijk et al., 1993; Rattay et al., 2000) as well as the applied stimulation parameters (Dimitrijevic et al., 1998). It is important to note that the selection of different monopolar or bipolar electrode combinations of the epidural array results in different locations of the cathode along the electrode array as well as different cathode-anode distances, affecting stimulation site and effective range. Monopolar (e.g. c+3-) and bipolar electrode combinations with largely spaced electrodes (e.g. 0+3-) provide a broader effective range of stimulation than narrowly spaced electrodes (e.g. 2+3-).

The rostro-caudal position of the active cathode with respect to the lumbosacral spinal cord segments can be identified by the elicitation of segmental muscle twitches in the lower limb muscles, based on their segmental innervations (Halter et al., 1983; Murg et al., 2000). According to the thresholds of responses evoked in Q and TS, two muscle groups with separate segmental innervations (L2-L4 and L5-S2, respectively), and vertebral cathode positions (identified by X-ray) along with standard anatomical data, the segmental stimulation sites can be estimated and categorized into 4 groups (Minassian et al., 2007b): Group 1, only thigh muscles respond even to maximally applied stimulation (10 V), cathode position: rostral to L2 cord segments; Group 2, thresholds $Q < TS$, cathode

position: L3/L4; Group 3, thresholds $Q = TS$, cathode position: S1/S2; Group 4, thresholds $Q > TS$, cathode position: caudal to S2. The same categorization will be used in the present study for the characterization of effective stimulation sites. Muscle responses elicited by stimulation delivered from a Group 2-position will be given special consideration, since this site was demonstrated to be of particular relevance for lumbar network activity (Dimitrijevic et al., 1998; Jilge et al., 2004; Minassian et al., 2004).

Stimulation protocol

Recordings utilized for the present study were collected according to 2 clinical stimulation protocols, the ‘muscle twitch’- and the ‘frequency-protocol’. All recordings were conducted with the subjects in a comfortable supine position.

The ‘muscle twitch-protocol’ was used for the identification of the rostro-caudal electrode position and in particular the effective site of SCS by eliciting segmental reflex responses (Murg et al., 2000). For this purpose, the pulse generator was programmed as to deliver repetitive pulses of 210 μ s width at the lowest available stimulation frequency of 2.1 Hz. For each monopolar or bipolar electrode combination of the epidural array, the stimulation was intensified in 1 V-increments up to a maximum of 10 V, but was never increased beyond the level that started to cause discomfort to the subject.

The ‘frequency-protocol’, on the other hand, was utilized to determine both the appropriate electrode combination and stimulation frequency that effectively suppressed motor unit excitability (Pinter et al., 2000). Again, the pulse generator delivered repetitive pulses of 210 μ s width. Stimulation was initially applied at 2.1 Hz for a given lead selection. Intensity was stepwise increased until muscle twitches were recorded in all lower limb muscles studied. At this level, the stimulation frequency was gradually increased up to 100 Hz, with steps specified by the pulse generator (2.1, 5, 11, 16, 22 Hz etc.). The same procedure was repeated for incremental stimulus intensities and eventually for different electrode combinations.

Surface-poly electromyography

Surface EMG recordings have a long history of various applications in biomechanics, motor control, neuromuscular physiology, and clinical evaluation of movement disorders. For the present study, multi-channel surface EMG was utilized as a non-invasive technique that provides a measure of the outputs of multiple lumbosacral motor pools, the latter representing common final pathways of spinal neuronal activity. Surface EMG allows for the recording from a relatively large volume of the muscle, hence assessing a corresponding large portion of the motor pools.

For the above introduced clinical stimulation protocols, EMG activity was recorded from Q, adductor, Ham, TA, and TS bilaterally (cf. Figure 2), and from the lower abdominal and lumbar paraspinal muscles. Pairs of silver-silver chloride surface electrodes were utilized with an inter-electrode distance of 3 cm. To obtain electrode impedances below 5 k Ω for enhancing signal quality, the skin was prepared with abrasive skin gel if necessary. The EMG signals were amplified using a Grass 12D-16-OS Neurodata Acquisition System (Grass Instruments, Quincy, MA, USA) adjusted to a gain of 2000 over a bandwidth of 30–700 Hz. Data were digitized at 2002 samples per second and channel using a Coda ADC system (Dataq Instruments, Akron, OH, USA).

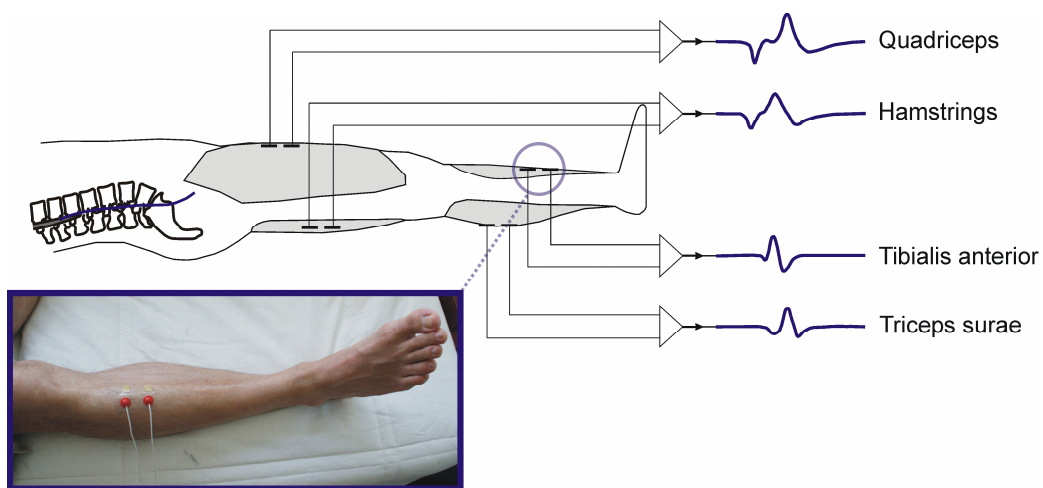


Figure 2. Sketch illustrating placement of surface-electrodes used to record EMG activity from various lower limb flexor and extensor muscle groups bilaterally.

Data analysis

Responses of Q, Ham, TA, and TS elicited by SCS at 2.1 Hz were analyzed for their EMG features in terms of onset, offset, duration, peak-to-peak amplitude and waveform. Electromyographically, the muscle responses were detected as CMAPs.

The lumbar paraspinal surface EMG electrodes were the ones closest to the stimulation site and therefore most readily picked-up the volume-conducted stimulus pulses generated by the epidural electrodes as artifacts. These artifacts were used for the temporal identification of single pulses within the applied 2.1 Hz-trains, permitting us to unequivocally relate the CMAPs to the pulses which had triggered them. This simple stimulus-response relation allowed for the analysis of EMG characteristics of single CMAPs captured from the continuous recordings.

Figure 3 illustrates the analyzed CMAP features. The onset latency and the offset of a CMAP were defined as the times between the stimulus application and the first and last EMG deflections from baseline larger than 5% of the corresponding CMAP peak-to-peak

amplitude, respectively (Fig. 3a). The CMAP width was the duration between the onset latency and the offset. Averages of these time parameters were calculated as the mean values of all responses consecutively elicited with constant stimulation parameters (generally 20–35 CMAPs).

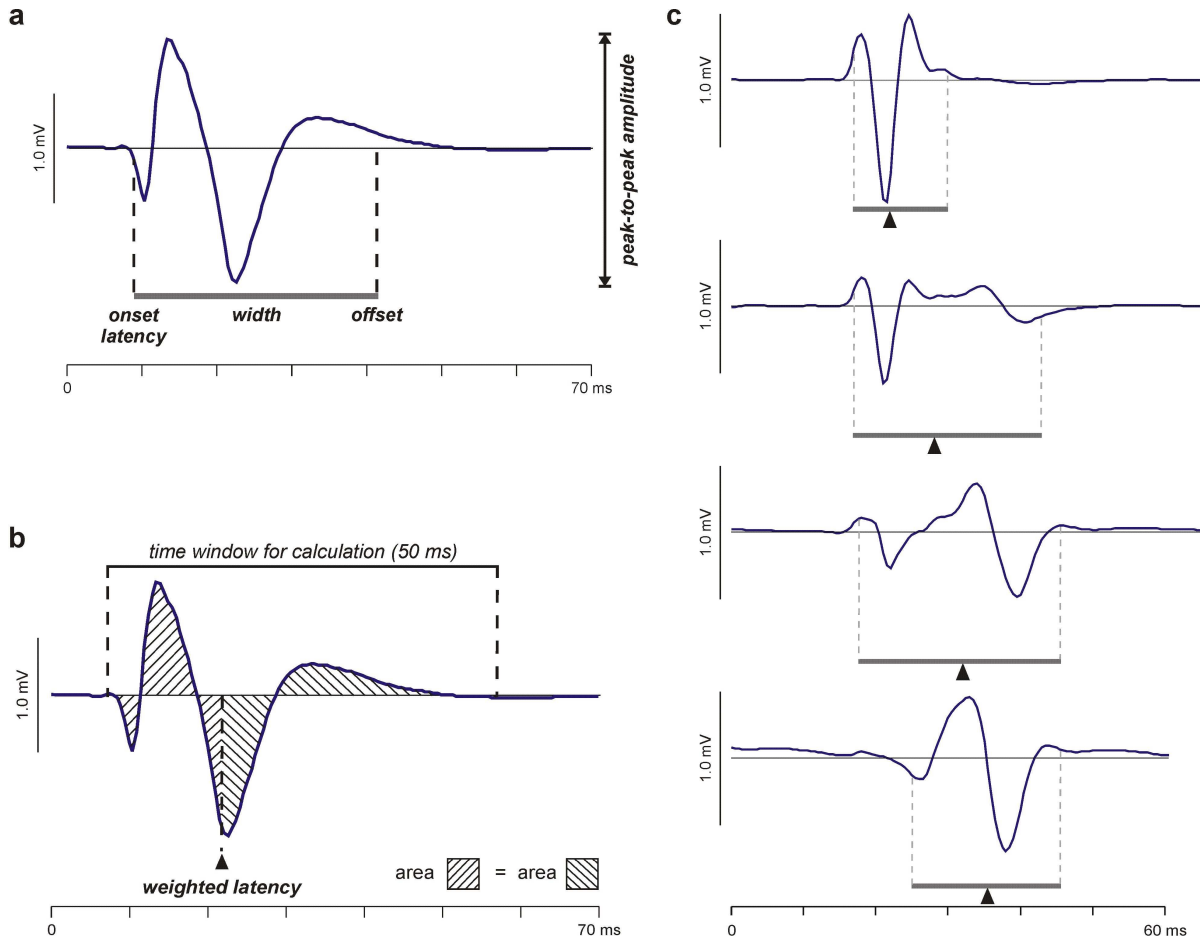


Figure 3. Evaluated electrophysiological features describing CMAPs associated with PRM reflexes. **a** Peak-to-peak amplitude, onset latency, offset, width. **b** The definition of weighted latency of a PRM reflex is the time in the waveform measured when the area under the curve for the full 50 ms time window is divided equally. All latencies measured from stimulus onset. **c** PRM reflexes elicited in tibialis anterior during a single recording session with constant stimulation intensity of 6 V and epidural electrode combination 0+2-, subject 1. Stimulation frequencies from top to bottom: 2.1 Hz, 11 Hz, 16 Hz, and 22 Hz. Delayed EMG components emerge as from 11 Hz and eventually become the predominant responses constituents (22 Hz). At 11 Hz and 16 Hz, the early response component diminishes; still the onset latencies as compared to the short response elicited at 2.1 Hz are unchanged. Only when the early components are fully suppressed (22 Hz), the onset latency shows a considerable shift. As opposed to that, weighted latencies are gradually shifted to prolonged latencies in consistency with the growing dominance of the delayed EMG components of the responses illustrated from top to bottom.

In addition to the conventional time parameters, a novel parameter was defined, referred to as weighted latency (Fig. 3*b*). Weighted latency is a calculated value, as opposed to the measurable onset latency, and provides a measure for changes in the CMAP morphology and reflects the contribution of late peaks to the CMAP waveform (Fig. 3*c*). Arithmetically, weighted latency is the time between the stimulus application and the weighted median of the rectified EMG activity associated with a CMAP. For its calculation, time windows, each covering a single response, were introduced. The left margins of the time windows were defined as the onset latencies of the corresponding responses minus 2 ms, to entirely include the initial CMAP deflections from baseline. Time window length was 50 ms, a duration longer than any CMAP width measured, hence covering the cessation of all stimulus-induced events within this period. Signal contributions after the complete decay of the physiological response but still within the time window were negligible. Finally, within each time window, the area under the rectified CMAP was evaluated. Weighted latency was then defined as the time between the stimulus and the moment that separated the calculated integral into 2 equal parts (see differently hatched areas of the CMAP given in Fig. 3*b*).

To identify standard CMAP shapes, all stimulus-triggered responses within a sequence with constant stimulation parameters were averaged. Average shapes were established for each subject, muscle, and incremental intensity. Finally, the calculated CMAP shapes were categorized according to the number of EMG phases, positive or negative initial peaks, and CMAP widths.

Additionally, response thresholds for consistently eliciting PRM reflexes with peak-to-peak amplitudes $> 50 \mu\text{V}$ were identified and recruitment curves were calculated as the relation between the mean response-magnitudes and the respectively applied stimulus intensities for each muscle studied. To obtain group results, the individual recruitment curves were normalized in two steps as follows: (i) Mean amplitudes of a given muscle were related to the respective maximum response, and applied stimulus intensities were given as multiples of the response threshold. (ii) The values of all subjects were grouped into intervals of 0.5 times of the threshold intensity. Relative maximum applied intensities amounted to 5 times the threshold. Within each interval, the average amplitude was calculated from the six subjects for each muscle pair.

Data were analysed off-line using WinDaq Waveform Browser playback software (Dataq Instruments) and Matlab 6.1 (The MathWorks, Inc., Natick, MA, USA).

Results

This study generated three main findings which will be presented in separate sections. First, standard PRM reflexes in the lower limbs elicited by low rate-SCS (2.1 Hz – the lowest possible stimulation frequency of the pulse generator) will be described. The associated EMG activities are identified as CMAPs with short and constant onset latencies and electrophysiological features of segmental two-neuron-arc reflexes. Subsequently, PRM reflexes are presented that are modified either by interactions between antagonistic muscles at higher stimulation rates or by the emergence of additional delayed EMG components at 2.1 Hz-SCS that are superimposed on the simple monosynaptic TA response.

Simple segmental posterior root-muscle reflexes elicited by low-rate SCS

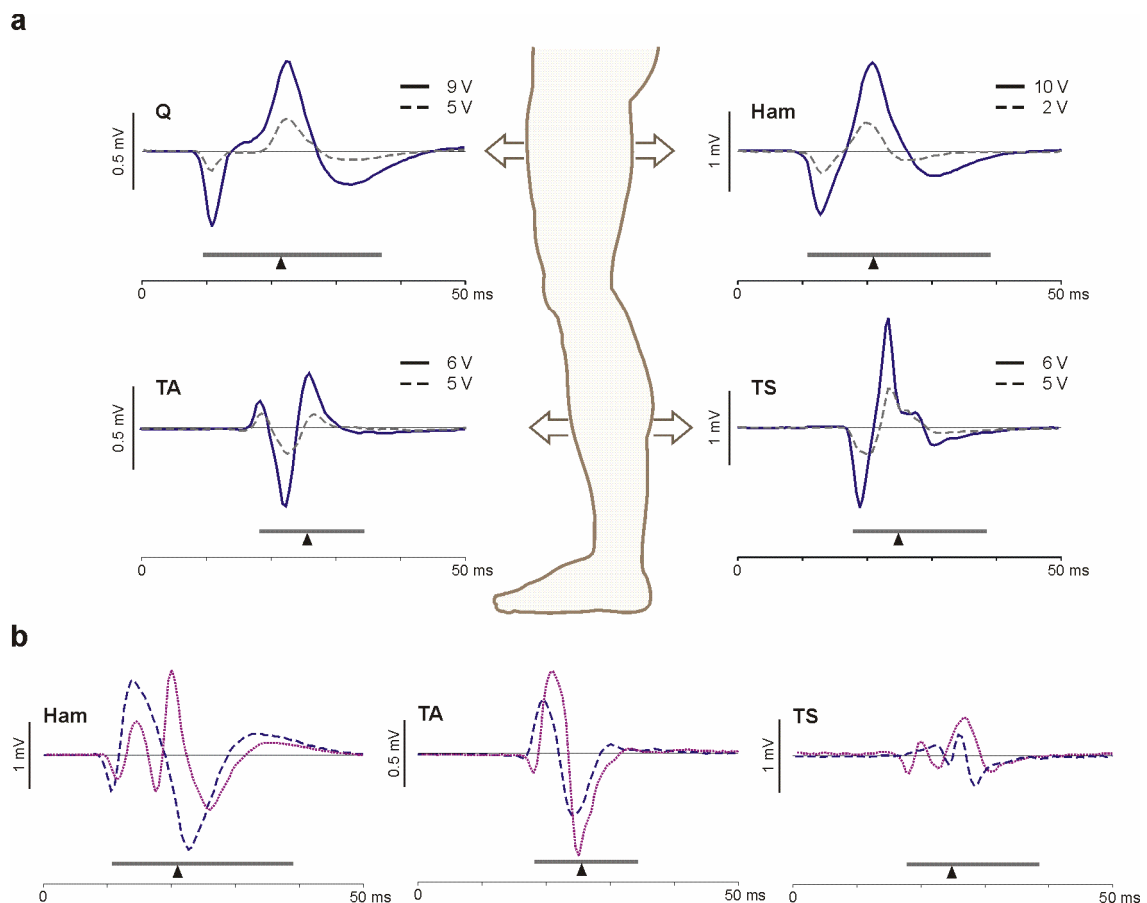
Epidural stimulation of the lumbosacral spinal cord at a low rate of 2.1 Hz elicited PRM reflexes in Q, Ham, TA, and TS simultaneously. When elicited under constant stimulation conditions, these responses had consistent CMAP latencies, amplitudes and waveforms and were therefore referred to as ‘simple PRM reflexes’. They never yielded a build-up of additional delayed EMG components beyond their distinctive short offsets, not even in response to maximum stimulation that could reach 5 times the threshold intensity.

Some variations of CMAP waveforms could be observed at slight increases of the stimulus intensity above threshold. CMAP shapes of PRM reflexes with magnitudes of 80% and above of the corresponding maximum responses stayed constant with yet stronger stimulation. By categorizing the CMAP shapes with maximum amplitudes, distinct templates were identified that were characteristic for the different muscles studied. Figure 4a illustrates representative simple PRM reflexes of Q, Ham, TA, and TS with maximum (solid lines) and lower (dashed lines) amplitudes, the latter elicited just at threshold intensities or slightly above. Exceptions from these standard templates are shown in Figure 4b. Quadriceps had a triphasic CMAP shape, detected in all twelve limbs of the six subjects studied. Hamstrings showed most inter-individual variabilities of CMAP shapes. The template displayed in Fig. 4 was recorded in eight limbs. In two further cases, CMAPs featured the standard shape being mirrored in the abscissa with a short initial positive phase. In the remaining two limbs, five-phasic CMAPs with a first positive deflection were detected. Tibialis anterior responses featured two characteristic templates, triphasic in seven cases and biphasic in four cases. Both shapes had same widths and started with a negative peak. In one case, a polyphasic shape was detected that did not exceed the offset of the other templates. Triceps surae had a CMAP shape dominated by two major peaks starting with a positive deflection. Exceptions were only found in two limbs with responses demonstrating four and five distinct phases, respectively, but the same CMAP widths as the standard template.

Given a functional stimulation site estimated at L3/L4 segments (Group 2-position), maximum peak-to-peak amplitudes were larger in the thigh than in the leg muscles. Mean values evaluated in all six subjects amounted to Q, $2100.4 \pm 1170.1 \mu\text{V}$; Ham, $2416.7 \pm 944.2 \mu\text{V}$; TA, $687.7 \pm 315.7 \mu\text{V}$; and TS, $1284.9 \pm 847.4 \mu\text{V}$. No evidence for reciprocal interaction between antagonistic muscle groups was found.

Mean thresholds for eliciting simple PRM reflexes were Q, $3.0 \pm 0.6 \text{ V}$; Ham, $3.0 \pm 0.6 \text{ V}$; TA, $4.1 \pm 1.2 \text{ V}$; and TS, $3.9 \pm 0.8 \text{ V}$ given stimulation sites estimated at L3/L4 segments (Group 2-position). At intensities above 4.1 V on average, SCS was effective to induce PRM reflexes in all recorded lower limb muscles bilaterally. While the recruitment curves of the thigh muscles had steeper initial slopes than the ones of the leg muscles, they all reached a plateau at stimulus intensities of 2 times the respective thresholds. In Ham, TA, and TS, the recruitment curves remained steady at the plateau level up to the maximum applied intensity, whereas the recruitment curve of Q declined with further increase of stimulus intensity.

In two subjects (# 4 and 6) the potential for post-activation depression of PRM reflexes elicited at 2.1 Hz -SCS in Q, Ham, TA, and TS at intensities from the threshold of 2 V to the maximum of 10 V was studied. The responses to the first stimuli within the trains did not demonstrate any post-activation effects on the PRM reflexes elicited by the immediately following pulses.



◀ **Figure 4.** Standard PRM reflexes of quadriceps (Q), hamstrings (Ham), tibialis anterior (TA), and triceps surae (TS) derived from sequences of SCS at 2.1 Hz. **a** Characteristic CMAP waveforms of PRM reflexes with maximum amplitudes (solid lines in blue color) are illustrated together with CMAP widths (horizontal bars, margins marking onset latencies and offsets) and weighted latencies (filled arrowheads). CMAP templates are derived from single individuals; time parameters are group results of all subjects. CMAPs in dashed grey lines show PRM reflexes at threshold intensity or slightly above. Q, electrode combination 0–3+, 9 V, subject 2; Ham, 1–3+, 10 V, subject 4; TA, 0+2–, 6 V, subject 1; TS, 0+2–, 6 V, subject 1. **b** Exceptions from the standard CMAP templates detected in Ham, TA, and TS as described in the text. Ham (dashed line in blue color), epidural electrode combination 0+3–, 5 V, subject 4; Ham (solid line in purple color), epidural electrode combination 0+3–, 6 V, subject 3; TA (dashed line in blue color), epidural electrode combination 0+2–, 5 V, subject 1; TA (solid line in purple color), epidural electrode combination 0+3–, 7 V, subject 4; TS (dashed line in blue color), epidural electrode combination 0+3–, 6 V, subject 5; TS (solid line in purple color), epidural electrode combination 1–3+, 5 V, subject 4.

Mean time parameters of maximum PRM reflexes based on the whole subject group are illustrated in Figure 4 and listed in Table 2. With a variability of 0.5 ms, a value equal to the sampling interval, the onset latencies of repetitively elicited responses of a given muscle were confirmed to be constant. The onset latencies of CMAPs detected in the thigh muscles were shorter than in the leg muscles. At the same time, CMAP widths of the thigh muscle responses were longest. The response cessations of the various muscle groups were synchronized to a high degree. The corresponding offsets compared in pairs did not show significant differences (paired t-test, $p < 0.05$), except when comparing Ham with TA.

Table 2. Time parameters of PRM reflexes of quadriceps (Q), hamstrings (Ham), tibialis anterior (TA), and triceps surae (TS) with maximum peak-to-peak amplitudes

	Onset latency	Weighted latency	Offset	Width
Q	9.8 ± 0.9	21.5 ± 1.9	36.8 ± 4.8	27.0 ± 4.8
Ham	10.9 ± 0.9	21.1 ± 1.0	39.2 ± 1.8	28.3 ± 2.3
TA	18.5 ± 0.9	25.9 ± 1.9	34.7 ± 3.0	16.4 ± 3.5
TS	18.1 ± 1.0	25.1 ± 1.7	38.8 ± 4.9	20.7 ± 4.7

Values (mean \pm SD) are in ms and averaged from all subjects.

Modulated posterior root-muscle reflexes elicited by SCS at higher rates

Epidural SCS delivered at the lowest available repetition rate of 2.1 Hz exclusively entailed independent PRM reflexes in all four muscle groups studied, without interactions between responses to successive stimuli or between antagonistic muscles. At higher stimulation frequencies up to 22 Hz different types of stable patterns (i.e., lasting for at least 5 s) of periodic reflex modulations could be identified (cf. Fig. 5). The oscillation period of the simple periodic patterns covered only two successive responses, unlike the PRM reflex modifications forming a spindle-like shaped EMG burst as described in previous studies (Minassian et al., 2007b).

In the thigh muscles, the modulations affected the response magnitudes as well as the CMAP shapes. Yet, with respect to the time parameters, all responses were of monosynaptic nature. In the leg muscles, the modified reflexes typically involved the emergence of delayed EMG components that could even become the predominant response constituents. However, such complex, dynamic modulations are beyond the scope of the present study. Only results recorded from Q and Ham will be presented in the following section.

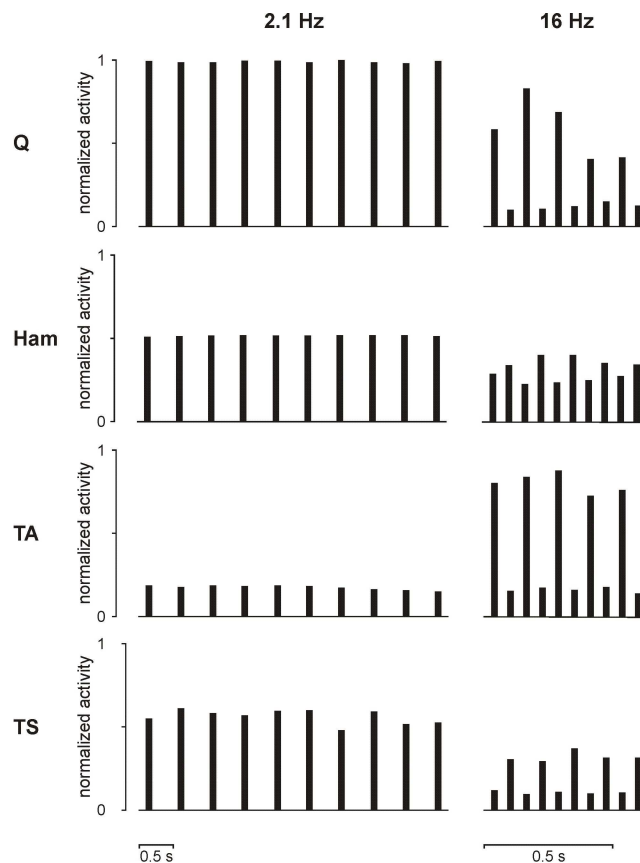
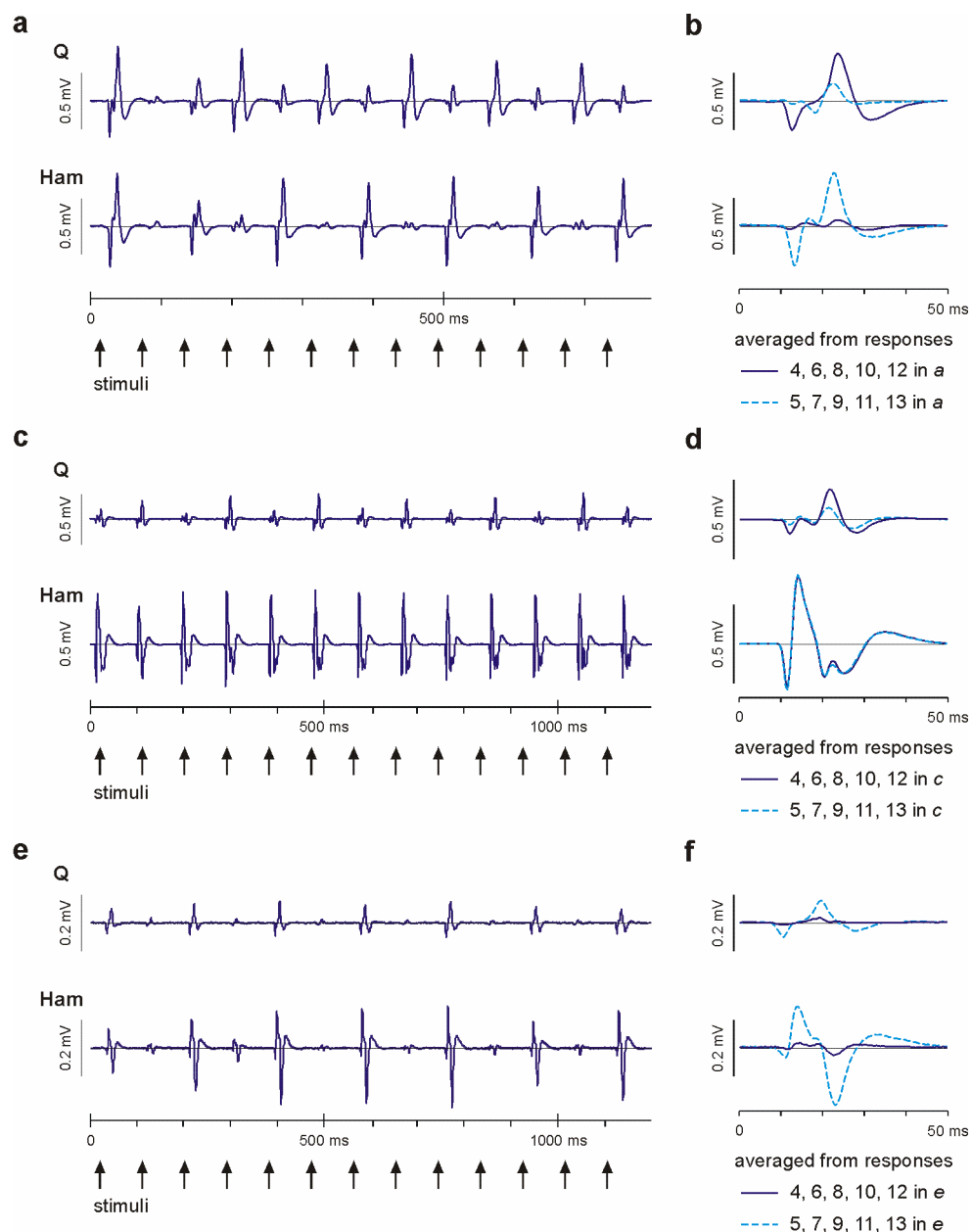


Figure 5. Independent un-modulated PRM reflexes elicited at 2.1 Hz (left) compared to responses featuring one type of simple periodic patterns at 16 Hz-SCS (right). Bars represent integrated activities of successive PRM reflexes. All data derived from subject 2, epidural electrode combination 0+3–, 5 V.

Of all available data sets for responses to 5, 11, 16, and 22 Hz, 20.8% showed simple periodic patterns. Among these cases, the pattern most frequently detected (58.7%) was characterized by the out-of-phase attenuation of responses elicited in Q and Ham (Figs. 6a, b). This type of modulation was most readily elicited when SCS was delivered at 16 Hz (20.9% of all tested data sets), followed by stimulation at 22 Hz (15.1%) and 11 Hz (4.2%). No examples were found at 5 Hz or above 22 Hz. The mean durations for a stable pattern were 15.0 ± 3.4 s (16 Hz); 15.6 ± 3.7 s (22 Hz); and 11.6 ± 3.4 s (11 Hz). Moderate stimulation intensities of 1-1.5 times the threshold were most effective to result in this pattern out-of-phase attenuation of Q and Ham PRM reflexes (66.7% of all samples showing this pattern). The pattern could also be induced at intensities of 1.6-2.5 times the threshold (33.3%). No examples were found at even higher stimulus intensities. Stimulation sites estimated at S1/S2 segments most frequently elicited this pattern in Q and Ham (17.8% of all tested samples corresponding to a Group 3-position), followed by stimulation sites corresponding to L3/L4 segments (Group 2-position; 10.3%).



◀ **Figure 6.** Periodic PRM reflex modulations elicited by SCS at frequencies above 2.1 Hz. Displayed responses of quadriceps (Q) and hamstrings (Ham) are first 13 within a series, arrows depict the times of stimulus application. **a** Stable pattern characterized by out-of-phase attenuation of Q and Ham PRM reflexes is established after the first 3 responses. **c** Pattern featuring attenuation of every second Q response, while Ham responses remain un-modulated. **e** In phase-modulation of Q and Ham responses. **b, d, f** Averaged CMAPs of Q and Ham derived from the continuous recordings in *a*, *c*, and *e*, respectively. Solid dark lines calculated from responses 4, 6, 8, 10, 12, dashed light lines from responses 5, 7, 9, 11, 13, respectively. Data from top to bottom derived from: subject 2, epidural electrode combination 0+3-, 5 V, 16 Hz; subject 2, 0+3-, 5 V, 11 Hz; and subject 4, 0-3+, 6 V, 11 Hz.

Occasionally, two additional patterns could be detected in Q and Ham: (i) attenuation of every second response within one muscle group (either Q or Ham), but un-modulated, constant motor output resembling that at 2.1 Hz-SCS in the antagonistic one (28.8% of all cases featuring simple periodic patterns; Figs. 6*c, d*); (ii) in-phase modulation of successive Q and Ham PRM reflexes (12.5% of all samples featuring simple periodic patterns, Figs. 6*e, f*).

Complex posterior root-muscle reflexes in tibialis anterior elicited by low-rate SCS

More complex PRM reflexes were occasionally elicited in TA by 2.1 Hz-SCS. These responses featured additional EMG components beyond the offsets of the simple CMAP templates. They still had short and constant onset latencies, but polyphasic CMAP shapes, longer widths and delayed weighted latencies.

Figure 7 compares representative simple (Fig. 7*a*) and complex (Fig. 7*b*) PRM reflexes of TA elicited with incremental intensities. Both examples were derived from the same subject during a single recording session. By selecting different active epidural electrode combinations, the effective site of the bipolar electrode with same contact separation was shifted by 9 mm in rostral direction from *a* to *b*. Characteristically for the complex PRM reflexes, graded stimulation not only yielded an increase in the response magnitudes, but also led to the build-up of additional late EMG components beyond a certain threshold (Fig. 7*b*, 4 V). As opposed to that, the simple PRM reflexes in Fig. 7*a* responded only with increased amplitudes to higher stimulus intensities. Another prominent feature making up the complexity of the polyphasic PRM reflexes in TA was the stochastic variability of their appearance. Late EMG potentials in addition to the simple CMAP components were not consistently evoked within series of responses elicited under constant stimulation conditions. Particularly at moderate stimulus intensities, complex and

simple PRM reflexes were elicited in a random order with rather constant amplitudes of the prominent late peak (Fig. 7b). At higher stimulation intensities every single stimulus pulse eventually resulted in a complex PRM reflex. Under such conditions, the late peak rapidly increased in size with yet increasing intensity. Furthermore, the amplitudes of the late positive peaks demonstrated profound variations (Fig. 7b). These were not subject to characteristic, patterned modulations, but appeared randomly within series of consecutively elicited responses under constant stimulation conditions. The variations did not affect the onset latency or the initial slopes of the CMAPs. Temporarily, the influence of the late EMG components started approximately with the 1st negative peak of the response.

To identify any relation between the elicitation of complex PRM reflexes and the effective electrode position as well as the utilized epidural electrode selection, all different monopolar and bipolar electrode combinations of the implanted electrode array were evaluated that were tested within single recording sessions in the 6 subjects. Responses with delayed peaks were detected in 5 of the 6 subjects and occurred in 30.8% of all tested electrode selections. With a probability of occurrence amounting to 32.6%, they were most likely to be elicited in case of stimulation sites estimated at L3/L4 segments (Group 2-position). Given a stimulation site estimated at S1/S2 segments (Group 3-position), 25.8% of the TA responses yielded a polyphasic shape. No examples of complex PRM reflexes were found with SCS delivered from sites caudal to S2 segments (Group 4-position). However, few data were available for the latter case. In a single subject, complex TA PRM reflexes were not detected. In this case, maximum applied intensities corresponded to 1.5 times the response threshold of TA.

Regarding the applied epidural electrode combinations, bipolar stimulating electrode selections with largely spaced electrodes (e.g. 0+3-) most frequently elicited complex PRM reflexes. With such electrode set-ups, they occurred in 75% of all cases and were thus the common type of spinal reflexes in TA. In monopolar stimulation mode (e.g. c+3-) the probability for their elicitation was 43.2%. Bipolar stimulation employing moderately (e.g. 1+3-) or narrowly spaced electrodes (e.g. 2+3-) were least likely to evoke complex responses, with probabilities of occurrence of 21.4% and 10.8%, respectively.

Independently from the applied monopolar or bipolar stimulation mode, polyphasic PRM reflexes were evoked in 70.6 % of all cases when the most caudal lead electrode, # 3, was selected as cathode. The probabilities for complex responses to be evoked with the other lead electrodes operated as cathode were: # 2, 21.9%; # 1, 4.0%; and # 0, 23.1%.

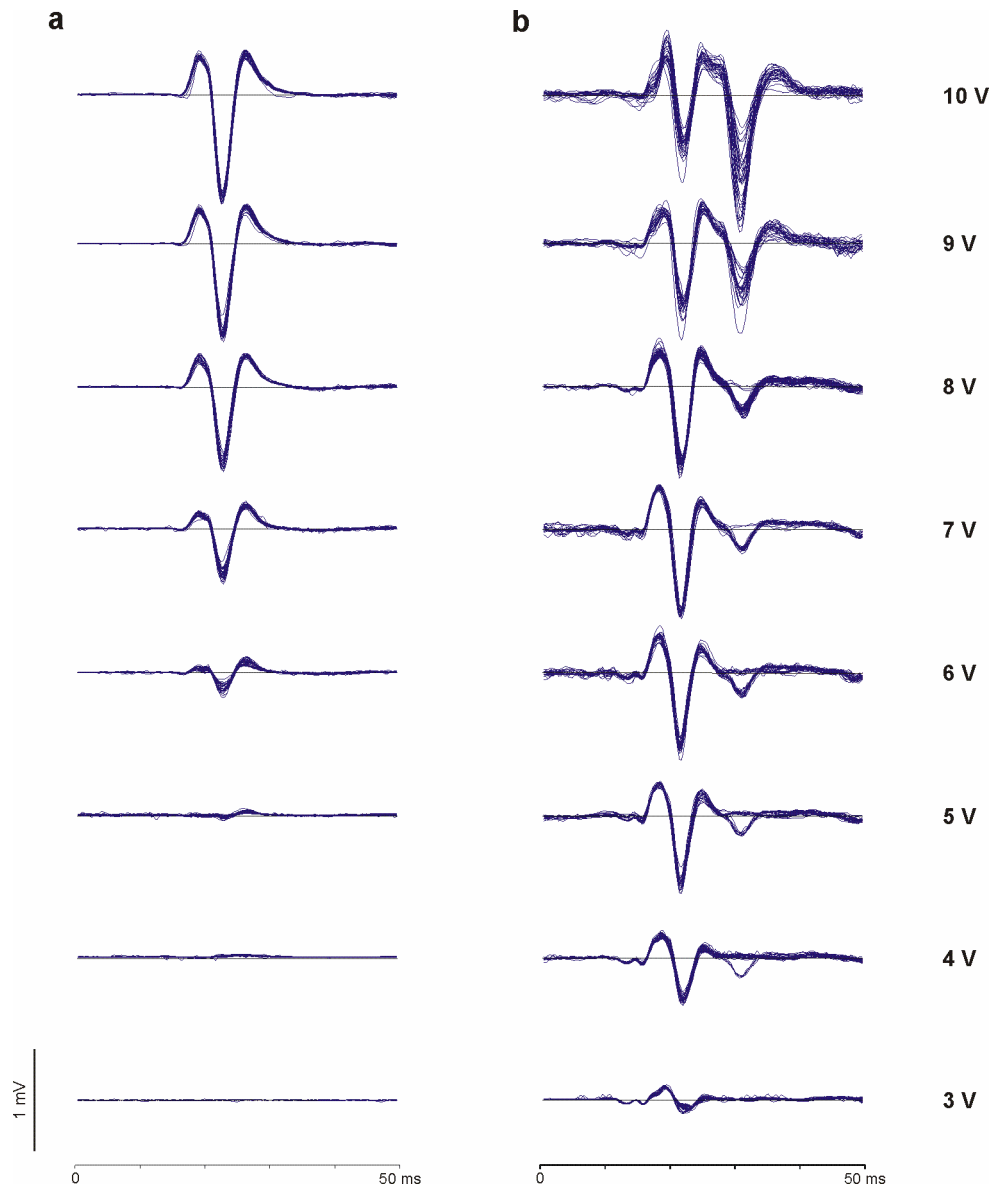


Figure 7. Tibialis anterior PRM reflexes elicited by graded SCS. **a** Simple PRM reflexes; epidural electrode combination 0+2-. **b** Complex PRM reflexes with additional delayed peaks were obtained when shifting the dipole in rostral direction (epidural electrode combination 1+3-). Inserted values are applied stimulus intensities. At each intensity, 27-34 consecutive responses are shown superimposed. Same scaling for all traces. All recordings derived from subject 1 during a single recording session.

To evaluate the effect of incremental intensities on the occurrence of delayed PRM reflex components, the number of complex PRM reflexes elicited by stimulation with constant parameters in relation to the total number of responses was analyzed. This value corresponds to the probability for eliciting complex PRM reflexes with given parameter settings. This probability was calculated for a given epidural electrode selection only if

complex PRM reflexes were elicited at all with given epidural electrode selections in response to incremental intensities. The probability for the occurrence of complex TA PRM reflexes increased with graded stimulation. At threshold intensity, $20 \pm 37\%$ of consecutively elicited CMAPs demonstrated late EMG components. Any increase of stimulus intensity above threshold significantly ($p < 0.05$) increased the number of complex PRM reflexes. At intensities of 2.5-3 times the response threshold, more than half of the PRM reflexes successively elicited were complex ($55 \pm 40\%$). At the maximum applied intensities corresponding to 4.5-5 times the threshold, all of the CMAPs demonstrated additional late peaks. The mean threshold required to evoke the standard TA CMAP calculated from this distinct data set was 3.7 ± 1.8 V. The corresponding value for the elicitation of the additional delayed peak amounted to 6.1 ± 2.1 V, being 1.9 ± 0.9 times the threshold of the simple response.

Figure 8 illustrates representative CMAP templates of simple and complex PRM reflexes elicited in TA with different active electrode combinations and stimulus intensities. Examples were all derived from a single subject and recording session to allow direct comparisons. Traces arranged from top to bottom show the simple triphasic template (Fig. 8a (i)) and complex CMAPs with similar initial potentials but different contributions of delayed peaks (Fig. 8a (ii)-(iv)). The CMAP widths of all complex responses were similarly extended, while weighted latencies increased considerably from (ii)-(iv), thereby reflecting the growing dominance of the late EMG components. In detail, weighted latencies of the CMAPs from (i)-(iv) amounted to 21.2 ± 0.2 ms; 21.8 ± 0.8 ms; 28.2 ± 2.0 ms; and 29.8 ± 0.8 ms, respectively.

The influence of incremental intensities on weighted latencies is presented in Fig. 8b. The examples from top to bottom differ in the dominance of the late PRM reflex component, as exemplified accordingly in Figs. 8a (i)-(iv). The graph in the top row (Fig. 8b (i)) is derived from a recording consistently featuring the simple triphasic CMAP shape without any build-up of late components with incremental intensities. In such case, mean weighted latencies of responses to graded stimulation demonstrated variations of less than 1 ms (Fig. 8b (i)) and were only slightly shifted from 20.3 ± 0.5 ms at the response threshold to 21.2 ± 0.3 ms at the highest applied intensity of 10 V. The stimulation conditions from (i) to (iv) were more and more effective in eliciting complex PRM reflexes. This was also manifested in the calculated mean weighted latencies. In case of complex responses with delayed peaks of small amplitudes as compared to the initial phases of the response (cf. Fig. 8a (ii)) weighted latencies were moderately shifted from 21.5 ± 0.7 ms at threshold to 25.4 ± 1.7 ms at 10 V (Fig. 8b (ii)). The increasing contribution of late components could also be seen from mean weighted latencies with incremental stimulus intensities; the respective values amounted to 22.4 ± 0.6 ms and 29.4 ± 1.7 ms (Fig. 8b (iii)), and 22.3 ± 1.2 ms and 30.4 ± 0.2 ms (Fig. 8b (iv)), evaluated at threshold intensity and at 10 V, respectively. Under the most favorable conditions for the elicitation of complex PRM reflexes (Fig. 8b (iv)), mean weighted latencies were delayed as soon as stimulation intensity was increased beyond threshold. The values rapidly approached a maximum and stayed constant thereafter.

Figure 8c illustrates the relation between the mean rectified amplitudes of the 2 dominant positive peaks of the PRM reflexes examined in Figs. 8a and 8b and the applied stimulus intensities. The first positive peak P_1 is representative for the early contributions to the PRM reflexes, while the second one, P_2 , describes the late components. The P_1 -recruitment curve displayed in Fig. 8c (i) started with a steady slope, until a plateau was reached. There was no elicitation of any late P_2 -peaks up to the maximum applied intensity. The threshold of late components including P_2 -peaks decreased in the examples according to the sequence of their presentation from (ii) to (iv) in Fig. 8c. At threshold and moderate stimulus intensities, the P_2 -recruitment curves did not increase systematically with graded stimulation, but had rather constant amplitudes. At approximately 2 times the threshold for the elicitation of late PRM reflex components, the P_2 -peaks rapidly increased in size. A concomitant effect was the decline of the P_1 -recruitment curves.

The maximum P_1 -peak amplitudes were limited to values of approximately 1 mV in the examples presented in Fig. 8. The maximum P_2 -peak, on the other hand, could attain amplitudes above 2 mV when being part of complex PRM reflexes with a dominating late EMG component, as shown in Fig. 8a (iv). Amplitude variations of the delayed potential peak were more distinct than of the early one, particularly when the P_2 -peak became the predominant CMAP deflection as can be seen from the standard deviations of the displayed recruitment curves. The standard deviations as percentage of the respective mean peak amplitudes amounted to 4.1% of P_1 in Fig. 8c (i) and 14.4% of P_2 in Fig. 8c (iv), both evaluated at 10 V.

The dominant positive peak P_2 of the complex responses was clearly delayed as compared to the positive peak P_1 of the simple PRM reflex. Neither of the peak latencies demonstrated a measurable jitter. The mean peak latency of P_1 derived from the simple PRM reflex in Fig. 8a (i) amounted to 22.6 ± 0.1 ms, the mean peak latency of P_2 evaluated for the example in Fig. 8a (iv) was 30.1 ± 0.2 ms.

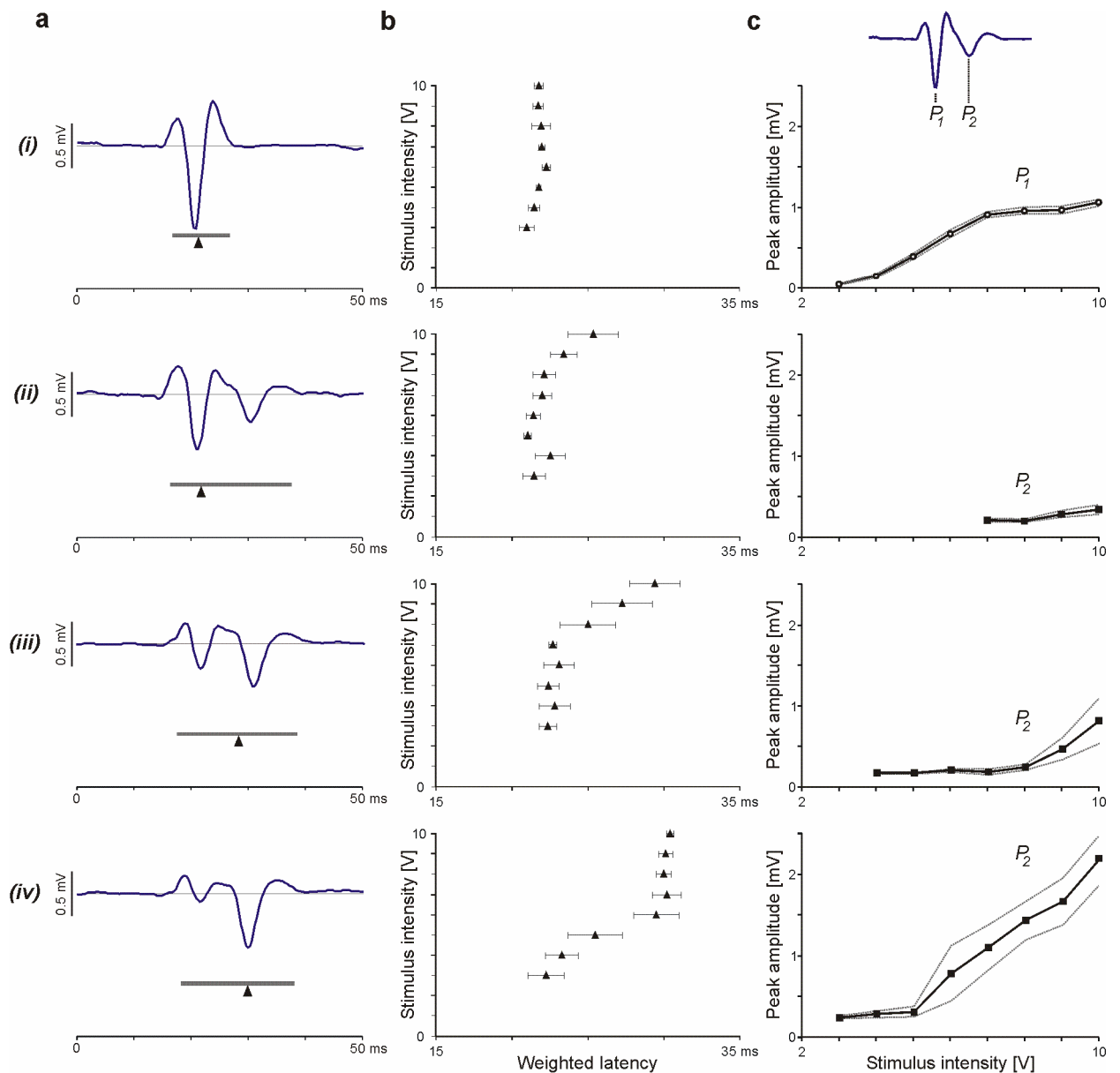


Figure 8. Tibialis anterior PRM reflexes without (i) and with (ii-iv) additional delayed peaks. **a** Characteristic templates with different contributions of late EMG components, each averaged from 22-34 consecutively elicited PRM reflexes. Bars illustrate CMAP widths (margins marking onset latencies and offsets) and arrowheads the corresponding weighted latencies. SCS parameters from top to bottom: 0+2-, 6 V; c+2-, 10 V; 1+3-, 10 V; and c+3-, 7 V. **b** Relation between graded SCS and mean weighted latencies (\pm SD) calculated from data sets exemplified in *a*. **c** Recruitment curves of the positive peaks P_1 and P_2 , prominent in the early and late parts of the PRM reflexes, respectively. Data derived from subject 1.

The various CMAP shapes given in Figs. 7b and 8a suggest that the complex, polyphasic PRM reflexes are in fact composite CMAPs with two distinct constituents. This implication could be readily verified by arithmetic subtraction of two amplitude-matched complex and simple CMAPs, chosen from the available data sets to have almost

congruent initial potential phases. Two variants of the simple triphasic CMAP were utilized for this procedure, shown as templates T_1 , T_2 in Fig. 9a. Subtraction of T_1 , T_2 from amplitude-matched polyphasic responses resulted in the 3 representative templates T_3 , T_4 , T_5 given in Fig. 9a. The common features of the latter, calculated templates were their resemblance to physiologic CMAPs, with a width prolonged by 6.5-11.5 ms compared to the respective value of the simple CMAP. In particular, the onset latencies of these contributions to the polyphasic CMAPs were shifted by 2-4 ms to larger values. The prominent positive peaks had latencies of 30.5-31 ms, values delayed by 8.5-9.5 ms compared to the positive peak of the T_1 , T_2 templates. The differences in the shapes of the templates T_3 - T_5 were mainly in their initial phases. By linear combinations of the standard templates T_1 or T_2 and one of the templates T_3 - T_5 polyphasic TA responses could be artificially constructed that were closely resembling to recorded complex PRM reflexes elicited with various stimulation parameters as well as in different subjects. Three examples of the reconstructed polyphasic CMAPs are given in Fig. 9b. The initial phases of the templates T_4 and T_5 accounted for the influences on the early peaks of the polyphasic responses, i.e., increase of the first negative and decrease of the first positive peaks due to the contributions of the delayed templates.

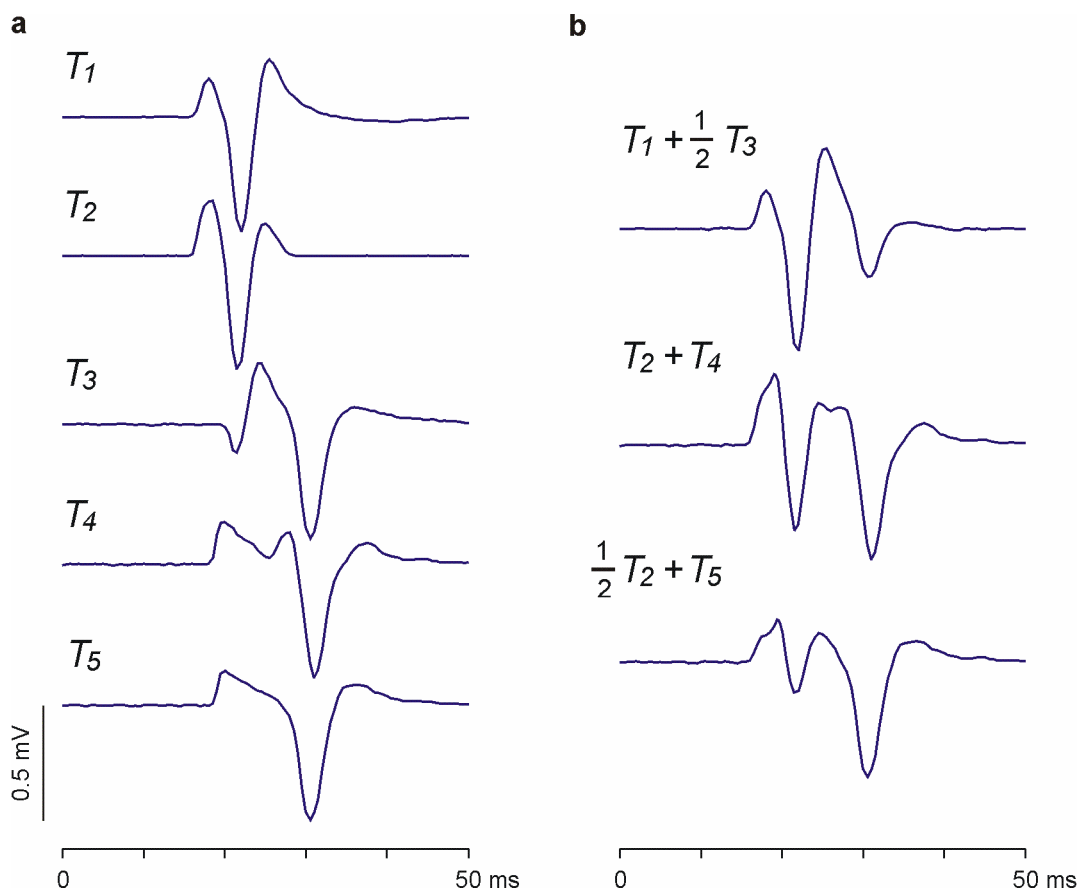


Figure 9. Calculated templates of early and delayed contributions to the complex PRM reflexes. **a** T_1 and T_2 are variants of the simple triphasic template; T_3 , T_4 , and T_5 are constructed by subtraction of EMG signals representing a simple and a complex CMAP, respectively. **b** Polyphasic CMAPs built by superposition (linear combination) of templates T_1 or T_2 with T_3 , T_4 or T_5 .

To summarize, the complex PRM reflex detected in TA in response to 2.1 Hz-SCS represents a new reflex type with some complex electrophysiological features. Comparable responses were not detected in the other muscle groups studied.

Discussion

The present study has shown that the human cord physiologically isolated from supraspinal input responds to low-rate stimulation (2.1 Hz – the lowest programmable stimulation frequency) of several lumbar and the first sacral posterior roots with monosynaptic, segmental PRM reflexes in multiple lower limb flexor and extensor muscles. These responses, recorded by surface EMG from Q, Ham, TA, and TS bilaterally, have short and constant onset latencies and simple bi- or triphasic CMAP waveforms that are characteristic for a given muscle group. Their appearance as a CMAP with invariant EMG features when elicited under constant stimulation conditions as well as their low stimulation thresholds suggest that the simple PRM reflexes result from the activation of large-diameter group Ia fibers within the posterior roots and the efficacy of the monosynaptic Ia input in discharging the spinal motoneurons (Mendell & Hennemann, 1971; Willis & Coggeshall, 1978). This strength of Ia excitation mainly depends on the number of Ia afferents projecting to the motoneurons and on inhibitory effects on the Ia terminals including post-activation depression – which is known to be reduced in spastic patients – and influences of other inhibitory circuits (Pierrot-Deseilligny & Burke, 2005a). As opposed to findings derived from H reflex studies in humans with intact nervous system, the PRM reflexes analyzed here revealed a high efficacy of motoneuron excitation by Ia afferents, most probably due to the absence of connectivity between segmental neural circuits and suprasegmental structures.

PRM reflexes elicited by 2.1 Hz-stimulation were of segmental nature. This independence of PRM reflexes from the activity of other muscles could be lost when higher rates of stimulation up to 22 Hz were applied, while stimulation site and intensity were kept constant. Under such conditions, the central state of excitability was increased, and the invariant segmental responses were replaced by periodically modulated PRM reflexes with reciprocal patterns in antagonistic muscles that the. Since the focus of the present study was to illustrate electrophysiological characteristics of the simplest type of PRM reflexes, the investigation of possible mechanisms underlying the modification of the spinal cord organization at higher rates of stimulation will be a subject for further studies.

More complex responses to 2.1 Hz-stimulation occurred in the ankle flexor muscle TA in about one third of the recordings. These responses had short onset latencies corresponding to those of the simple responses, but polyphasic CMAP shapes as well as considerably longer widths. Most probably, the additional delayed EMG components resulted from the concomitant inconsistent recruitment of group II muscle spindle afferents with disynaptic excitatory input to the TA motor pool (Pierrot-Deseilligny & Burke, 2005b).

Simple segmental posterior root-muscle reflexes elicited by SCS at 2.1 Hz

The simple PRM reflexes evoked under constant stimulation conditions at 2.1 Hz had invariant EMG features. Increasing the stimulus intensity up to 5 times the response threshold did not evoke delayed EMG components. The simple PRM reflexes were recognized in previous studies as segmental muscle twitches. They were the responses with the shortest onset latencies recorded from a given muscle following epidural lumbosacral cord stimulation (Murg et al., 2000; Jilge et al., 2004; Minassian et al., 2004; Dimitrijevic et al., 1980; Halter et al., 1983). When elicited at 2.1 Hz, they were suggested to be monosynaptic in nature (Jilge et al., 2004; Minassian et al., 2004). These findings were confirmed and further elucidated by the present study.

The onset latencies were constant for a given muscle group. They were longer in the distal muscles due to the longer efferent limb of the reflex arcs. Still, the response offsets of proximal and distal muscles were statistically the same, compensated by differences in the CMAP widths that could probably be attributed to the anatomical characteristics of the studied muscles and the placement of the EMG electrodes. The distinct short offsets of the simple PRM reflexes delimited short-latency excitatory compound events induced by SCS delivered at a low rate of 2.1 Hz.

The CMAP shapes of the simple PRM reflexes evoked under constant stimulation conditions demonstrated no variations. Changes of low-amplitude CMAPs evoked by graded stimulation were most likely due to spatial-temporal superpositions of the contributions of additionally recruited motor units. Large-amplitude responses were rather invariable in shape with further increase in stimulus intensities, and had characteristic CMAP waveforms that were characteristic for the different muscles, probably depending on the anatomy of the activated motor units with respect to the pair of surface recording electrodes. In particular, influencing factors could be the end plate distribution, the length of muscle fibers and the size of their population (Basmajian, 1979) as well as the mono/oligosynaptic reflexive recruitment of motor units.

The maximum attainable peak-to-peak amplitudes of the simple, monosynaptic PRM reflexes were larger in the thigh than in the lower leg muscles. This might be due to differences in the generation of CMAPs in muscles of diverse forms and sizes as well as to the biophysical conditions given by different distances between posterior roots/rootlets of different cord segments to stimulation sites estimated at L3/L4 segments (Group 2-position; Murg et al., 2000; Minassian et al., 2004, 2007b). The monosynaptic PRM reflexes with smallest amplitudes were elicited in TA, being 1.8 to 3.5 times smaller than in the other muscles. Anatomically, motoneurons of TA might have a low number of terminals from group Ia fibers, resulting in a smaller total monosynaptic excitatory postsynaptic potential (Hunt & Perl, 1960). A physiological explanation could be a low excitability of the monosynaptic reflex arc of TA due to tonic presynaptic inhibition (Schieppati, 1987; Willis, 2006). Moreover, TA motor nuclei may have a different segmental organization as compared to those of the other muscle groups considered. Further studies are required to test these hypotheses. The monosynaptic PRM reflexes of

Ham, TA, and TS systematically increased in magnitude with incremental intensity, until reaching a plateau. Unexpected results were found when analyzing the recruitment curves of Q PRM reflexes that declined at stimulus intensities above 2 times the threshold. This decline might be attributed to the recruitment of group Ib fibers in addition to Ia afferents or the concomitant activation of muscle spindle secondary afferents with inhibitory effects on extensor muscle groups (Pearson & Gordon, 2000). However, the fact that the suppression was only found in Q needs to be investigated in future studies.

No evidence for interactions between PRM reflexes recorded from antagonistic muscle groups of thigh and leg was found at 2.1 Hz-SCS, suggesting that interneurons involved in pre- or postsynaptic inhibition were inactive under such conditions. Alternatively, the absence of reciprocal inhibition could be due to mutual inhibition of Ia inhibitory interneurons of antagonistic motor cells. The synchronous monosynaptic excitation of antagonistic motor pools could be accompanied by simultaneous actions on Ia inhibitory interneuron populations that also receive their main segmental input from Ia afferents (Jankowska & Roberts, 1972). Furthermore, Renshaw cells are particularly effective in depressing activity of Ia inhibitory interneurons. In her review on interneurons, Jankowska (1992) elaborated that mutual inhibition of subpopulations of Ia inhibitory interneurons and inhibition by Renshaw cells can adjust the degree of co-activation of flexors and extensors.

In humans with intact nervous system, reciprocal Ia inhibition at the ankle can be assessed by amplitude changes of the soleus H reflex following a conditioning stimulus applied to the antagonistic common peroneal nerve. Thereby, conditioning-test intervals must range between 2-4 ms (Crone et al., 1987), which is in contrast to the synchronous activation of afferents of antagonists as in case of epidural SCS. Moreover, volitional co-activation of antagonistic leg muscles in healthy subjects has been shown to depress reciprocal inhibition (Nielsen et al., 1992).

Further evidence against the occurrence of reciprocal inhibition induced by 2.1 Hz-SCS can be deduced from the finding that segmental interactions were not even detected at threshold intensities (cf. Fig. 2, responses in dashed lines). This is in contrast to earlier studies on the soleus H reflex showing that the amount of reciprocal inhibition depends largely on the magnitude of the control reflex, reaching a maximum at amplitudes corresponding to 5-15% of that of the maximal direct motor response (Crone et al., 1985). However, the question as to whether the same mechanisms are active in the intact nervous system as in the human lumbar cord deprived of brain control needs to be addressed in future studies.

Posterior root-muscle reflexes elicited by SCS at higher rates

Without changing the site or strength of epidural SCS and only by increasing the stimulation frequency to 11-22 Hz, series of periodically modulated PRM reflexes with reciprocal interactions between antagonistic muscle groups could be elicited (cf. Figs. 5,

6). It was shown in earlier studies that cathode positions close to L3/L4 cord segments (Group 2-position) are particularly relevant for eliciting functional EMG activities in the lower limbs at frequencies up to 50 Hz (Minassian et al., 2007b). Therefore, responses of Q (L2-L4 segmental innervation) and its antagonist will be focused on, rather than further elucidating the rather well-established reciprocal Ia inhibition at the ankle (Pierrot-Deseilligny & Burke, 2005c).

The transition from invariant PRM reflexes at 2.1 Hz to ones featuring simple periodic patterns at higher frequencies hints at the activity of interneurons. The proposition is that the central state of excitability was increased by the higher rate of the afferent input, most probably by temporal summation of interneuronal activity. Putative circuits concomitantly activated in addition to segmental PRM reflex pathways could include Ia inhibitory interneurons that transfer information from primary muscle spindle afferents more effectively than other interneurons (Jankowska, 1992) and Renshaw cells.

The crucial role of an increased level excitability for the operation of interneurons was shown p.e. in the spinal cat by Jankowska and Riddell (1995) who applied glutamate ejections in order to induce a tonic discharge of a single interneuron. Sherrington described reciprocal inhibition when superimposed on the exaggerated tonus in 'decerbrate rigidity' and in various hindlimb reflexes (reviewed by Burke 2007). Reciprocal inhibition between antagonistic muscle groups was also shown to be present during increased levels of spasticity when eliciting phasic knee, Ham, and Achilles tendon jerks in spastic posttraumatic SCI subjects (Dimitrijevic & Nathan, 1967). The human lumbar cord deprived of suprasegmental influence will presumably respond with reciprocal inhibition only when the central state of excitability is increased as achieved here by the higher stimulation rates. Preliminary studies also suggested that the modification of spinal reflex activity is related to a specific range of stimulation frequencies (Persy et al., 2005). The finding that reciprocal inhibition depends on a range of stimulation frequencies can be explained by the fact that Ia inhibitory interneurons require some summation of excitatory influences (Eccles et al., 1956). In the absence of spatial summation, i.e., without the convergence of supraspinal pathways on Ia inhibitory interneurons, their excitation depends most probably on temporal summation at higher stimulation rates. Further studies of the model of the human lumbar cord chronically deprived of brain influence are required to test the hypothesis that spinal interneurons are 'rate-sensitive' to afferent input.

Jankowska (1992) stressed that inhibitory Ia interneurons respond with single spikes to a synchronous Ia afferent volley. Moreover, she pointed out that Ia inhibitory interneurons may also discharge in bursts following stimulation of specific afferents, p.e. flexor reflex afferents, in the non-anesthetized high decerebrate cat. Hence, the efficacy of Ia afferents to activate Ia inhibitory interneurons may not only depend on the level of the lumbar network-excitability, but probably also on the synchronicity of the excitatory input and the involved types of afferents.

Complex posterior root-muscle reflexes elicited by SCS at 2.1 Hz

The complex PRM reflexes elicited in TA at 2.1 Hz-SCS had polyphasic CMAP shapes as opposed to the bi- or triphasic ones of the simple responses. Their onset latencies corresponded to a monosynaptic reflex, but their weighted latencies as well as their offsets were considerably delayed, due to a new contribution to the EMG signal in addition to the short-latency compound recruitment of motor units. The new contribution to the EMG signal was most probably made up of the activity of a motor unit population of TA that was recruited with some delay with respect to the monosynaptic latency, due to an increased central latency. In segmental reflexes, the central delay is increased by excitatory interneurons interposed between the directly, electrically stimulated afferents and the synaptically recruited motoneurons (Renshaw, 1940). Several observations have been shown in the present work allowing for the assumption that the polyphasic TA responses consisted of separate modes, with the motoneurons being fired in at least two groups due to a monosynaptic and a delayed, oligosynaptic recruitment.

In a dorsal root the whole range of afferent fibers is present, exhibiting diameters from 1 to 20 μm with various peripheral origins (Lloyd, 1943b). Fibers of different sensory modalities are admixed in a dorsal root and present elements of different reflexes (Lloyd, 1944). Externally applied pulses of increasing intensity excite fibers in order of decreasing axonal diameter (Rattay et al., 2000; Struijk et al., 1993). It was shown to be difficult with dorsal root stimulation (Lloyd, 1943a), and with stimulation of afferent nerves from muscles (Lloyd, 1943b), to obtain a pure group I volley in cats. With all but the weakest stimuli, group II fibers were concomitantly activated in these experimental studies. A similar situation was found in humans with intact nervous system by Magladery and colleagues (1951) when stimulating the posterior tibial nerve and recording the afferent impulses in the dorsal roots, the reflex outflow through anterior roots, as well as slow internuncial potentials by needle electrodes placed within the spinal theca. It was concluded that the degree to which fiber thresholds in the group I and II fibers overlapped was even greater than would have been expected from animal experiments (Magladery et al., 1951).

There were characteristic differences in the thresholds and the recruitment of the monosynaptic and of the delayed CMAP components of the complex PRM reflexes. Statistically, the delayed recruitment of motoneurons had higher thresholds than the monosynaptic recruitment, both contributing to a complex PRM reflex. The monosynaptic simple PRM reflex of TA had a systematic stimulus-response relation, with increasing magnitudes when graded stimulation was applied, until a plateau was reached. On the other hand, the late positive peak of the complex PRM reflexes initially had rather small and constant amplitudes with incremental stimulus intensity, with an abrupt rise at about twice its threshold intensity.

The probability for the elicitation of complex PRM reflexes was higher, when monopolar or bipolar stimulation with largely spaced active lead electrodes was employed. Both stimulation modes have a broader effective range than narrowly spaced epidural electrode

combinations. At the same time, their stimulation effect is stronger at a given distance from the stimulating cathode. Furthermore, stimulation sites corresponding to a Group 2-position – estimated with its center at L3/L4 segmental levels and a caudal range up to the L5 segmental levels (Minassian et al., 2007b) – most effectively evoked complex PRM reflexes. Employing the most caudal lead electrodes as cathode within the Group 2 category additionally increased the probability of complex PRM reflex elicitation. Such stimulation sites must be close to the continuum of rootlets entering the spinal cord at the levels L4 and L5, both associated with the TA muscle. At the same time the stimulation of posterior roots/rootlets is favoured by monopolar or bipolar stimulation employing largely spaced electrodes (Holsheimer et al., 1995; Rattay, 1987).

Another typical feature of the delayed components of the complex PRM reflexes were their profound amplitude variations, a characteristic similarly found in multineuron-arc reflexes (Lloyd, 1943a). Two different types of fluctuation could be distinguished. First, at threshold and moderate stimulus intensities, the delayed response components were either present with rather constant amplitudes, or were completely absent at all. This observation hints on some stochastic effects determining the ‘opening’ of the central pathways mediating the delayed CMAP components. These effects were at the same time stimulus intensity-dependent, since the probability of occurrence of a delayed response increased with incremental stimulation. At higher stimulus intensities, when eventually every single stimulus yielded complex PRM reflexes, the central reflex pathways transmitting the delayed response were effectively ‘opened’, but with the late potentials of successively elicited responses demonstrating considerable amplitude variations. The different variations of early and late components of the polyphasic CMAPs generated by the same stimulus pulse is particularly revealing in that it suggests the activation of different reflex pathways.

The recruitment of monosynaptic and more complex reflex responses to graded dorsal root stimulation was studied in detail in the segmental spinal reflex by Lloyd (1943a). It was found that as the size of dorsal root volleys was stepwise increased, the magnitude of the elicited monosynaptic reflex rapidly increased. At 50% of the maximum afferent volley, the group I reflex reached 90-95% of its maximum. Some group II reflex discharge pertaining to the more complex reflex arcs were evoked as soon as a group I discharge was identifiable. However, intense development of the delayed reflex occurred only as the dorsal root volley was increased beyond 50% of its maximal size. The reflex magnitude became half of its maximum after the dorsal root volley was 70-85% maximal. The delayed dorsal root-ventral root discharge increased rapidly thereafter. There are thus evident similarities between the recruitment of group II dorsal root-ventral root reflexes described in experimental studies (Lloyd, 1943a) with the recruitment of the delayed components of the polyphasic PRM reflexes of TA, respectively.

The electrophysiological properties of the early and delayed phases of the complex PRM reflexes led us to the assumption that the latter are composite CMAPs constituting of at least two independent contributions. These two contributions could be identified by

calculating the difference in the EMG signals of simple and complex PRM reflexes. Such calculations are valid, since the principle of EMG signal generation is by simple superposition of individual components (Basmajian, 1979). In this fashion, the polyphasic CMAP of TA could be decomposed in two contributions (cf. Fig. 9). One had all features of the simple monosynaptic PRM reflex. The other one resembled a CMAP with delayed onset and extended duration. Different shapes of the calculated delayed CMAP were found, mainly with different initial phases of the waveform. The assumed monosynaptic and delayed contributions to the polyphasic CMAPs overlapped in time. Therefore the onset, as well as the initial phases of the calculated delayed CMAP is most probably obscured by contributions of the monosynaptic waveform. The exact identification of the onset latency of the calculated delayed CMAP is thus not possible. However, the onset latencies and the latencies of their dominant positive peaks allow a reasonable estimation. It can be assumed that the onset latency of the delayed contribution to the polyphasic composite CMAP is prolonged by some milliseconds, within the range of 2-9.5 ms, with respect to the monosynaptic onset latency. The minimum reflex pathway transmitting the delayed response component contained at least one more neuron in series than did the monosynaptic reflex pathway.

All facts considered, it can be assumed that the complex PRM reflexes indicate the irregular recruitment of group II muscle spindle fibers in addition to group Ia afferents. The most direct effective linkage of group II pathways is disynaptic via group II interneurons that are located particularly in the midlumbar segments (Pierrot-Deseilligny & Burke, 2005b). Similarly to the present results, the interposed interneurons as well as the slow down of the conduction velocity in secondary spindle afferents within the spinal cord were shown to lead to central delays of peripheral nerve-induced group II excitation of 4.9-6.7 ms (Marque et al., 2005), values similar to those derived here.

Effects of Golgi Ib afferents, also of large diameter, can be excluded since in the presently analyzed non-functional reflex activity they would have an inhibitory, and not an excitatory effect on TA motoneurons. Furthermore, the large amplitudes of the late components of the polyphasic PRM reflexes can readily exclude peripheral explanations of their generation. Phenomena in the muscle, like satellite potentials or potentials generated distant from the recording site due to termination of electrical activity at the muscle-tendon junction (Lateva & McGill, 1999), can be thus ruled out. The large attainable magnitudes of the late response components can also exclude heteronymous facilitation of TA motoneurons as a potential explanation, since heteronymous volleys produce smaller excitatory postsynaptic potentials than homonymous volleys (Hunt & Perl, 1960).

The oligosynaptic reflexes were confined to TA, a physiological flexor muscle, and had large attainable magnitudes. The high excitability of the oligosynaptic reflex hints at the physiological relevance of the corresponding reflex pathway directed to a flexor muscle. These facts together with the association of group II afferents with flexor reflexes implies, that the revealed oligosynaptic reflex arc might be part of the flexor reflex pathways.

Previously, polysynaptic PRM reflexes were described that were part of patterned EMG activities, elicited by epidural lumbar cord stimulation in complete spinal cord injured subjects (Minassian et al., 2001). Stimulation at 25–50 Hz and 6–10 V was shown to elicit locomotor-like EMG patterns, characterized by rhythmic activity with alteration between flexor and extensor muscles in the paralyzed lower limbs (Dimitrijevic et al., 1998; Minassian et al., 2004). The prolonged latency PRM reflexes were found in TA when being part of burst activities of the stimulation-induced locomotor-like movements (Minassian et al., 2004, 2007b). Their onset latencies were delayed by about 10 ms as compared to the monosynaptic PRM reflexes elicited at 2.1 Hz (Minassian et al., 2004). Other investigators have detected polysynaptic TA responses during spinal cord stimulation-induced locomotor-like activity in chronic paraplegic persons elicited when utilizing epidural needle electrodes (Gerasimenko et al., 2001).

However, the present results suggest that the locomotor-related, polysynaptic PRM reflexes elicited in TA are not related to the oligosynaptic PRM reflex contributions as described here. The oligosynaptic group II reflex components of the composite TA PRM reflexes never occurred without the monosynaptic group I reflex component. On the other hand, the occurrence of the locomotor-related, polysynaptic PRM reflexes was associated with the concomitant full suppression of the monosynaptic PRM reflex. Furthermore, the latency of the dominant positive peak of the CMAPs associated with locomotor-related PRM reflexes (Minassian et al., 2004) was even more delayed than the one of the oligosynaptic PRM reflex component detected at low-rate SCS as described here.

Conclusions

The simple PRM reflexes elicited in the lower extremities by epidural SCS at 2.1 Hz provide evidence for the monosynaptic activation of spinal motor cells via Ia afferents. The PRM reflexes successively elicited under such conditions occurred independently from preceding events as well as from responses simultaneously elicited in other muscles. The simple, monosynaptic PRM reflexes were previously suggested to be the functional equivalent of the ‘classical’ H reflex (Minassian et al., 2004, 2007a, 2007b). Both are initiated in Ia sensory axons, either within the posterior roots or in the periphery.

The complex, polyphasic PRM reflexes detected in TA suggest that low-rate posterior root stimulation may, partially depending on the applied intensity, additionally excite group II fibers with disynaptic connections to spinal motor cells. In the attempt to relate these complex PRM reflexes to more classically defined reflexes, no equivalents elicited in TA from periphery were detectable (Burke et al., 1989; Hallett et al., 1994).

At higher stimulation rates up to 22 Hz, the independent segmental responses were replaced by periodically modulated PRM reflexes hinting at the concomitant activation of lumbar cord interneurons.

The electrophysiological characterization of the simple PRM reflexes will be essential for understanding the reorganization of reflex systems occurring during sustained SCS. Conditioned polysynaptic PRM reflexes may be revealing in understanding the oscillatory states of human lumbar spinal cord circuits, particularly when the lumbar locomotor pattern generator is activated by SCS (Dimitrijevic et al., 1998; Jilge et al., 2004; Minassian et al., 2004, 2007b). Further studies on the initiation of segmental interactions by SCS may enlighten the sensory-motor mechanisms involved in the configuration of human lumbar networks at higher frequencies that may even lead to functional motor outputs.

Simulation of reciprocal spinal segmental circuitries – A biologically realistic mathematical model

Summary

Non-patterned stimulation of the lumbar spinal cord delivered at a low rate (2.1 Hz) can elicit independent monosynaptic PRM reflexes in multiple lower limb muscles simultaneously. By increasing the stimulation frequency to 11-22 Hz, successive responses were shown to be modified with periodic patterns that suggested the influence of interneuronal circuits. The alternation of large and small responses in spite of constant stimulation as well as the predominantly anti-phase relation of these responses in the antagonistic thigh muscles hinted on the influence of interneuronal circuits. It was suggested that the generation of simple periodic patterns was due to an increased central state of excitability induced by the higher rates of stimulation and to temporal summation of various interneuronal activities. Specifically, Ia inhibitory interneurons as well as Renshaw cells were assumed to be reasonable candidates involved in modifying the motor outputs.

The aim of the present modeling study was to test whether a relatively simple network deprived of supraspinal influences but fed by tonic external input at 16 Hz can produce simple periodic patterns of motoneuron pool firing. The network consisted of monosynaptic reflex circuits of two motor pools, completed by recurrent and reciprocal inhibition. Interneuronal populations of the same type were connected by mutual inhibition. Parts of the complete network were explored for their role in the generation of the motor outputs. The widely used *Leaky Integrate-and-Fire* model was modified to account for specific, biologically-realistic time courses of postsynaptic potentials.

Given an ‘appropriate stimulation code’ similar to that used in the neurophysiological study (i.e., 16 Hz, stimulus intensities of 1-1.5 times the PRM reflex threshold) the model network produced simple periodic patterns expressed as alternating numbers of motoneurons firing within the pools. Particularly, it could be shown that the robust generation of the periodic outputs mainly depended on the activity of Renshaw cells and less on that of Ia inhibitory interneurons. Asymmetric network models including two antagonistic circuits with different numbers of connectivities between neuron populations most efficiently produced anti-phase alternations of the responses elicited in the two motor pools. In the complete model network including both Renshaw cell and Ia interneuron populations, the capacity to produce stable periodic patterns was lost.

Overall, it can be concluded that a relatively simple model network may re-produce rhythmic motor outputs that closely resemble those derived from the neurophysiological study described within this thesis. The specific value of the biologically realistic model developed here lies in its capacity to closely investigate spinal cord motor systems in humans by assessing the functional roles of particular cell populations in modulating the motor output.

Introduction and Background

Posterior root-muscle reflexes and lumbar spinal locomotor circuits in humans

Dimitrijevic and coworkers (1998) demonstrated that non-patterned epidural stimulation of the posterior lumbar cord can induce patterned, locomotor-like lower limb activity in subjects with complete, long-standing spinal cord injury (SCI). Locomotor-like activity was only induced within a certain range of stimulation parameters (i.e., cathode location close to upper lumbar cord segments, stimulus strength 5-10 V, stimulation frequency 25-60 Hz). Subsequent studies (Minassian et al., 2004; 2007) showed that the rhythmic muscle activities were produced by patterned, periodic modulations of successive posterior root-muscle (PRM) reflexes, during of the constant stimulation conditions (Figure 10*a, b*). In particular, the rhythmically contracting muscles responded with alternation between two phases: (i) Phases of successively elicited PRM reflexes featuring characteristically modulated amplitudes, thus forming the spindle-like shape of an electromyographic (EMG) burst; and (ii) phases of PRM reflex suppression in-between the bursts. A complete cycle (i.e., a burst and a phase of PRM reflex suppression) had periods of 0.8-1.9 s. The timing and the magnitudes of the EMG bursts and the distribution of activity among the thigh and lower leg flexor and extensor muscles were appropriate to produce lower limb movements that resembled stepping in the supine individuals.

From these studies it could be concluded that the generation of rhythmic lower limb muscle activity in humans does not require connectivity between the brain and the spinal cord. Locomotor-like activity can be produced by epidural spinal cord stimulation (SCS)-

induced repetitive PRM reflexes, i.e., by chains of ‘simple’ spinal reflexes, that integrate the operation of human lumbar cord interneuronal circuits.

PRM reflexes evoked in series with distinct repetition rates co-activate functional circuits within the lumbar spinal cord, which do not subserve a pure reflex function (Brown, 1911; Grillner, 1985). On the basis of the exerted actions, these circuits were recognized as locomotor rhythm and pattern generating networks – the ‘human lumbar locomotor pattern generator’ (LLPG) (Minassian et al., 2004; Kern et al., 2005). The network action is directly reflected in the locomotor-like amplitude modulations of successive PRM reflexes and the delay of PRM reflexes during flexion phases of rhythmic activity (Minassian et al., 2004).

The activation of the human lumbar locomotor circuits was hypothesized to base on the direct electrical stimulation of posterior root afferents and the indirect, trans-synaptic activation of spinal circuitries via the afferent projections. Frequency-dependent summation processes of the generated inputs would then become effective to set the functional circuitry to operation that are otherwise not active (Jilge et al., 2004; Minassian et al., 2004).

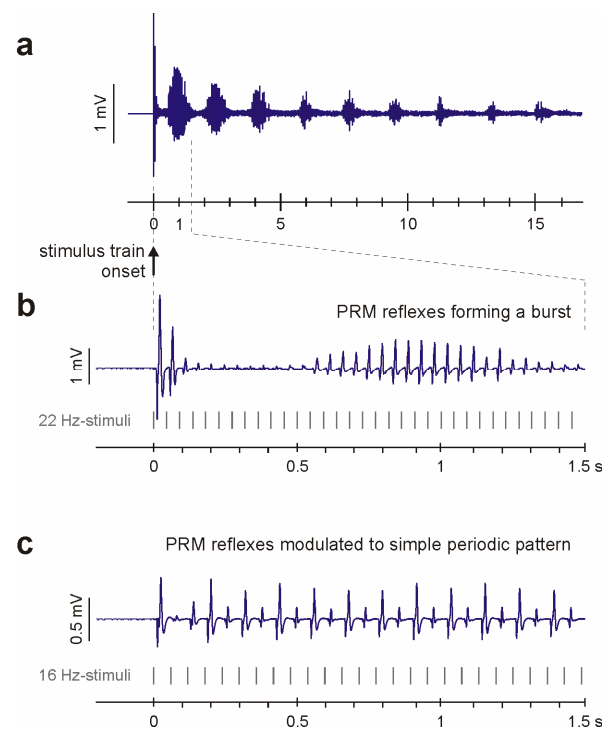


Figure 10. **a** Rhythmic EMG activity elicited in quadriceps by sustained epidural lumbar cord stimulation at 22 Hz-SCS in a complete SCI individual. **b** The initial portion of the same EMG signal as in *a* in extended time scale shows the first PRM reflex together with the PRM reflexes elicited by the immediately following stimuli of the train. The latter responses were modulated to the spindle-like shape of an EMG burst. **c** Simple periodic pattern as derived from the electrophysiological study described above elicited with 16-Hz stimulation, displayed for direct comparison.

To induce locomotor-like lower limb activity, the stimulation intensity had to be within the range of 1.2-3.3 times the threshold of PRM reflex elicitation. At such intensities, stimulation is predominantly confined to large-diameter posterior root afferents of group I, and is extended to group II afferents at the upper range of intensities. There are supportive animal experiments demonstrating direct access of various group I and II afferent pathways to locomotor central pattern generators (CPGs) in spinalized or decerebrated cats (Hultborn et al., 1998; Rybak et al., 2006). It is plausible to assume that in humans the epidurally stimulated posterior root fibers, that convey feedback information from periphery, have also access to functional locomotor circuits via axonal collaterals. Concerning the relatively simple repetitive stimulation provided by SCS, there is an agreement that such tonic signals delivered at constant frequencies can activate locomotor CPGs (Pearson & Gordon, 2000).

A general schematic for the spinal CPG generating rhythmic alternating activity of flexor and extensor motoneurons during locomotion was proposed by Brown (1914). The so-called 'half-center' model bases on an intrinsic spinal organization of interneuron populations with strong mutual inhibition between each other. Each CPG contains two groups of excitatory interneurons (i.e., the half-centers) that control the activity of flexor and extensor motoneurons, respectively. Mutual inhibitory connections between the half-centers ensure that only one center can be active at a time. Phase switching occurs when the reduction in the excitability of one half-center falls below a critical value and the opposing center is released from inhibition (McCrea & Rybak, 2008). Thus, in this model the alternating activity in flexor and extensor motoneurons directly results from the alternating activities in the two populations of interneurons. Since then, other CPG models have been suggested that allowed e.g. for a variety of motoneuron recruitment patterns (multiple, coupled, unit burst generators – UBGs; Grillner et al., 1981) or that separated the tasks of rhythm generation and motoneuron activation during locomotion (CPGs with two-level architecture, Rybak et al., 2006).

Posterior root-muscle reflexes modulated with simple periodic patterns

The rhythmic motor outputs to 11-22 Hz SCS featuring simple periodic patterns (Figure 10c) as described from the neurophysiological study were different from the locomotor-like ones in several aspects. The oscillation period of the simple periodic patterns covered only two successive responses. The resulting fast oscillation periods of 90-182 ms along with the low frequency of synchronized motoneuron firing (i.e., absence of any continuous muscle contraction) did not result in the generation of muscle force, torques at joints or any functional movement.

Yet, the simple periodic patterns clearly reflected the activity and the influence of some spinal circuitries capable of modulating the PRM reflex output in a rhythmic fashion as well as of providing for interconnections between antagonists. Moderate stimulation intensities of 1-1.5 times the threshold were most effective to result in out-of-phase

attenuation of quadriceps (Q) and hamstrings (Ham) PRM reflex series. Additionally, the effective frequency range was below the one producing locomotor-like patterns. The moderate stimulus intensities confined the electrical stimulation to large-diameter group I afferents and the lower frequency of afferent volleys generated would play a role in the temporal summation effects and in the trans-synaptic activation of interneurons. Both facts together clearly suggest that the simple periodic patterns were not produced by the LLPG, but either by a subset of it or spinal circuits ‘outside’ of the LLPG (Hultborn et al., 1998).

Rhythmicity in a neuronal network does not solely depend on the cellular properties of specialized, CPG-related neurons, like spontaneous bursting (*endogenous bursters*) or plateau potentials. A simple network can generate rhythmicity if it includes some time-dependent processes that enhance or reduce activity within some of the neurons, depending on the patterns of interconnections between the network neurons. ‘Building blocks’ for such connections include, amongst others, reciprocal inhibition and recurrent inhibition (Pearson & Gordon, 2000).

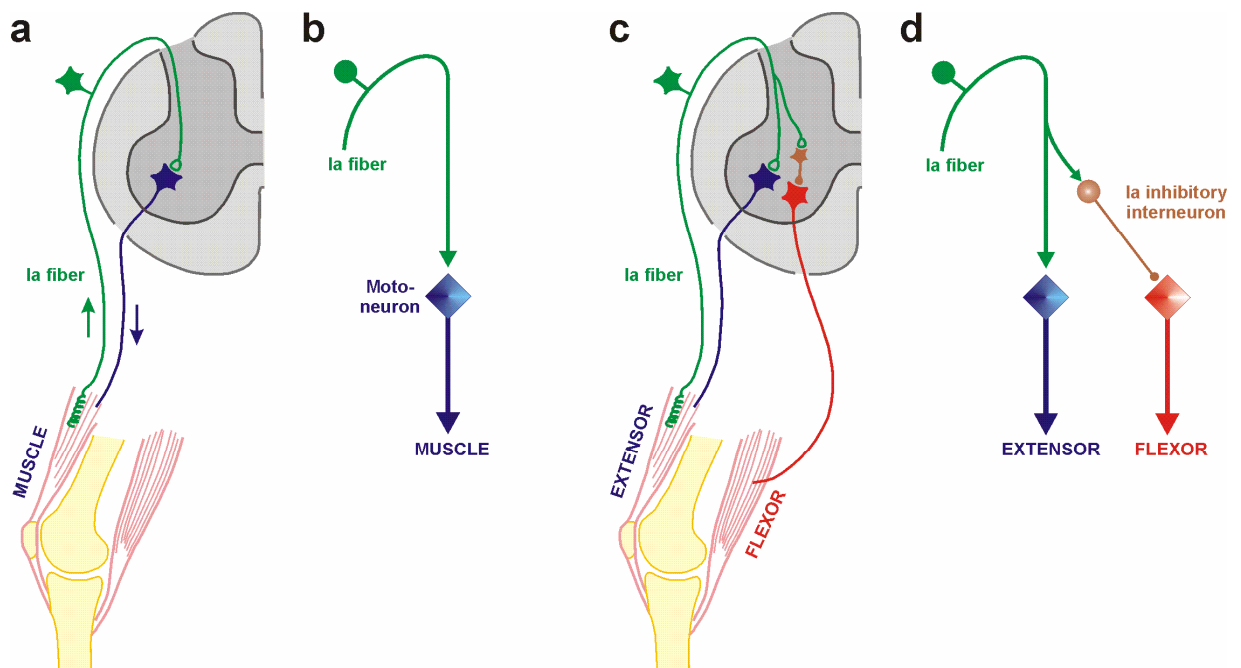


Figure 11. Spinal circuits of monosynaptic reflex arc and reciprocal inhibition. **a** Anatomical drawing of the monosynaptic two-neuron reflex arc with group Ia muscle spindle afferents (green) and extensor motoneurons (blue) along with **b**, a simplified schematic diagram of the same neural circuitry. In **c** and **d** the illustrations are extended to include the disynaptic inhibitory circuit of antagonist flexor motoneurons (red). Ia inhibitory interneurons are displayed in brown color. Note that anatomically, the extensor and flexor motoneurons can be at different spinal segmental levels.

The simplest neural systems providing reciprocal inhibition of antagonistic motoneuron pools are formed by disynaptic inhibitory circuits, mediated by Ia inhibitory interneurons (Jankowska, 1992). In animal vertebrates and humans with intact nervous system, Ia inhibitory interneurons are used to adjust the excitability of motoneurons during monosynaptic stretch reflexes and other spinal reflexes, as well as during a variety of movements including locomotion. Within the disynaptic inhibitory circuits, Ia inhibitory interneurons are monosynaptically activated by Ia muscle spindle afferents and project directly to motoneurons of antagonistic muscles (Figure 11c, d). Ia inhibitory interneurons are more effectively activated by group Ia afferents than any other type of interneurons (Jankowska, 1992). Thus, it can be assumed that Ia inhibitory interneurons are of the first interneuronal populations to be trans-synaptically activated by the group Ia afferent input produced by SCS. Hence, the involvement of Ia inhibitory interneurons within the generated patterns can be readily assumed.

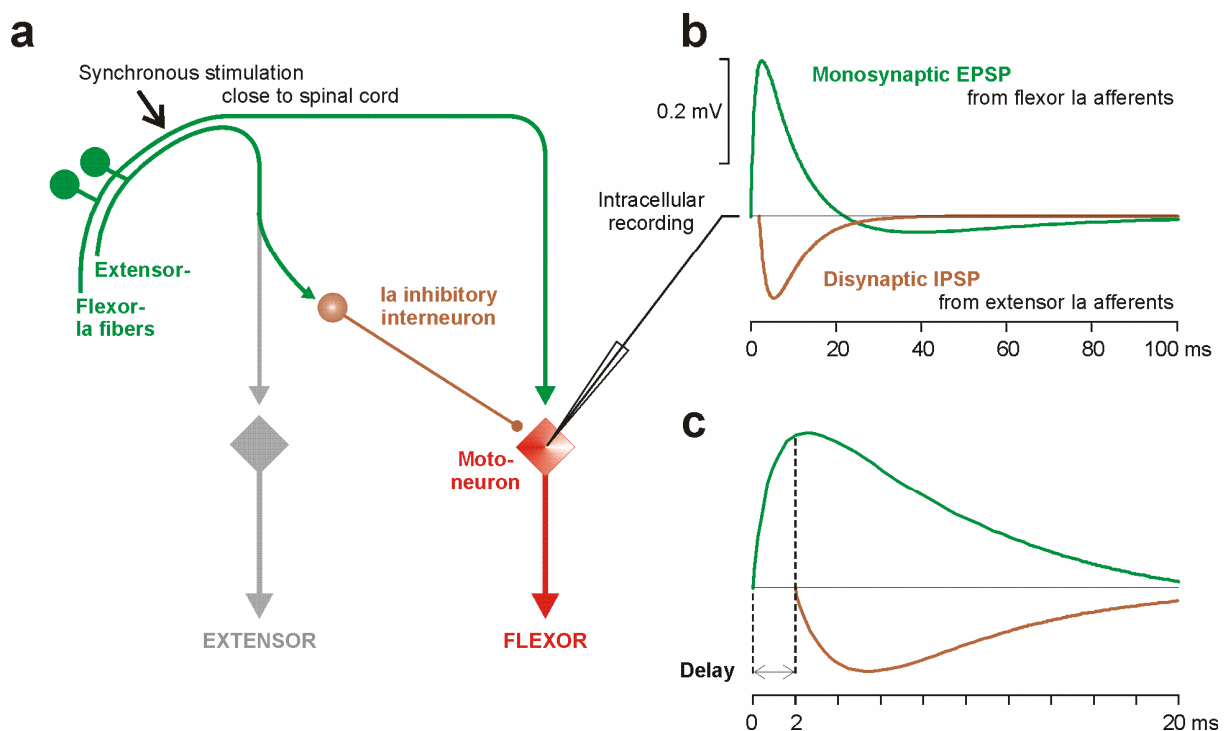


Figure 12. Convergence of a monosynaptic excitatory postsynaptic potential (EPSP) and a disynaptic inhibitory postsynaptic potential (IPSP), both produced by the same stimulus (but within different posterior root afferent populations), upon a motoneuron. **a** Diagram of the involved neural circuitry. **b** Schematic sketch illustrating the time course of EPSPs and IPSPs (for details see *Material and Methods*). **c** shows the initial portion of the EPSP and the IPSP, highlighting the relative delay of the latter due to the additional interneuron within the conducting neural pathway.

Ia interneurons respond with single spikes to synchronous Ia afferent volleys (Jankowska, 1992). The produced inhibitory postsynaptic potentials (IPSPs) upon the motoneurons are rather short-lasting and their main effect decays within the first milliseconds (see *Material and Methods*). Multisegmental afferent volleys evoked by a single pulse of SCS and entering the spinal cord simultaneously can elicit monosynaptic Ia excitatory postsynaptic potentials (EPSPs) as well as disynaptic IPSPs (via Ia inhibitory pathways) in the same motoneurons (Figure 12).

The rise time of the EPSP is assumed to be sufficiently long that the discharge of the last recruited motoneurons evoked by the monosynaptic input can be influenced by the arrival of a disynaptic IPSP (Pierrot-Deseilligny & Burke, 2005c). From experimental work this delay was found to be within the range of 0.5-1.0 ms relative to the beginning of the monosynaptic EPSP due to the intercalated interneuron and can be assumed to be about 2 ms in humans (Crone & Nielsen, 1994).

In human studies, the disynaptic inhibitory pathway from muscle spindle Ia afferents to motoneurons of the antagonist muscle is classically demonstrated as a short-latency depression of the Hoffmann reflex in soleus (or triceps surae) following a conditioning stimulation of the antagonist nerve, i.e., the deep peroneal nerve (Pierrot-Deseilligny & Burke, 2005c). The characteristic time course of the inhibitory effect has an onset at conditioning-test intervals of +1 ms, and reaches a maximum 1-2 ms later (both values consider a difference of -1 ms in conduction times to the spinal cord, since the conditioning stimulus is delivered about 6 cm more distally than the test). The time course has furthermore a brief overall duration of approximately 3 ms (Crone et al., 1987).

In contrast to the conditioning-test paradigms of stimulating nerves from antagonistic muscles with some interstimulus delays, the same antagonistic nerve fibers are activated by SCS within the posterior roots synchronously. Due to delay of the disynaptic pathway with respect to the direct monosynaptic one, it can be assumed that reciprocal inhibition of antagonistic motoneuron pools might only reduce the size of PRM reflexes to some degree. However, a considerable suppression by this mechanism is unlikely.

Considering the short duration (approximately 3 ms) of the effect exerted by a synchronous Ia inhibitory interneuron discharge (Crone et al., 1987), temporal summation might not enhance this effect since PRM reflexes within the simple periodic patterns (elicited at frequencies of 11-22 Hz) occurred at intervals between 45 ms and 91 ms. Consequently, the circuitry involved in the simple periodic patterns must include neurons that produce synaptic events with much longer durations, such that activity of one stimulus can affect activities of the following one delivered after 45-91 ms.

Renshaw cells are reasonable candidates for a circuitry involved in the simple periodic patterns, since a brief activation of alpha-motoneurons elicits a high-frequency discharge of Renshaw cells lasting for tens of milliseconds (e.g. Eccles et al., 1961). Renshaw cells are the interneurons that mediate the so-called recurrent inhibition. They are excited by

recurrent collaterals from the motoneurons themselves and in turn inhibit the motoneurons within the same and agonist motor pools (Figure 13).

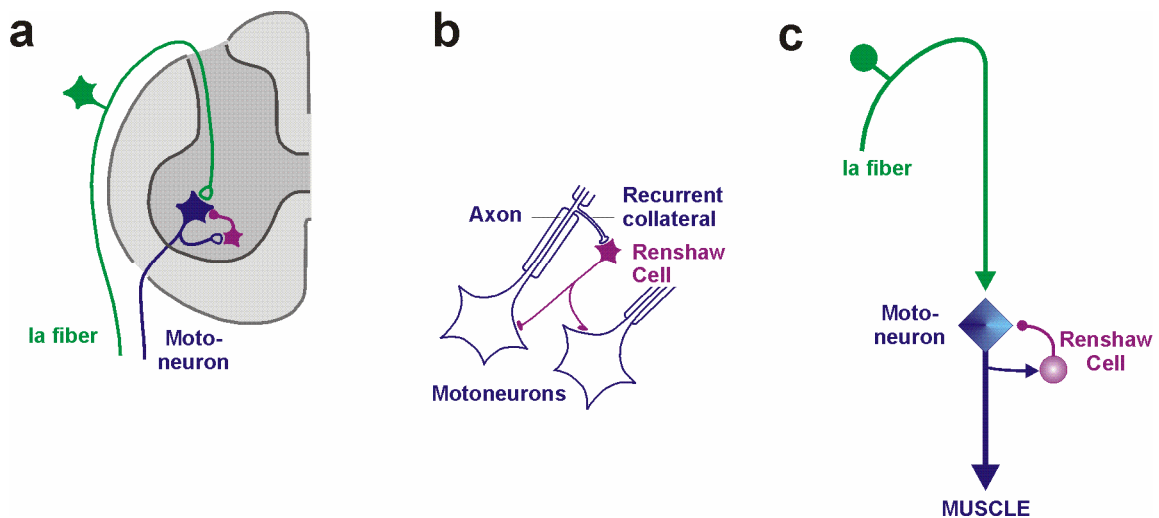


Figure 13. Spinal circuits involved in recurrent inhibition. **a, b** Anatomical drawings along with **c**, a simplified schematic diagram of the neural circuitry.

Like the Ia inhibitory interneurons, Renshaw cells are located just outside the motor nuclei in the laminae VII of the spinal gray matter and are involved in adjusting and stabilizing the activity in the motor pools. Due to the long durations of Renshaw cell activity, a discharge caused by a given stimulus pulse can be responsible for a decrease of excitability of motoneurons exposed to a following stimulus. The decreased number of motoneurons responding to a second stimulus (of same intensity) would then also activate a smaller population of Renshaw cells. Such mechanism might potentially result in simple periodic patterns within a single motoneuron pool (Figure 14).

Renshaw cells not only synapse with motoneurons, but also with Ia inhibitory interneurons activated by the Ia afferents from the same muscle group (Figure 15a). In fact, they are particularly effective in inhibiting Ia inhibitory interneurons (Jankowska, 1992).

This connectivity together with the long lasting activity of the Renshaw cells can result in an effect referred to as ‘recurrent facilitation’, which is a reduced efficacy of reciprocal inhibition mediated by Ia interneurons to the antagonistic muscle group (Hultborn et al., 1971a; 1971b). Recurrent facilitation can be a potential mechanism involved in the simple periodic patterns of PRM reflex modulation since: (i) Ia inhibitory interneurons are assumed to have a tonic background activity. This activity is either due to a ‘spontaneous firing’ or facilitation ‘by other sources’. The resting discharge frequencies are between 20-130 Hz (Hultborn et al., 1971b; the maximum of the frequency range could be also lower around 50 Hz, personal communication with Prof T. Deliagina, 2009). (ii) The tonically active Ia inhibitory interneurons produce a sustained, steady hyperpolarization of the

motoneurons. (iii) The long lasting activity of Renshaw cells inhibits the tonic background activity of the Ia inhibitory interneurons and thereby causes a long lasting dis-inhibition of the motoneurons. The effect of recurrent facilitation thus lies in a dis-inhibition of motoneurons, i.e., a release of the motoneurons from their sustained hyperpolarization evoked by tonically active inhibitory interneurons (Hultborn et al., 1971b). Recurrent facilitation could hence potentially contribute to the simple periodic PRM reflex patterns (Figure 15b).

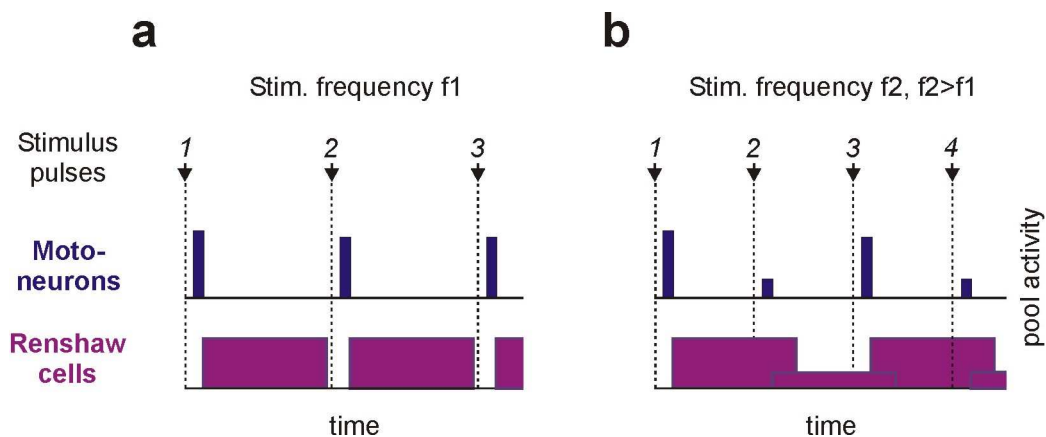


Figure 14. Drawing of a simple, qualitative model that could potentially explain two findings of the neurophysiological study: **a** Series of independent PRM reflexes at low stimulation frequencies and **b**, the occurrence of simple periodic patterns with increased SCS frequencies featuring the alternation of large and small responses in a single motoneuron-pool. At the low stimulation frequency in **a**, each stimulus pulse evokes a (monosynaptic) response in a similar population of the motoneurons (bars in blue color). Each response causes a burst in Renshaw cells (bars in purple color), which terminates before the next pulse is applied. Thus, the Renshaw cells do not affect the motoneuron activity. At the higher frequency in **b**, the afferent volley produced by the second pulse arrives at the motoneurons before the cessation of the Renshaw cell-burst (as a consequence of the first pulse). Hence, a smaller population of motoneurons responds. This smaller response causes fewer Renshaw cells to fire and, therefore, a reduction of motoneuron inhibition when the latter respond to the third pulse. (Personal communication with Prof T. Deliagina, 2009).

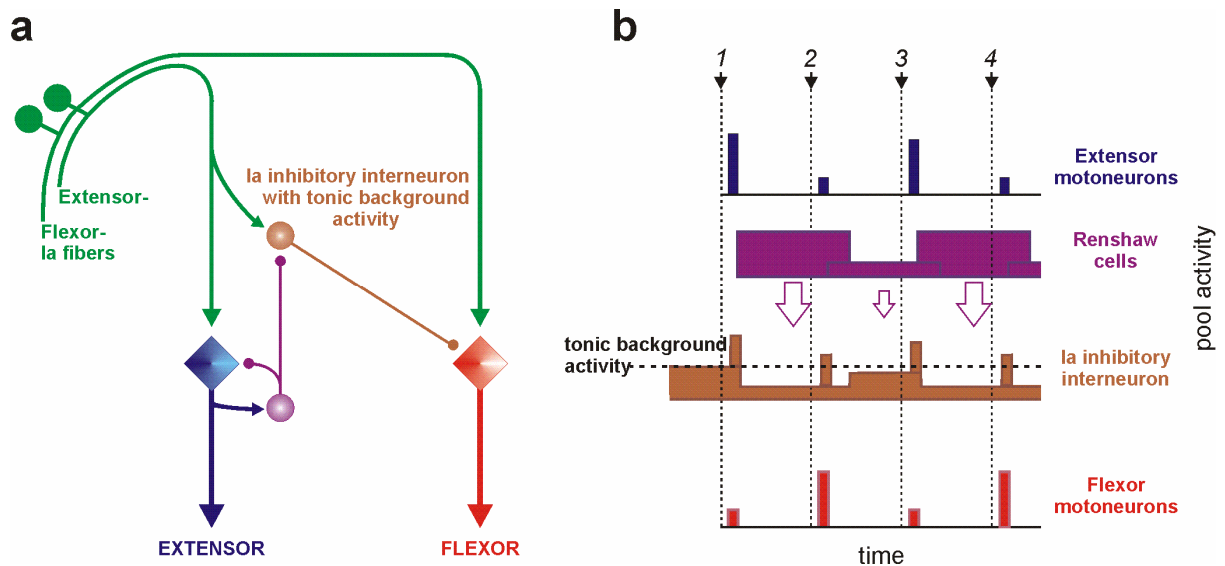


Figure 15. Spinal circuits including recurrent inhibition and reciprocal inhibition. **a** Simplified schematic drawing of the neural circuitry that could potentially produce the simple periodic PRM reflex patterns. **b** At higher frequencies of SCS, alternations occur in the Renshaw cells associated with the extensor motoneuron pool generated as in Fig. 14b. Due to the inhibitory input from Renshaw cells, the activity of the Ia inhibitory interneurons of the extensor alternates in anti-phase to these Renshaw cells. The Ia inhibitory interneurons affect the flexor motoneuron pool, causing alternation of the flexor responses in anti-phase to alternations of extensor responses.

To complete the model network, the remaining effective connectivities of the considered interneurons must be included. The only interneurons found to be affected by Ia inhibitory interneurons are other Ia inhibitory interneurons (Jankowska, 1992). Subpopulations of interneurons with opposite actions, those mediating Ia reciprocal inhibition from flexors to extensors and from extensors to flexors of a given joint, inhibit each other. These connectivities present a mutual inhibition between Ia inhibitory interneurons. At the same time, only two groups of interneurons are known to receive recurrent inhibition from motor axon collaterals via Renshaw cells: the interneurons mediating reciprocal Ia inhibition and the Renshaw cells themselves (Hultborn et al., 1971b). Thereby, the inhibitory connectivity is between populations of Renshaw cells that are associated with antagonistic motoneuron pools. The patterns of connectivity of the network model including monosynaptic segmental reflex arcs as well as reciprocal and recurrent inhibition are displayed in Figure 16.

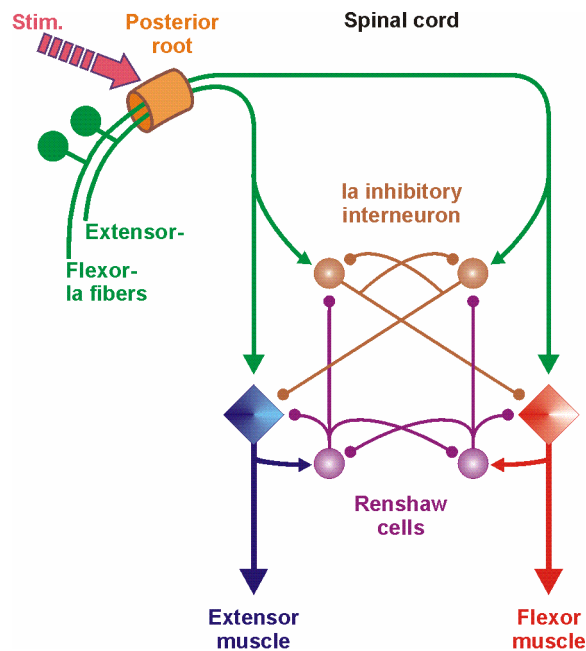


Figure 16. Patterns of connectivity of the network model to be studied. Input to the network is provided by spinal cord stimulation (*Stim.*), that generates action potentials in Ia afferents of extensor and flexor muscles. The afferents make monosynaptic excitatory synapses on homonymous alpha-motoneurons and Ia inhibitory interneurons. The latter mediate reciprocal inhibition of antagonist motoneurons and are also connected by mutual inhibition. Renshaw cells are excited by axon collaterals of the corresponding motoneurons and inhibit these motoneurons, the corresponding Ia inhibitory interneurons as well as Renshaw cells associated with antagonistic motoneurons (Jankowska, 1992). For the rostro-caudal architecture, as well as population size, qualitative connectivities, neuron properties etc. see *Material and Methods*.

The hypothesis of the present study is that the network as described in Figure 16 can produce simple periodic patterns of motoneuron pool firing with an oscillation period covering two successive responses. These rhythmic motor outputs shall be elicited by repetitive inputs provided by SCS at 16 Hz. Supraspinal influences will not be considered to mimic complete SCI. The capacity of the spinal network to produce simple periodic motor outputs shall be tested by a biologically realistic mathematical model that will be stepwise developed by adding additional neural elements. Thus, the function of network modules shall be assessed in isolation of the spinal circuit in which it is embedded. The complete network model will eventually include four cell types within eight neuron populations, i.e., flexor and extensor motoneuron populations as well as corresponding populations of group Ia afferent fibers, Ia inhibitory interneurons and Renshaw cells, mediating reflex interactions. Furthermore, it will incorporate populations of neurons with mutual inhibition between each other and considers long lasting time-dependent processes

that reduce or enhance (recurrent *inhibition* and *facilitation*) activity within the neuron populations. Thus, the hypothesis is based on the similarity of the suggested network model and its properties to the ones of the half-center CPG model. The suggested network is assumed to be relatively simple, including only interneurons close to the motor nuclei. In view of rhythmic activity, both Ia inhibitory interneurons as well as Renshaw cells are locomotor related neurons, primarily used to modulate motoneuron excitability during locomotion (Jankowska, 2001).

The significance of the present work lies in that it may enlighten the contribution of various neuronal elements on the function of the lumbar spinal machinery controlling lower limb activity. In particular, it provides a physiologically based tool for investigating the segmental motor system in humans.

Material and Methods

Modeling a spiking neuron – General aspects and biological abstractions

The activity of spinal circuits and segmental reflexes has been a subject of many studies throughout the last decades (e.g. MacGregor, 1987; McCrea, 1992; Bashor, 1998). Yet, in spite of technological advances, ethical considerations limit the extent to which spinal reflexes can be investigated in man by experimental techniques traditionally employed in neuroscience. Hence, computer simulations provide a means of complementary analysis methods ‘for characterizing what nervous systems do, determining how they function, and understanding why they operate in particular ways’ (Dayan & Abbott, 2001a).

Single neurons are the basic constituents of neuronal networks (Jolivet et al., 2008) and provide insight into the mechanisms of intrinsic neuronal signal transmission (Trappenberg, 2007a). The information gained at such level may then be expanded to networks of neurons, ultimately leading to an understanding of how neuronal populations encode afferent signals and interact to function as a complex system.

One of the most popular neuron models describing the generation and propagation of action potentials is based on the *Hodgkin-Huxley*-equations, a set of four coupled nonlinear differential equations, originally formulated for the giant squid axon (Hodgkin & Huxley, 1952; Rattay, 1990). The equations given below calculate the currents passing through 1 cm² of the axon cell membrane (hence allowing for the independence of the specific cell geometry; for details see Rattay, 1990):

$$\begin{aligned}\dot{V} &= [-g_{Na}m^3h(V - V_{Na}) - g_Kn^4(V - V_K) - g_L(V - V_L) + i_{st}]/c \\ \dot{m} &= [-(\alpha_m + \beta_m) \cdot m + \alpha_m] \cdot k \\ \dot{n} &= [-(\alpha_n + \beta_n) \cdot n + \alpha_n] \cdot k \\ \dot{h} &= [-(\alpha_h + \beta_h) \cdot h + \alpha_h] \cdot k\end{aligned}$$

with

$V = V_i - V_e - V_{rest}$ being the reduced voltage (0 in the steady state) of the cell where V_i , V_e , and V_{rest} denote the intracellular and extracellular potential as well as the resting voltage, respectively;

c , capacity per cm^2 ;

$i_{st} = \frac{I_{inj}}{2\pi \cdot r \cdot l}$, density of experimentally injected current;

$k = 3^{0.1T - 0.63}$, coefficient for temperature in $^{\circ}C$, chosen according to the ionic conductances derived from experimental studies;

m, n, h , probabilities for opening of the ionic channels with $m(0) = 0.05$, $n(0) = 0.32$, and $h(0) = 0.6$;

and α and β fitting the ionic conductances of experimental data:

$$\alpha_m = \frac{2.5 - 0.1V}{e^{2.5 - 0.1V} - 1}, \beta_m = 4e^{\frac{-V}{18}};$$

$$\alpha_n = \frac{1 - 0.1V}{10(e^{1 - 0.1V} - 1)}, \beta_n = 0.125e^{\frac{-V}{80}};$$

$$\alpha_h = 0.07e^{\frac{-V}{20}}, \beta_h = \frac{1}{e^{3 - 0.1V} + 1}.$$

The advantage of this approach is its ability to precisely describe biologically realistic model neurons under the influence of externally applied electrical stimulation. However, when several or even huge numbers of different types of neuronal populations are incorporated in a simulated network, the Hodgkin-Huxley-framework is often computationally too consumptive. Moreover, it highlights very specific features that may be beyond the scope of the particular question addressed and may hence be neglected as not relevant. Consequently, the question arises how the anatomically and physiologically complex neuronal networks can be represented by computer models that on the one hand

provide a reasonable biological abstraction and on the other hand leave the computational processes tractable.

Based on the work done by Louis Lapicque more than one hundred years ago (Lapicque, 1907; Brunel & van Rossum, 2007), another type of neuron model has been established and extensively used in the context of studying dynamics of spiking neurons at the network level – the simplified phenomenological neuron models. Though often assumed to be biologically questionable because of their simplicity (Jolivet et al., 2008), many phenomena observed in experimental work can be reproduced by adjusting only a few model parameters (Bashor, 1998; Brunel & van Rossum, 2007).

The most widely used representative of the phenomenological neuron models is the so-called Leaky Integrate-and-Fire (LIF) model. It is based on the fact that spike generation by neurons is quite stereotyped and therefore neglects a detailed description of the biophysical mechanisms responsible for the initiation of an action potential. Rather, it provides an approximation of the total membrane potential in terms of presynaptically exerted facilitatory and inhibitory influences (Trappenberg, 2007b). The LIF model, its advantages and drawbacks, will be further discussed in the following.

The leaky Integrate-and-Fire Model and its refinement in the present work

The Leaky Integrate-and-Fire Model

The LIF model represents an example of a formal spiking neuron model. Its main characteristic making up its simplicity lies in the fact that it solely deals with subthreshold dynamics of the membrane potential: Whenever the membrane potential V of the modeled neuron reaches a critical value V_{thr} , an action potential is fired. In the classical LIF model, the membrane potential is subsequently set to its resting value $V_{rest} < V_{thr}$ (e.g. Dayan & Abbott, 2001b). Thereby, the main effects are captured by the following equation (Trappenberg, 2007b):

$$\tau_m \frac{dV(t)}{dt} = -V(t) + RI(t),$$

with

τ_m ... denoting a membrane (m) time constant determined by the average sodium and leakage channel conductances and describing the exponential decay of the membrane potential; and

$$I(t) = \sum_j \sum_{t_j^f} \omega_j a(t - t_j^f) \dots$$
 being the sum of individual synaptic currents arriving at the target neuron where each of the stereotyped responses of the postsynaptic potential depends on the efficiencies ω_j of each synapse; a parameterizing the stereotyped postsynaptic response. t_j^f denotes the firing time of the presynaptic neuron at the j -th synapse.

Alternatively, the neuron under consideration may be described by a LIF model without a reset of the membrane potential to V_{rest} after the generation of an action potential (Jilge et al., 2004). This version of the LIF model is especially beneficial if the driving current is assumed to consist of elements either equal to zero or V_{AP} (i.e., the input required for the initiation of an action potential). Given an equidistant distribution of elements V_{AP} within these sequences, the input of epidural SCS at constant stimulation frequencies may hence be simulated. The particular value of the adapted LIF model lies in that it allows to some extent for an approximation of temporal summation processes of various excitatory and inhibitory inputs. The postsynaptic potential P of the n -th neuron at a discrete time point t_k would then be recursively calculated by the following equation (Jilge et al., 2004):

$$P_n(t_k) = P_n(t_k - 1) \exp\left(-\frac{\Delta t}{\tau_n}\right) + \sum_m \omega_{mn} V_{mn}(t_k)$$

with

$$t_k = k\Delta t, k \in \mathbb{N}_0;$$

$\tau_n > 0$... time constant describing the repolarization of the membrane potential;

V_{mn} ... synaptic input to n -th neuron provided by neuron m ;

$\omega_{mn} V_{mn}$... induced (excitatory or inhibitory) postsynaptic potential.

Figure 17 illustrates two examples of LIF neurons. The first one (Fig. 17a) is driven by a constant external input and the membrane potential is set to V_{rest} after each spike generation. The second one (Fig. 17b) shows the behavior of a neuron simulated according to the adapted LIF model in response to a periodic *all-or-nothing* input current without an immediate reset of the membrane potential to V_{rest} .

As is obvious from the examples given in Figure 17, the postsynaptic potentials provided by the LIF model represent only a rough approximation. Yet, when taking into account that temporal summation processes of various (inhibitory as well as facilitatory) synaptic inputs are hypothesized to be the leading mechanism in the generation of simple periodic patterns (cf. *Introduction*), a neuron model permitting a more detailed description of the time courses of postsynaptic potentials (PSPs) would be desirable, also with respect to the specific firing patterns of different types of neurons and the corresponding variety of

generated PSPs. This can be, for instance, accomplished by taking advantage of the numerous intracellular recordings from – mainly cat – motoneurons conducted since the early 1950s. These recordings provide a close description of both (monosynaptic) EPSPs and (disynaptic) IPSPs evoked by synchronous synaptic actions (e.g. Coombs et al., 1955), in terms of time course- and amplitude-characterizations of the produced membrane potential changes (Curtis & Eccles, 1959; Rall et al., 1967). Hence, a model combining the simplicity of the conventional LIF model with a more detailed definition of postsynaptic potentials appears to be a promising method to approach the questions addressed in the present work.

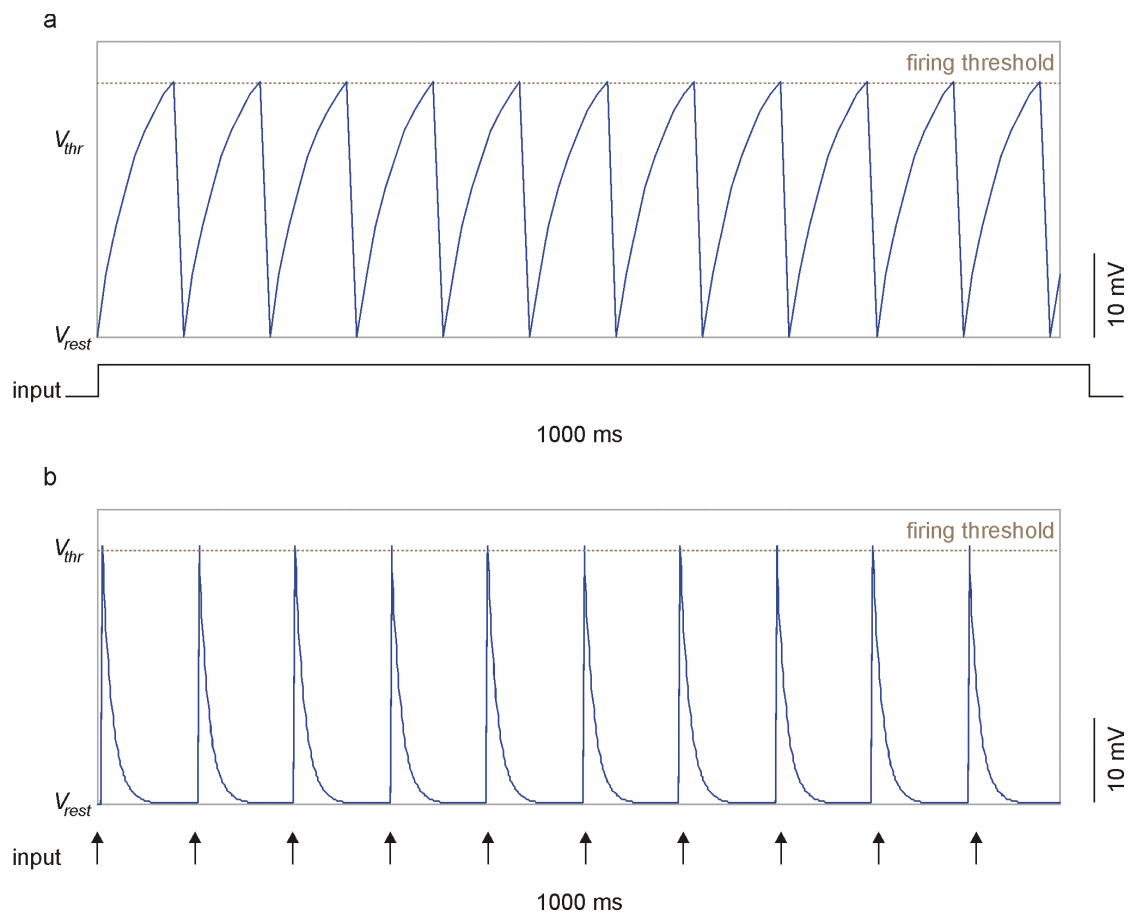


Figure 17. Typical behavior of the membrane potentials of leaky integrate-and-fire model neurons. **a** Action potentials are fired in response to a constant input current as soon as the membrane potential reaches a firing threshold V_{thr} . Subsequently, the membrane potential is set to its resting value V_{rest} . **b** Changes in membrane potential in response to periodic input made up of elements equal to zero or V_{AP} (indicated by arrows) without reset of the membrane potential after spike generation.

Excitatory and Inhibitory Postsynaptic Potentials

When recorded intracellularly in or near the soma of a motoneuron, EPSPs and IPSPs produced by group Ia afferent volleys demonstrate waveforms with steep initial rising phases and slower exponential-like decaying phases (Curtis & Eccles, 1959). Such evoked potentials are due to the synchronous activation of a population of Ia fibers (Rall, 1967) and are hence made up of multiple smaller subunits, termed miniature (or single-fiber) potentials which are in turn generated by the activity of single synapses (Sypert & Munson, 1984; Rall, 1967; Rall et al., 1967; Burke, 1967). The relatively long decaying phases of the evoked PSPs suggest that the synaptic terminals of group Ia afferents are widely distributed over the whole soma-dendritic receptive surface of motoneurons (Rall et al., 1967). The steep rising phases of the PSPs would then be attributable to the activity of synapses in close vicinity to the soma, while their decaying phases would be due to potentials produced by a fraction of synapses at rather distal dendritic locations. The latter potentials – transmitted by the dendrites that have electrically passive membrane characteristics – are subject to electrotonic attenuation (Burke, 1967).

Regarding the specific shapes of the observed time courses of the experimentally detected EPSPs and IPSPs, the steep initial phases in positive or negative direction, respectively, were found to be due to short (approximately 2 ms in duration), intense inflowing currents. The decaying phases of EPSPs declined to a slight hyperpolarization before returning to the resting level. The corresponding phases of IPSPs declined immediately back to the initial baseline. As a general rule, IPSPs approached the resting membrane potential faster than EPSPs, the latter most probably featuring a prolonged residuum of depolarizing current. Since the observed PSPs were evoked by the synchronous action of a population of Ia fibers, their time courses largely corresponded to those produced by single synaptic terminals (Curtis & Eccles, 1959).

A relevant information for modeling temporal summation is that the effect of – excitatory and inhibitory – potential summation at the motoneuronal level was shown to follow a near-perfectly linear process in the majority of trials and to never yield values greater than the algebraic sum (Burke, 1967). In cases not demonstrating a linear relation, the resulting compound potentials had still amplitudes amounting to at least 80% of the algebraic sum.

The Alpha Function

In the simulation of neuronal networks, EPSPs and IPSPs may be described without solving differential equations, but only by a single function defined as to match the empirical data. The change in the membrane potential P in time after a synaptic delay can be described by an *alpha*-function (Trappenberg, 2007a; Dyan & Abbott, 2001b):

$$P(t) = \omega \cdot t \cdot \exp\left(-\frac{t}{t_{peak}}\right)$$

with

ω	...	synaptic weight, and
t_{peak}	...	time at which the function reaches its peak, also specifying the time constant for rising and decaying phases.

Commonly, a combination of two or more exponentials is used to fit the shapes of the recorded PSPs (Trappenberg, 2007a).

Selection of neurons and interneurons involved in the present simplified reciprocal spinal network – Specification of model parameters

In designing the mathematical model of reciprocal spinal segmental circuits, the main focus was on the attempt to provide a simplified, yet biologically realistic neuronal circuit for investigating the mechanisms underlying the generation of simple periodic patterns of PRM reflex modulations as observed in the electrophysiological recordings in SCI subjects. The main patterns detected are summarized in Figure 18.

The present model was conceived as a pair of two segmental circuits associated with antagonistic (flexor and extensor) motor pools and interconnection in-between them, each composed of four different types of neuronal populations: Ia afferent fibers, alpha motoneurons, Ia inhibitory interneurons, and Renshaw cells (cf. Fig. 16). The synaptic conductances were described by alpha functions which will be discussed below in detail for each of the neuron types considered.

Altogether, the model contained 80 neurons within the 8 populations of the flexor and extensor circuits (10 per population). Neurons within a single population were considered to be identical and hence described by the same parameter settings. The number of recruited flexor and extensor Ia afferents could vary in each test run – thereby mimicking the effect of different stimulation intensities. At the same time, the numbers of projections between populations were set to constant values: 60% in case of the flexor (i.e., a single cell of a (flexor) source population projected to 60% of the cells in the target population), and 80% in the extensor, accounting for the fact of smaller total monosynaptic EPSPs detected in the former (Hunt & Perl, 1960). An example is given in Figure 19a showing a single Ia fiber projecting to the (homonymous) population of motoneurons. Cells within one population could contact with equal probability any of the cells within the target population and all interconnections between the populations were defined by a randomized procedure at the beginning of each simulation. As a result, target neurons, though otherwise conceived as identical, could feature different numbers of excitatory and inhibitory inputs.

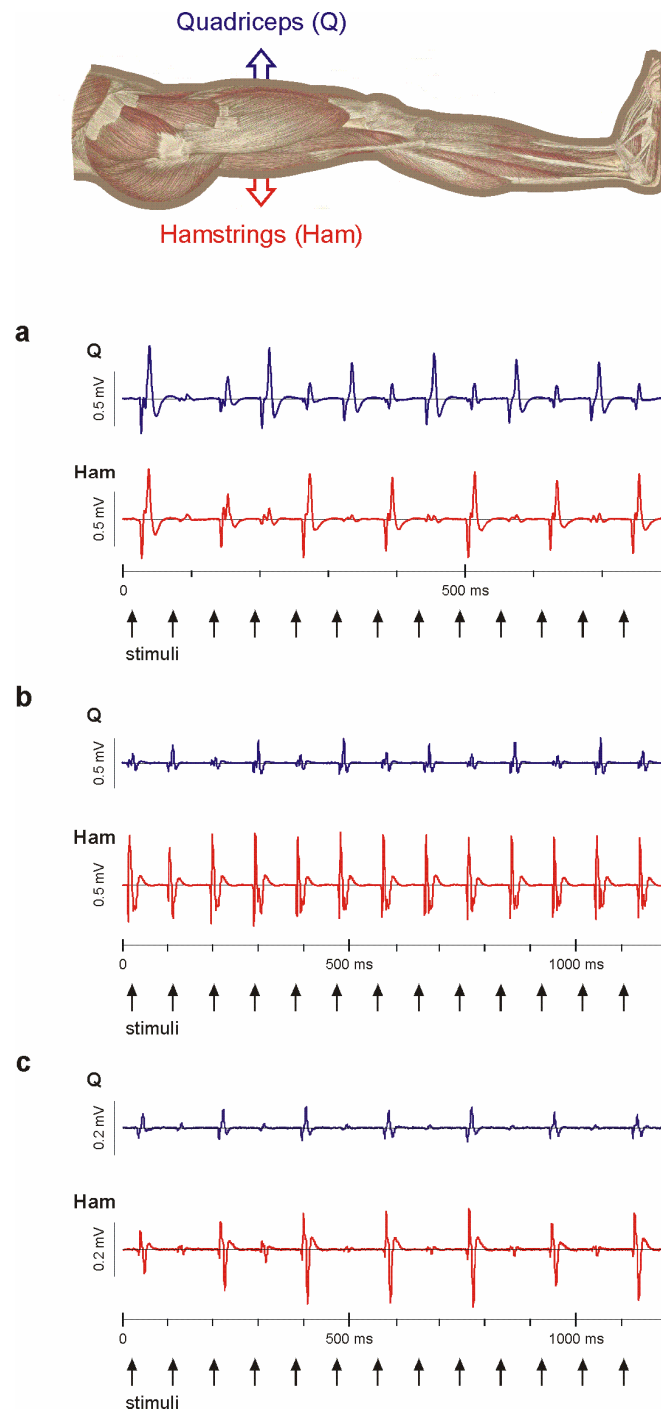


Figure 18. Simple periodic patterns elicited by epidural SCS in complete SCI subjects. Displayed are PRM reflexes recorded from quadriceps (Q) and hamstrings (Ham), arrows depict the times of stimulus application. **a** Reciprocal attenuation of Q and Ham responses. **b** Pattern characterized by attenuation of every second response recorded from Q and stable output in Ham. **c** In-phase modulation of Q and Ham responses. Data derived from *a*, subject 2, epidural electrode combination 0+3-, 5 V, 16 Hz; *b*, subject 2, 0+3-, 5 V, 11 Hz; and *c*, subject 4, 0-3+, 6V, 11 Hz. Only the traces shown in *a* are displayed as from the first stimulus application.

As stated above, the present model incorporated monosynaptic activation of alpha motoneurons via group Ia fibers as well as reciprocal inhibition mediated by Ia interneurons (that were in turn affected by mutual inhibition between each other) and recurrent inhibition via Renshaw cells acting on homonymous motoneurons and Ia interneurons as well as antagonistic cells of the same type. All model neurons were assumed to have a resting membrane potential $V_{rest} = 0$ at time $t = 0$.

Following Maynard et al. (1997) and Westmoreland et al. (1994), major innervations zones were defined for both the flexor and the extensor circuit. This means, that each muscle is innervated by motoneurons located in several segments, but one segment (and specifically its segmental reflex circuit) is particularly effective in activating the muscle. For reasons of simplicity, the segments with motoneurons innervating the muscles shall be called segments 1-3 (*Sgm1*, *Sgm2*, *Sgm3*) for both the extensor as well as the flexor muscle. Anatomically they could represent the segments L2-L4 (quadriceps) and L5-S2 (hamstrings), or alike.

To account for the major innervations zones, the simulated group Ia afferent fibers were classified as to belong to one of the spinal cord segments *Sgm1*-*Sgm3* (Figure 19b). Four of the 10 afferents were then associated with *Sgm2*, and three afferents with *Sgm1* and *Sgm3*, respectively. Specifically, the ratio of EPSP amplitudes was then chosen to be 100:85 for the monosynaptic EPSPs produced by *Sgm2*-afferents as compared to the ones of *Sgm1*- or *Sgm3*-afferents.

The simulated network was set into action by trains of pulses ‘externally’ applied to the flexor and extensor Ia afferent fibers. The trains were represented by sequences consisting of elements equal to zero or V_{AP} . The stimuli occurred at intervals corresponding to 16 Hz, since this was the rate at which most frequently simple periodic patterns were observed. All subsequent events (i.e., the generation of EPSPs and IPSPs) were time-locked to the incoming pulses and occurred with specific delays. Cell membrane potentials were computed and updated for all model neurons at a time resolution of 0.1 ms. If the total sum (composed of excitatory and inhibitory influences) of a PSP produced in a particular neuron was above threshold, an action potential was triggered (for details see below). Total time spans of simulations varied between 350 ms and 500 ms (corresponding to 3500 and 5000 steps, respectively). Finally, the number of motoneurons firing at each time was reported.

The model was simulated using Matlab 6.1 (The MathWorks, Inc., Natick, MA, USA). The maximal computing time for a single simulation amounted to 9575 s (approximately 2h40min) using a Pentium M, 1.5 GHz processor.

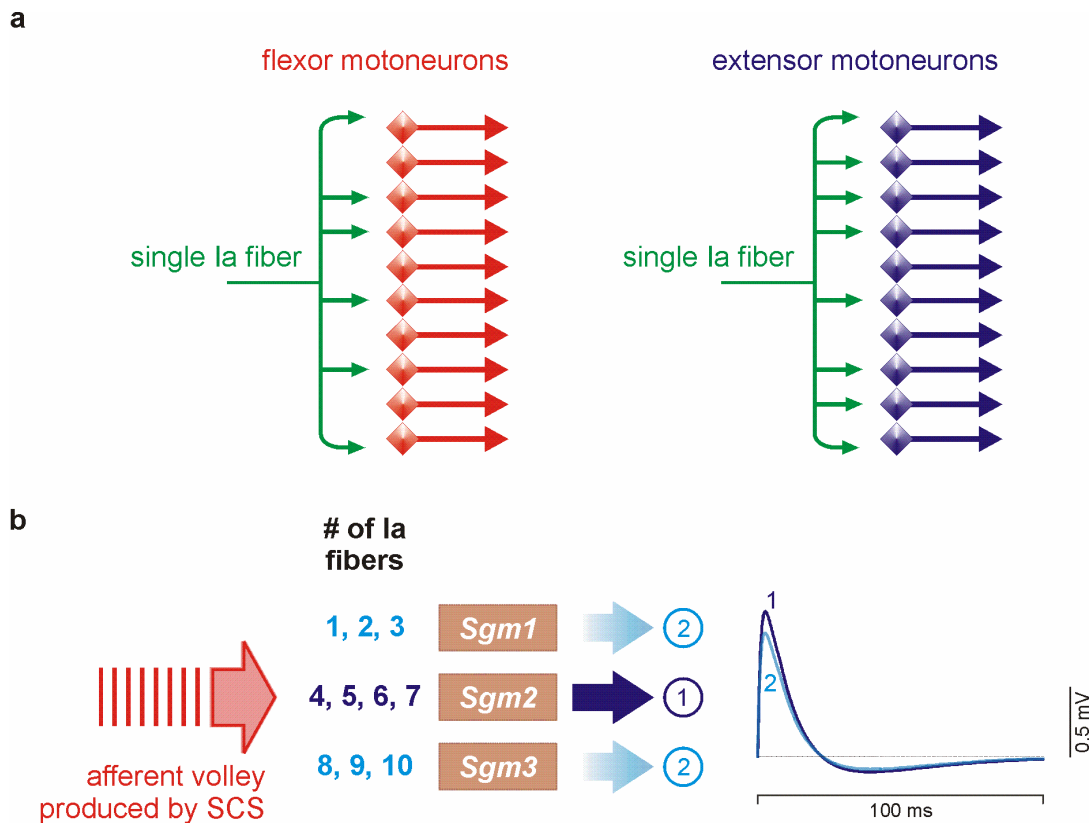


Figure 19. Specification of some model parameters. **a** As for the flexor, a single Ia afferent projects to 60% of all homonymous motoneurons, while in the extensor, this value amounts to 80%. **b** The major innervation zone of both the flexor and extensor was assumed to be the middle one of three adjacent arbitrary segments *Sgm1-Sgm3*. If a single Ia afferents associated with *Sgm2* was recruited, the resulting EPSPs in the motoneurons to which these fibers projected were larger in amplitude (potential in dark color, labeled as 1) as compared to others (potential in light color, labeled as 2).

Ia afferents and motoneurons

Within each segmental circuit of the model network, alpha motoneurons depend on the transmission of excitatory inputs provided by Ia afferents in order to fire. Since an EPSP produced by a single Ia fiber is too small to increase the motoneuron membrane potential to its firing threshold, the present model required at least 20% of the homonymous Ia fibers to be recruited to evoke – after a monosynaptic delay δ_{MN} – responses in the (flexor or extensor) motoneurons. The common threshold that ensured the elicitation of action potentials in both motoneurons in response to each applied stimulus was reached if 30% of all Ia fibers were recruited. These assumptions were based on findings from physiological studies conducted in SCI subjects showing the dependence between the applied stimulus intensities and the elicitation of reflex responses.

To characterize the input-output relation of the monosynaptic reflex pathway in response to single stimuli, so-called recruitment curves were established. Recruitment curves show the relation between stimulus intensity and the size of reflex output (Schieppati, 1987). For their calculation, the simulation was repeated five times for each ‘stimulation-intensity’ (i.e., number of recruited Ia afferents), with the particularly activated Ia fibers being randomized.

The average time course of an EPSP elicited in an alpha motoneuron by a single Ia afferent was closely fitted to experimental data (Curtis & Eccles, 1959; Burke, 1967) and was represented as superposition of four exponentials, two of them describing the initial excitatory (*e*) phase $EPSP_{MN,e}$, and two a slight afterhyperpolarization (AHP), $EPSP_{MN,AHP}$:

$$EPSP_{MN,e}(t) = \omega_{MN,e} \cdot \exp[(\tau_{MN,e,d} \cdot t) - \exp(\tau_{MN,e,r} \cdot t)],$$

$$EPSP_{MN,AHP}(t) = \omega_{MN,AHP} \cdot \exp[(\tau_{MN,AHP,d} \cdot t) - \exp(\tau_{MN,AHP,r} \cdot t)]$$

with

$$0 \leq t \leq t_{end}/10 \text{ (in steps of 0.1 ms),}$$

$\omega_{MN,e}$ and $\omega_{MN,AHP}$... scaling factors of the excitatory and afterhyperpolarization phases, respectively;

$\tau_{MN,e,r}$ and $\tau_{MN,AHP,r}$... time constants describing the rising phases of the excitatory and afterhyperpolarization components of the PSP, respectively; and

$\tau_{MN,e,d}$ and $\tau_{MN,AHP,d}$... time constants describing the decaying behavior of the excitatory and afterhyperpolarization phases, respectively.

The final EPSP for a motoneuron was then produced by the sum

$$EPSP_{MN} = EPSP_{MN,e} + EPSP_{MN,AHP}$$

with $EPSP_{MN,AHP}$ being shifted by approximately 8 ms, i.e., with its influence starting only 8 ms after the onset of the excitatory phase. The peak of the EPSP occurred 2 ms after the initial deflection from baseline and amounted to 1.0427 mV. The AHP phase reached a minimum of -0.1636 mV. The resulting EPSP had a peak-to-peak amplitude of 1.1527 mV (with the minimum being only -0.11 mV due to the summation process). All potentials are illustrated in Figure 20. For details on the parameter settings used in the equations see *Appendix A*.

Eventually, a single action potential was triggered as soon as the sum of all EPSPs produced in a motoneuron reached a threshold V_{thr} .

There were no differences in the computation of EPSPs in the flexor and extensor motoneuron pools. Differences only arose due to the different numbers of ‘internal’ synaptic connections between the neuron pools associated with the flexor (60%) and extensor circuits (80%).

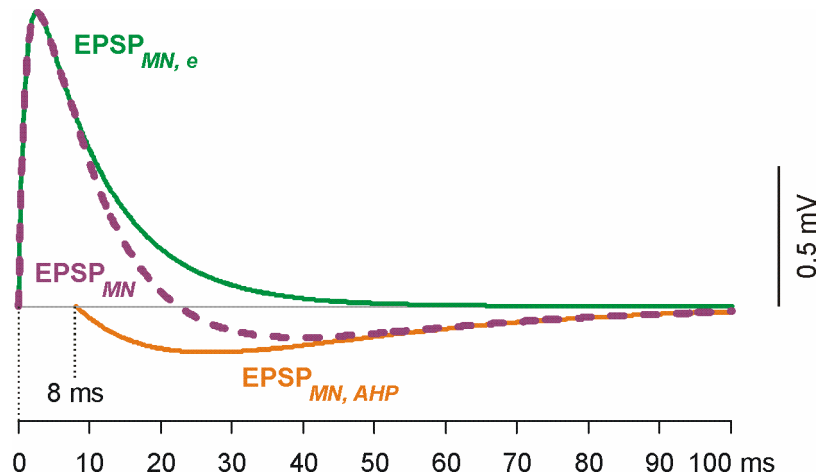


Figure 20. Excitatory postsynaptic potential (dashed line in purple color) elicited by a single Ia fiber in a motoneuron ($EPSP_{MN}$) of either pool (i.e., flexor or extensor) made up of an excitatory phase (green solid line labeled as $EPSP_{MN,e}$) and an afterhyperpolarization phase (solid line in orange labeled as $EPSP_{MN,AHP}$).

Ia inhibitory interneurons

In simulating Ia inhibitory interneurons, two characteristics were considered: (i) their ability to respond with single spikes to a synchronous Ia afferent volley (Jankowska, 1992); and (ii) their tonic background activity, here assumed to be within a range of frequencies of 20-100 Hz under resting state conditions (Hultborn et al., 1971b; personal communication with Prof T. Deliagina, 2009).

Ia inhibitory interneurons exert their inhibitory effect on antagonistic motoneurons as well as ‘opposite’ Ia interneurons (Hultborn et al., 1976a; Jankowska, 1992) via disynaptic pathways (cf. Fig. 12). The additional delay of the IPSP relative to the monosynaptic EPSP of 2 ms is assumed in the present model.

The amplitude of a single IPSP was chosen exceedingly small so that the activity of a considerable portion of Ia inhibitory interneurons was required to inhibit a target (motoneuron) cell (Pierrot-Deseignilly & Burke, 2005c). As for the time course, Ia IPSPs

have brief rising times with a peak assumed at approximately 2-2.5 ms after the onset of the potential (the respective value in the cat amounts to 1.0-1.5 ms; Davidoff & Hackman, 1984). The decay was simulated as to follow an exponential curve and to be shorter lasting than the one of the EPSP (Curtis & Eccles, 1959).

A single (flexor and extensor) Ia IPSP is illustrated in Figure 21 and was described by the alpha function:

$$IPSP(t) = \omega_{IPSP} \cdot [\exp(\tau_{IPSP,d} \cdot t) - \exp(\tau_{IPSP,r} \cdot t)]$$

with

$0 \leq t \leq t_{end}/10$ (in steps of 0.1 ms), ω_{IPSP} denoting the synaptic weight, and $\tau_{IPSP,r}$ and $\tau_{IPSP,d}$ the time constants for the rising and decaying phases, respectively. Details on the parameters are summarized in *Appendix A*.

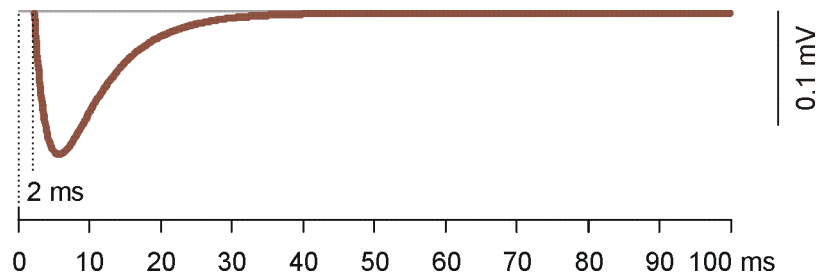


Figure 21. Time course of a single Ia IPSP as exerted on antagonistic motoneurons and Ia interneurons.

For the computation of the tonic background activity, repetitive IPSPs were assumed to be elicited by the Ia inhibitory interneurons on their target cells. The intervals in between two IPSPs were randomly set to values corresponding to any frequency between 20 and 100 Hz and individually determined for each cell. Finally, the tonic background activity exerted on a target cell was defined as the sum of the inhibitory actions provided by all Ia interneurons projecting to this cell. An example is given in Figure 22.

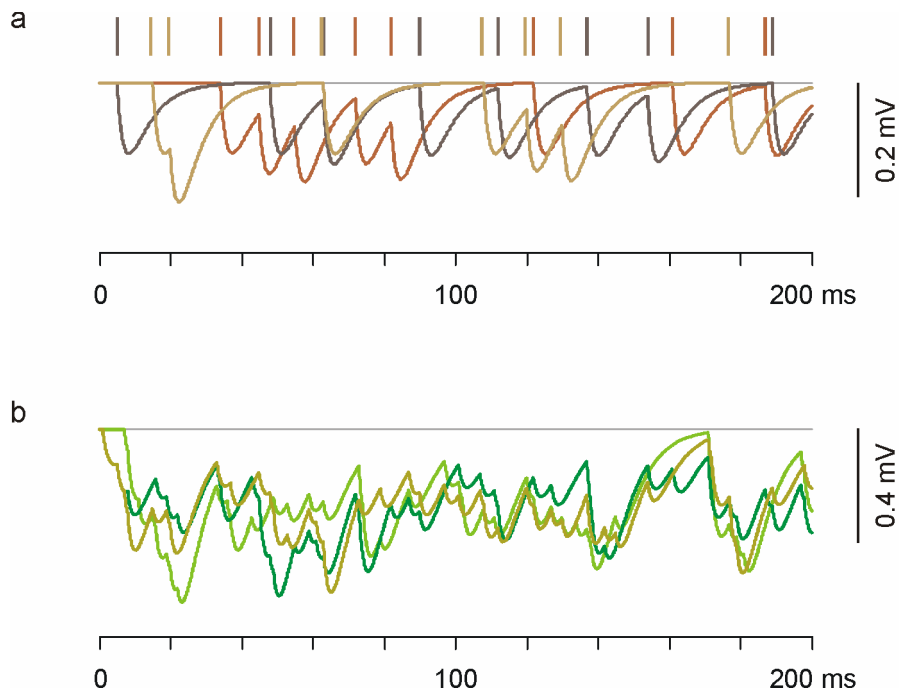


Figure 22. Tonic background activity of Ia interneurons as exerted on target cells. **a** Activity of three individual Ia interneurons (light, middle, and dark brown curves), firing at rates of 20-100 Hz. Vertical lines on the top illustrate the respective times of spike initiation. **b** Hyperpolarization of three different flexor motoneurons due to tonic background activity of Ia interneurons. The total hyperpolarizing effects are composed of the activities of 60% of all Ia interneurons each.

Renshaw cells and recurrent inhibition

As stated above (cf. *Introduction*), Renshaw cells mediating recurrent inhibition are excited by discharges of motoneurons. They have low firing thresholds (Pompeiano, 1984) and fire long bursts of spikes for tens of milliseconds in duration (Katz & Peirrot-Deseilligny, 1998; Uchiyama et al., 2003).

In the present model, the enhancement of the resting potential V_{rest} of a Renshaw cell by a single excitatory input (originating from motoneurons) was chosen according to the following criteria: The firing threshold was attained, if a Renshaw cell received excitation from 40% of all motoneurons projecting on it, with no inhibitory inputs acting at the same time. The excitatory input had to be correspondingly higher to overcome the inhibitory influence as exerted by the antagonistic Renshaw cells. If set into action, the Renshaw cell would fire a burst made up of individual spikes which would cause – after a delay δ_{RC} following stimulus application – a long lasting postsynaptic event composed of the superposition of single IPSPs (Figure 23a, b). The duration of a burst was adjusted so that its influence on the motoneurons had not ceased when the next stimulus pulse arrived at

the latter at intervals of 45-91 ms (i.e., 11-22 Hz, cf. Fig. 14*b*). A single spike within the burst was assumed to be rather short in duration and of small amplitude. (Due to the small size of the Renshaw cells, intracellular recordings are difficult to be obtained. Consequently, details on their intrinsic properties are hardly available.) At the beginning of a burst, the spikes occurred at short intervals which were slowly prolonged as the burst persisted (Figure 23*c*; Eccles et al., 1961; Uchiyama et al., 2003).

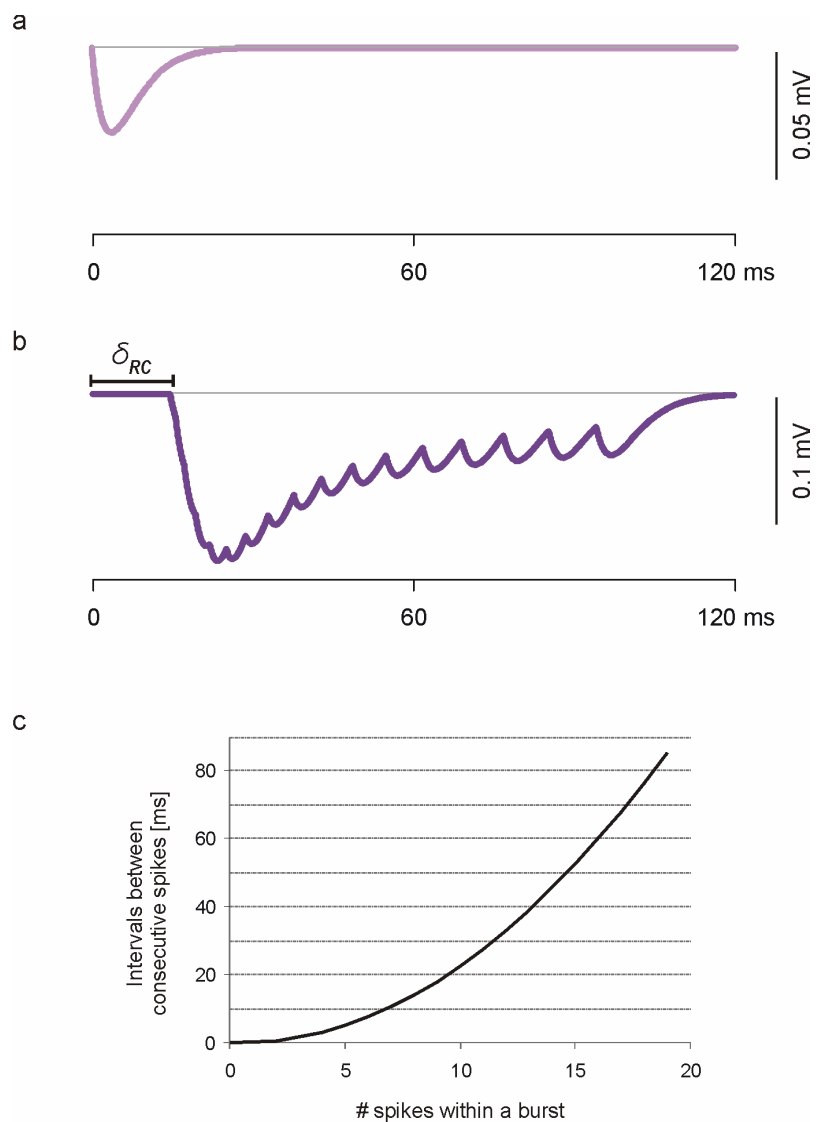


Figure 23. Recurrent inhibition mediated by Renshaw cells. The superposition of single IPSPs as shown in **a** account for the long lasting inhibitory events in **b**. δ_{RC} denotes the delay with respect to the incoming Ia afferent volley after which recurrent inhibition is set into action. **c** The single IPSPs potentials initially occur at short intervals that are prolonged towards the end of a burst.

The effect of recurrent inhibition was calculated equally for all target cells, i.e., homonymous motoneurons and Ia interneurons (Hultborn et al., 1971a) as well as antagonistic Renshaw cells. The time course of a single spike was calculated by the following equation:

$$IPSP_{RC}(t) = \omega_{RC} \cdot [\exp(\tau_{RC,d} \cdot t) - \exp(\tau_{RC,r} \cdot t)]$$

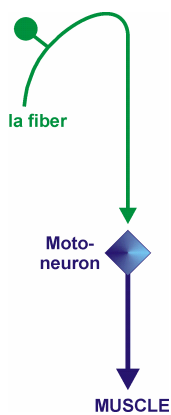
with

$0 \leq t \leq t_{end}/10$ (in steps of 0.1 ms), ω_{RC} denoting the synaptic weight, and $\tau_{RC,r}$ and $\tau_{RC,d}$ the time constants for the rising and decaying phases, respectively. Parameters for calculation as well as a simplified approach of modeling recurrent inhibition are presented in *Appendices A* and *B*.

Results

The complete network model containing monosynaptic activation of motoneurons, Ia inhibition, recurrent inhibition as well as mutual inhibition between interneurons of same types will be explored in steps featuring different levels of complexity. First, the most basic spinal network, the monosynaptic reflex circuits of flexor and extensor motor pools in isolation from each other, will be analyzed. Subsequently, the model will be stepwise expanded to integrate also interneuronal elements. The thereby produced results will be presented in separate sections and seek to enlighten the functional roles of particular cell populations, when isolated from the network they are embedded in, in modulating the motor output.

Model I: Ia afferent fibers monosynaptically projecting on homonymous motoneurons



The neurophysiological study presented in within this thesis revealed recruitment curves of the PRM reflexes recorded from several lower limb muscles that were characterized by steep initial slopes and reaching a plateau at stimulus intensities corresponding to two times the respective thresholds. On average, an intensity of approximately 1.3 times the response threshold was required to induce responses in all recorded muscles.

These results could be closely reproduced by the computer model. The calculated flexor recruitment curve that started with a rather moderate slope as compared to the one of the extensor, due to the different numbers of projections on motoneurons per Ia fiber associated with the antagonistic circuits (Figure 24). Consequently, the flexor curve reached its plateau (i.e., 100% of all homonymous motoneurons firing) when on average 60% of all Ia fibers were activated, while the corresponding value for the extensor amounted to 40%. The common threshold

for the elicitation of monosynaptic motoneuron discharges in response to each of the consecutively applied stimulation pulses corresponded to the recruitment of 30% in the flexor, and 20% of all homonymous Ia fibers in the extensor circuit, respectively.

The respective recruitment curves of a network neglecting major innervation zones was calculated with the same model and is presented in *Appendix B*.

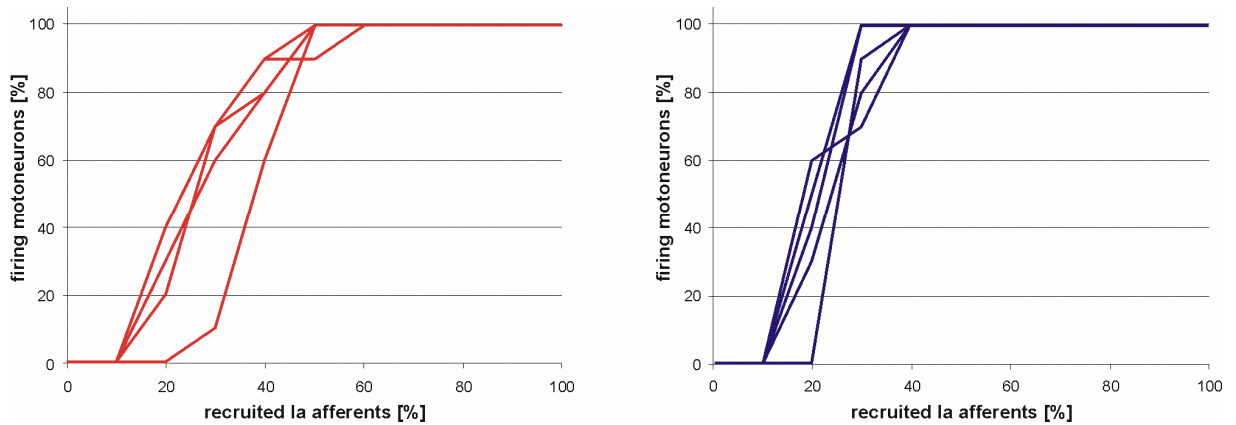
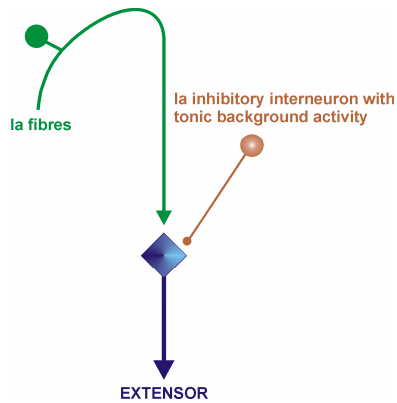


Figure 24. Recruitment curves of flexor (red) and extensor (blue) motoneuron populations activated by Ia afferent volleys. The recruitment curves are defined as the relation between the percentage of recruited Ia fibers and the percentage of firing motoneurons within each population. The differences in the recruitment curves displayed are due to the randomized selection of the particularly activated Ia fibers in each of the five simulation runs conducted for each stimulus intensity (i.e., number of recruited Ia fibers, here given as percentage of activated Ia fibers within a population).

Model II: The influence of tonic background activity exerted by Ia interneurons



The tonic discharges of Ia inhibitory interneurons considerably changed the recruitment curves of both motoneuron populations (Figure 25). The most obvious difference was the requirement for more Ia fibers to be recruited to reach the maximum output – the average values under the present conditions corresponding to 70% in the flexor and 50% in the extensor circuit, respectively. Additionally, as the mean common thresholds remained constant, the slopes of the recruitment curves appeared less steep as compared to those in the example without inhibitory influences.

Detailed information on the network behavior in response to ‘graded stimulation’ is given in Figure 26.

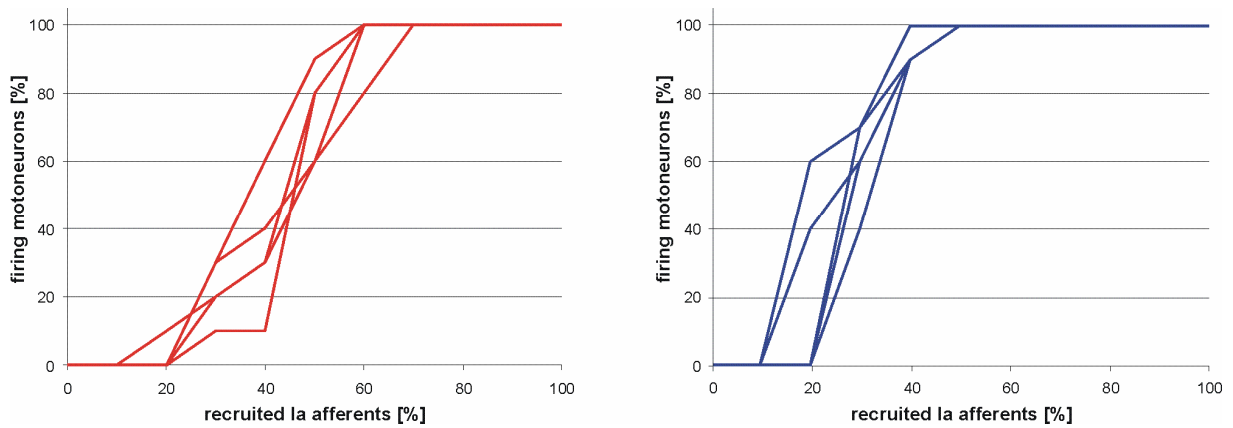
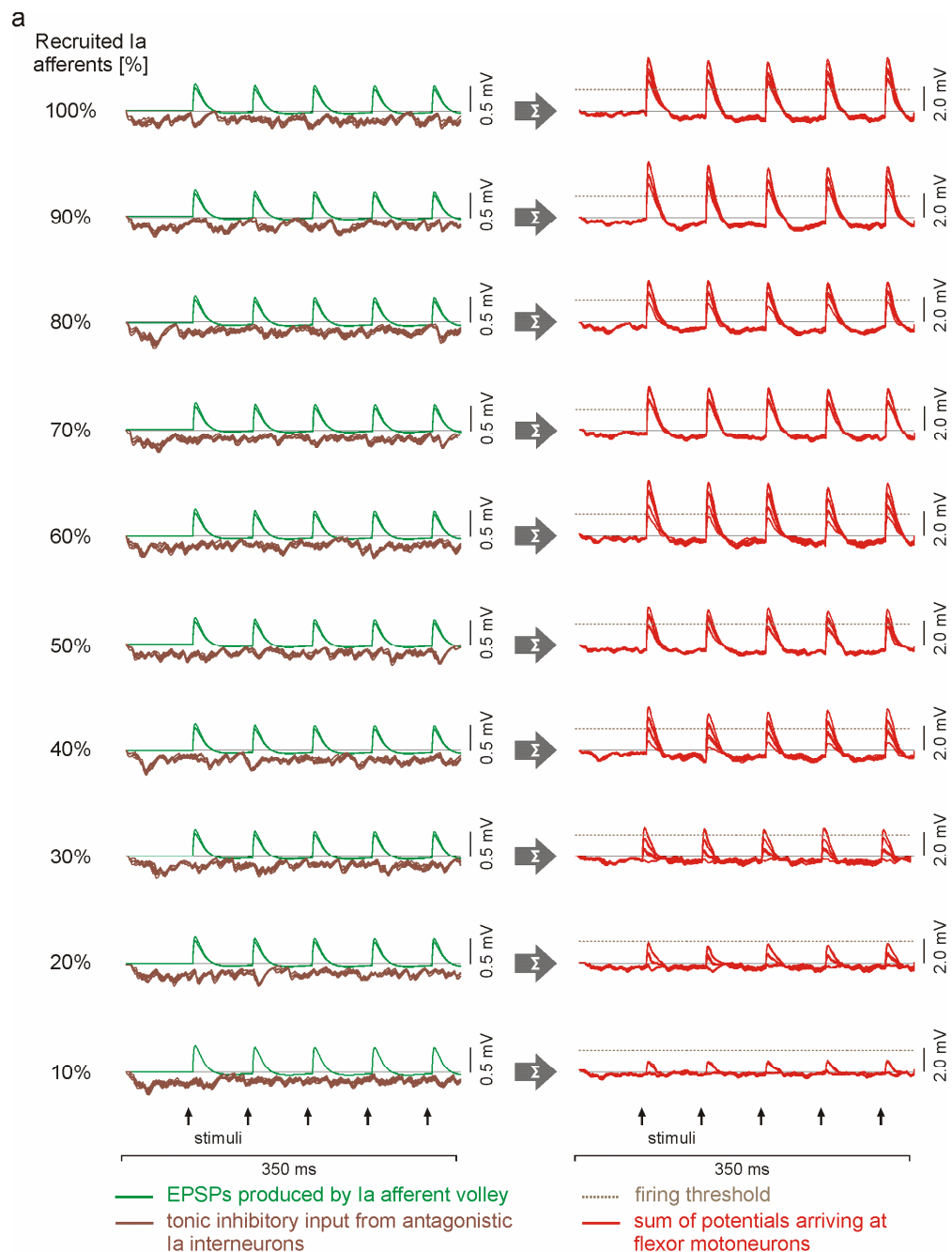
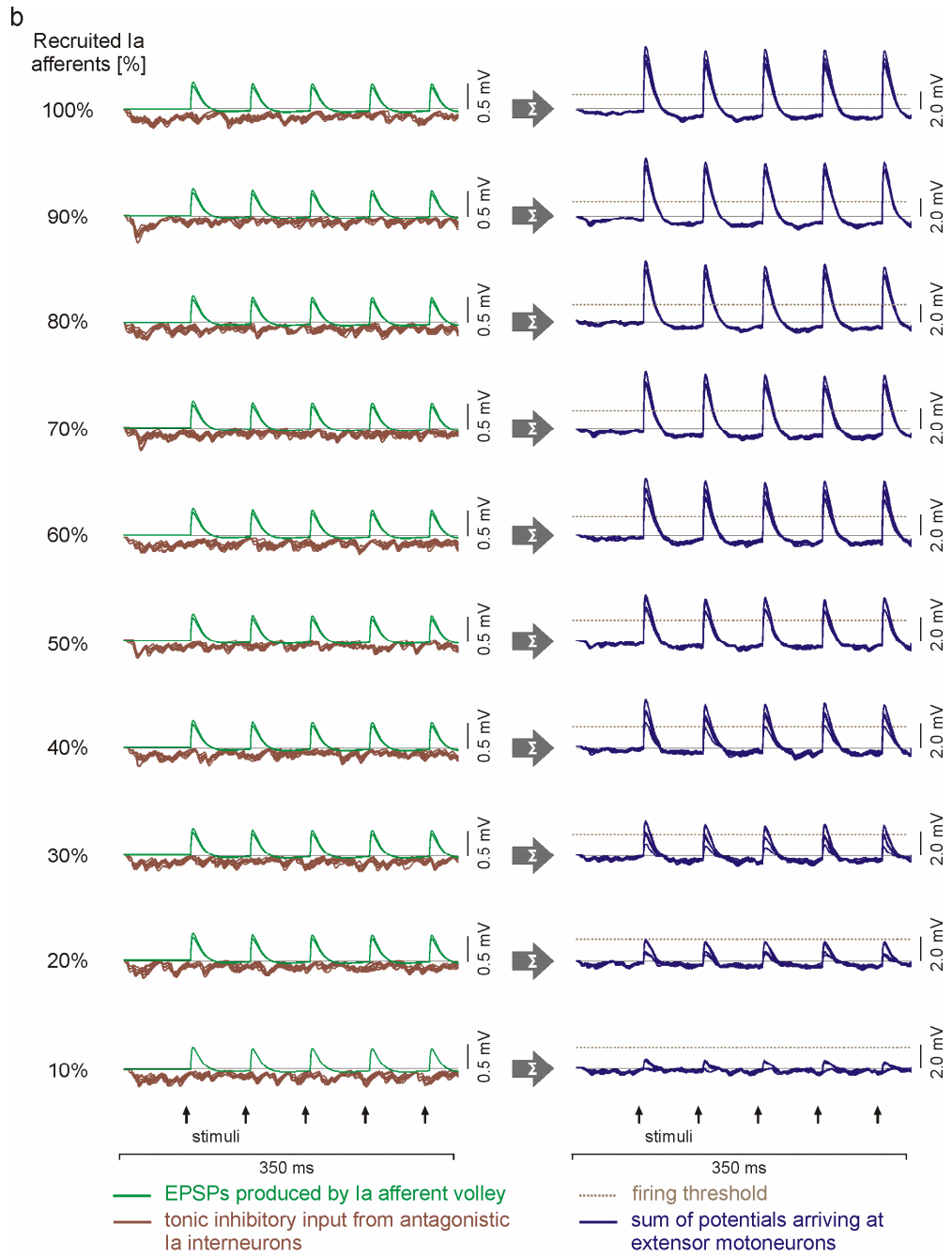


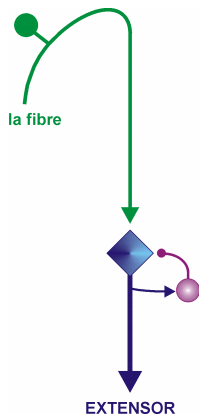
Figure 25. Recruitment curves of flexor (red) and extensor (blue) motoneuron populations affected by tonic background Ia inhibition. For each stimulus intensity (i.e., number of recruited Ia fibers, here given as percentage of activated Ia fibers within a population), the simulation was repeated five times. The randomized selection of particularly activated Ia fibers accounted for the different recruitment curves produced in each simulation run. Two facts account for the steeper extensor recruitment curves, i.e., the lower number of flexor Ia interneurons projecting to extensor motoneurons and the relatively strong monosynaptic drive of the latter.

Figure 26. Concept of synaptic integration of various excitatory and inhibitory inputs at the motoneuronal level in response to graded stimulation. EPSPs generated by homonymous Ia fibers (green) and tonic discharges of antagonistic Ia interneurons (brown) at rates of 20-100 Hz sum up as to result in a total motoneuron membrane potential of the flexor (**a**, red) and the extensor circuits (**b**, blue), respectively. Action potentials would be generated at times when the membrane potentials attain firing threshold. Arrows depict the times of stimulus application. Inserted values are applied stimulus intensities represented by the percentage of recruited Ia fibers within the respective population. Each of the ten superimposed lines of the graphs is the time course of membrane potential changes of a single motoneuron, influenced by PSPs.



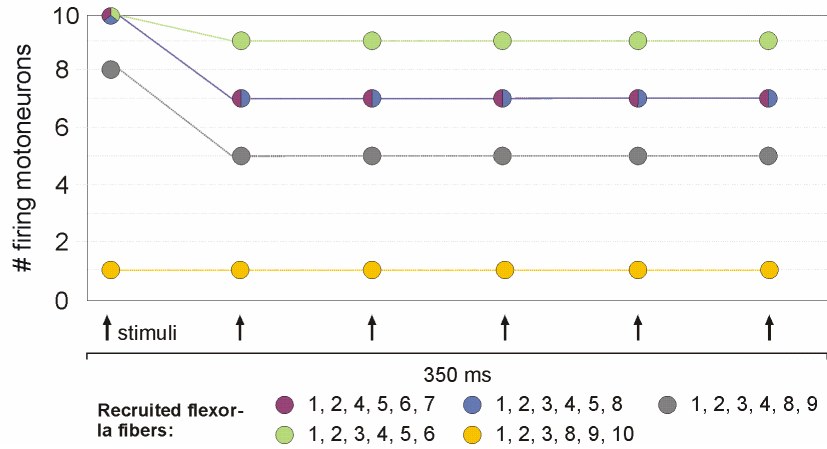
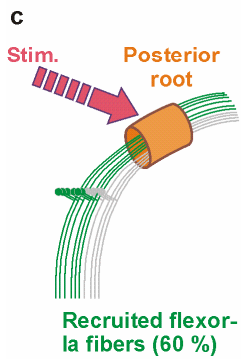
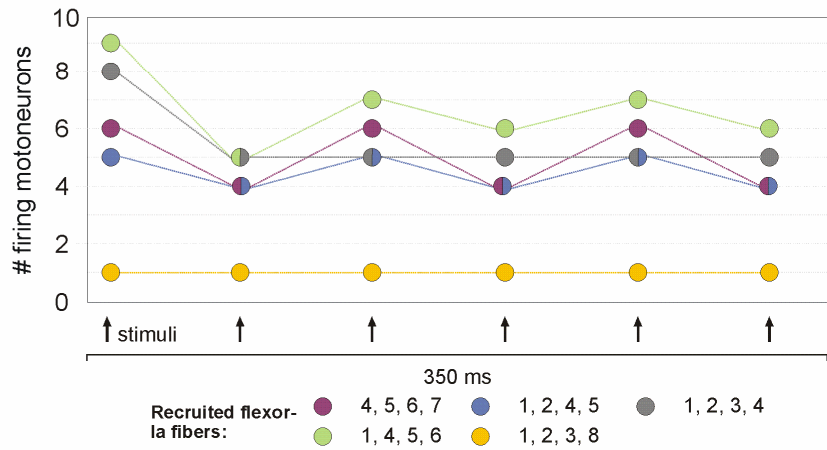
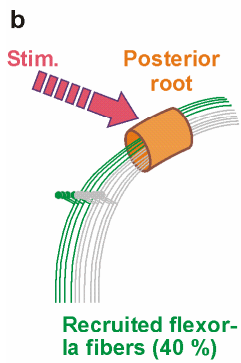
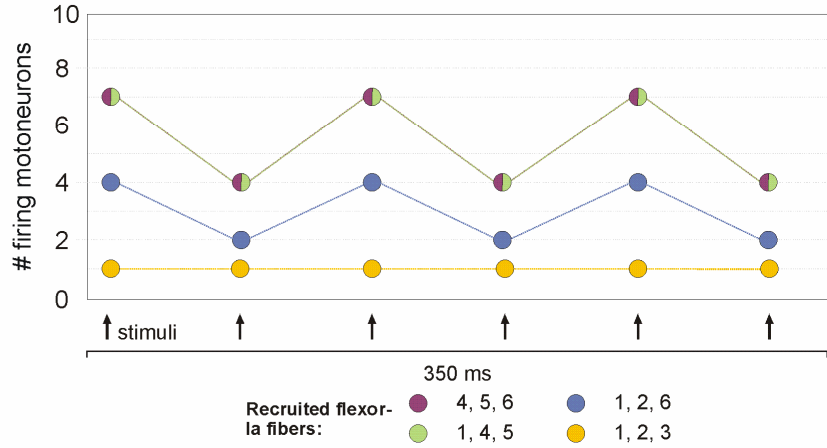
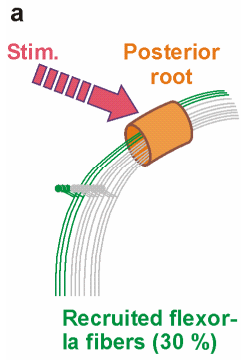
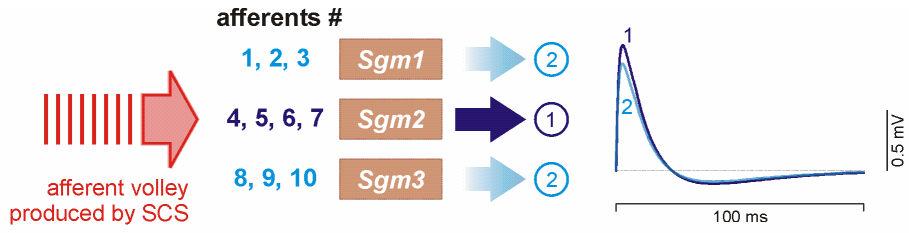


Model III: The effect of recurrent inhibition of a single motoneuron pool



Interesting results were found when testing the influence of recurrent inhibition of a single motoneuron pool, i.e., without considering any reciprocal interactions between the antagonistic network circuits. As hypothesized in the *Introduction*, the operation of Renshaw cells was in fact effective in generating simple periodic patterns. Furthermore, the computer model revealed a strong relation between the applied stimulation intensity (in terms of numbers of recruited Ia fibers) and the elicitation of simple periodic patterns – a finding closely resembling the results derived from the neurophysiological study described above.

As for the flexor circuit (Figure 27), simple modulation patterns were found in 75% of all cases tested at an intensity corresponding to the common threshold (i.e., 30% of Ia fibers being recruited; Fig. 27a). This value declined to 60% at intensities corresponding to 1.3 times the common threshold with the modulations being less pronounced than at common threshold-stimulation (Fig. 27b). No examples were found at even higher intensities. The various cases of simulation runs differed in the composition of the particularly recruited Ia fibers, i.e., either belonging to the major innervation zone or the adjacent segments. All combinations of fiber compositions were tested. Whenever simple periodic modulations were elicited, they featured stable patterns after the first applied stimulus pulse. At two times the common threshold (Fig. 27c), the first stimulus yielded maximum output (i.e., 100% of motoneurons firing) in 60% of all cases and 80% of the maximum in 20% of all cases. Thereafter, the outputs declined, but were unmodulated and remained steady at rather high levels (i.e., 90%, 70%, and 50% of motoneurons firing, respectively) with further stimulus application. Regarding the selection of the particularly stimulated Ia fibers with respect to the major innervation zone of the flexor, no modulations were induced if only afferents not associated with this zone were recruited, irrespective of the applied stimulus intensity. The combinations of activated Ia fibers that most readily yielded the generation of simple periodic patterns were those that featured a majority of fibers within the major innervation zone.



◀ **Figure 27.** Simple periodic patterns within the flexor motoneuron pool generated by recurrent inhibition exerted by homonymous Renshaw cells. The ordinate values marked by the filled circles are the numbers of motoneurons firing in response to successive stimuli. Different colors specify the particularly recruited Ia fibers. Each example represents a whole class of simulations under similar conditions (e.g., yellow, all possible combinations of recruited Ia fibers not associated with the major innervation zone; etc.). **a** Results derived at common threshold intensity corresponding to the recruitment of 30% of all flexor Ia fibers. Under such conditions, 75% of all cases featured simple periodic patterns. **b** Motoneuron firing induced by stimulation at 1.3 times the common threshold. Still, 60% of all cases yielded response modulations which appeared, however, less pronounced. **c** The simple periodic patterns were replaced by constant outputs if even higher intensities were applied. The examples here show the results derived from stimulation at 2 times the common threshold.

The results illustrated in Figure 27 implicit that the generation of periodic patterns by Renshaw cells solely relies on simple temporal summation processes at the motoneuronal level. This finding is further elaborated in Figure 28. The first pulse of the train induced responses in a rather large number of the – yet unconditioned – motoneurons that in turn activated a considerable portion of the Renshaw cell population. The resulting long lasting bursting of the latter would still have a decreasing effect on the motoneuron excitability when the next stimulus was applied. Hence, fewer motoneurons would respond and consequently, fewer Renshaw cells would subsequently be recruited, leading to a reduced inhibition of motoneurons to following stimuli. After two responses, the cycle would start again.

Recruited Ia afferents [%]

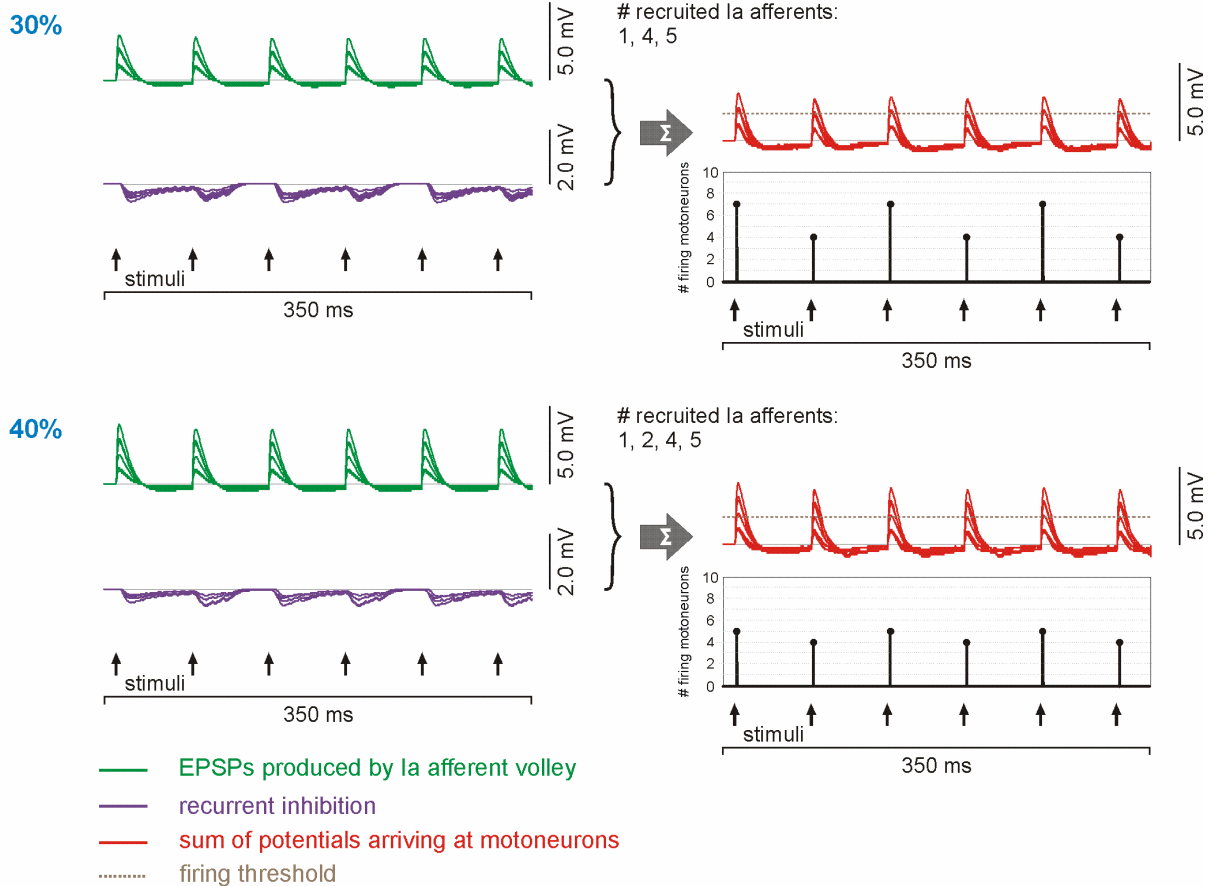


Figure 28. Simple periodically patterned motor outputs of flexor motoneurons (red) due to summation of excitatory Ia fiber (green) and inhibitory Renshaw cell (violet) inputs. Displayed are the respective postsynaptic potentials at stimulus intensities corresponding to the recruitment of 30% and 40% of Ia fibers (i.e., 1 and 1.3 times the common threshold intensity, respectively). Each line of the graphs is the time course of membrane potential changes of a single motoneuron, influenced by PSPs.

The assumption that temporal summation is the leading mechanism in generating modulated outputs was supported by testing the same network model at stimulation rates of 2.1 Hz and 5.0 Hz (Figure 29). Under such conditions, the activity of Renshaw cells induced by the first stimulation pulse had ceased before the next stimulus was applied. Hence, incoming volleys arrived at the motoneurons at resting state condition. Consequently, the number of cells within the motoneuron population responding to the successively applied stimuli only depended on the stimulation intensity and was not subject to any inhibitory influences exerted by Renshaw cells.

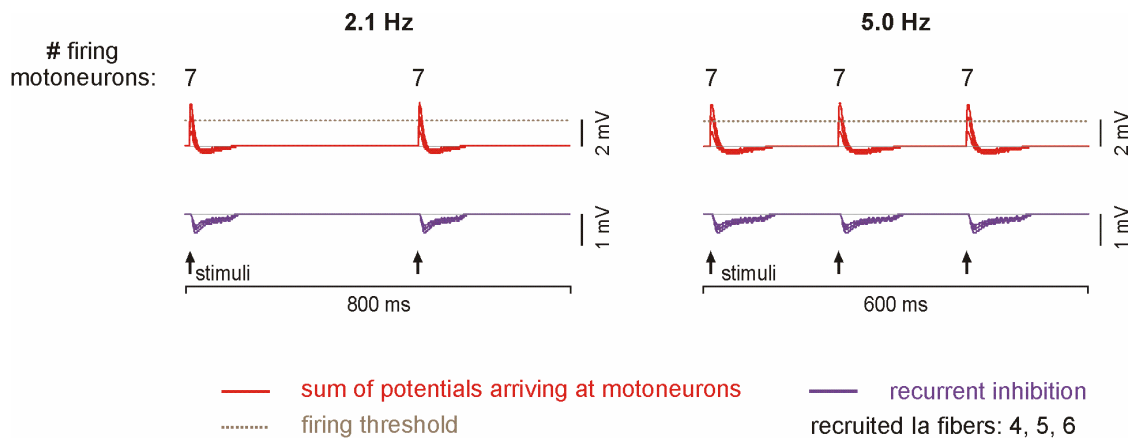


Figure 29. Network behavior in response to stimulation at 2.1 Hz (left) and 5.0 Hz (right). At such frequencies, Renshaw cell activity (violet) terminates before the application of a following stimuli, resulting in unmodulated motoneuron outputs (red). Both examples (2.1 Hz and 5.0 Hz) are calculated for circuits designed as flexors.

Similar results as for the flexor were obtained for the extensor circuit. At common threshold intensity and 1.5 times this threshold (i.e., 20% and 30% of extensor Ia fibers being recruited, respectively), simple periodic patterns were induced in even 100% of all cases (Figure 30*a, b*). Again, the modulations were less distinct at the higher intensity. Any further increase of intensity ‘destroyed’ the periodic patterns (Fig. 30*c, d*). If 60% of the Ia fibers were activated, maximum outputs (i.e., 100% of extensor motoneurons firing) in response to each stimulus were the common result. Due to the larger number of projections on motoneurons per each extensor Ia fiber, the produced network outputs were less sensitive to the recruitment of particular fibers within or outside the major innervation zones. With other words, the smaller magnitudes of EPSPs produced by the latter were compensated by the relatively large total number of Ia inputs.

The replacement of the simple periodic patterns at higher stimulus intensities was due to the strong bombardment of motoneurons by Ia afferent volleys under such conditions. The strong excitatory drive would then largely overcome the inhibitory actions exerted by the Renshaw cells, as illustrated in Figure 31.

◀ **Figure 30.** Simple periodically patterned outputs of the extensor motoneuron pool generated by recurrent inhibition exerted by Renshaw cells. The ordinate values marked by the filled circles illustrate the numbers of motoneurons firing in response to successive stimuli. Different colors specify the composition of the particularly recruited Ia fibers. **a** Results derived at common threshold intensity corresponding to the recruitment of 20% of all extensor Ia fibers. Under such conditions, all tested examples featured simple periodic patterns. **b** Qualitatively, the same results were obtained at stimulus intensities of 1.5 times the common threshold. However, the modulations were less pronounced than at common threshold intensity-stimulation. **c, d** Any further increase of the stimulus intensity yielded the elicitation of constant, unmodulated outputs.

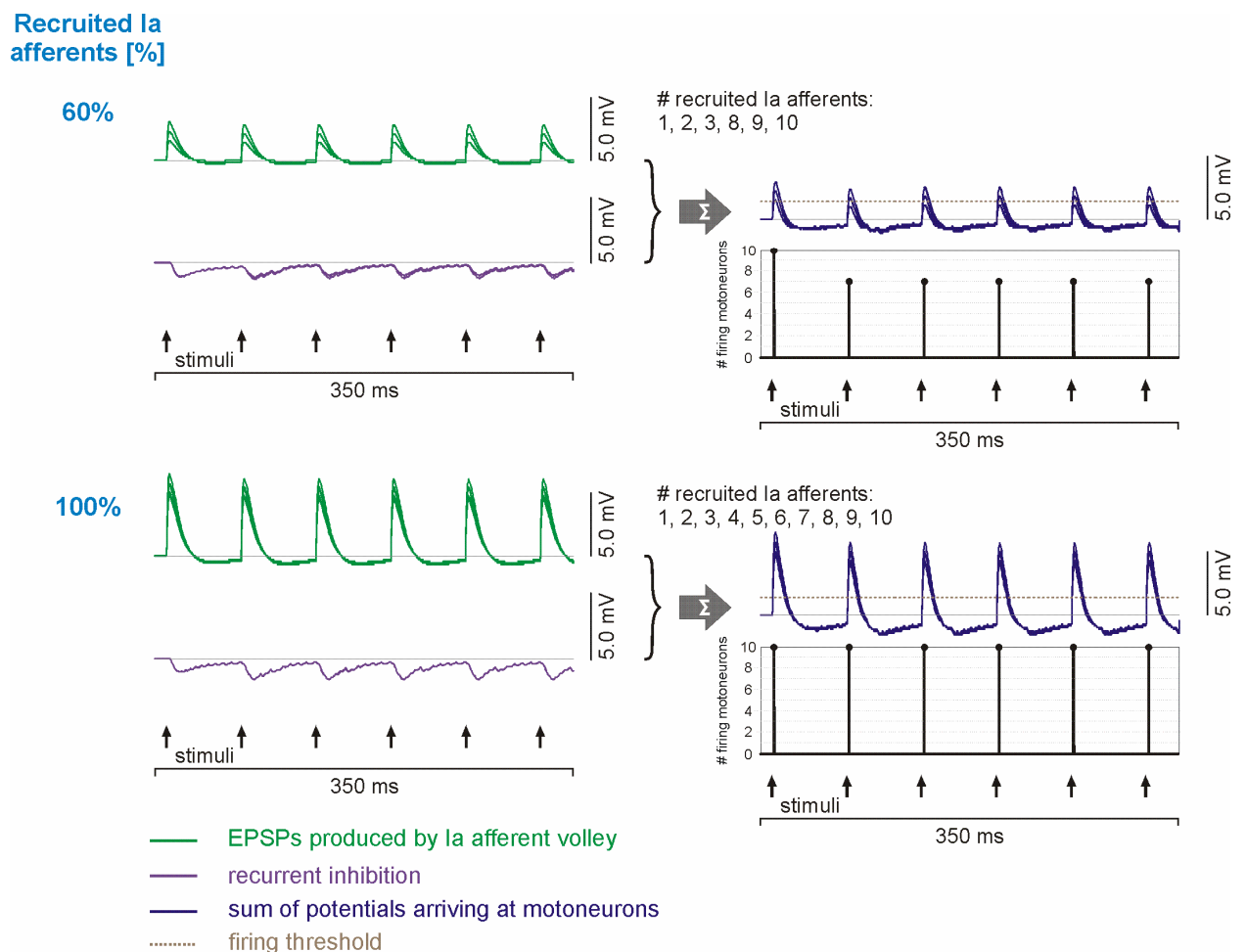


Figure 31. Replacement of simple periodic patterns observed in the extensor motoneuron population (blue) by constant outputs observed at higher stimulation intensities (60% and 100% of Ia fibers being recruited, respectively). Due to the strong drive of motoneurons by Ia afferent input (green), the role of recurrent inhibition (violet) on the produced output is neglectable.

Another feature of recurrent inhibition was that it reduced the output of the flexor motoneuron population in response to maximum stimulation (i.e., 100% of Ia fibers being recruited). With other words, the maximum attainable output in the flexor was reduced to 90% of that in the model without considering recurrent inhibition mediated by Renshaw cells (cf. *Models I, II*). At the same time, there was no change in the number of firing extensor motoneurons to maximum stimulation. The respective firing patterns of the flexor and extensor motoneuron pools are displayed in Figure 32.

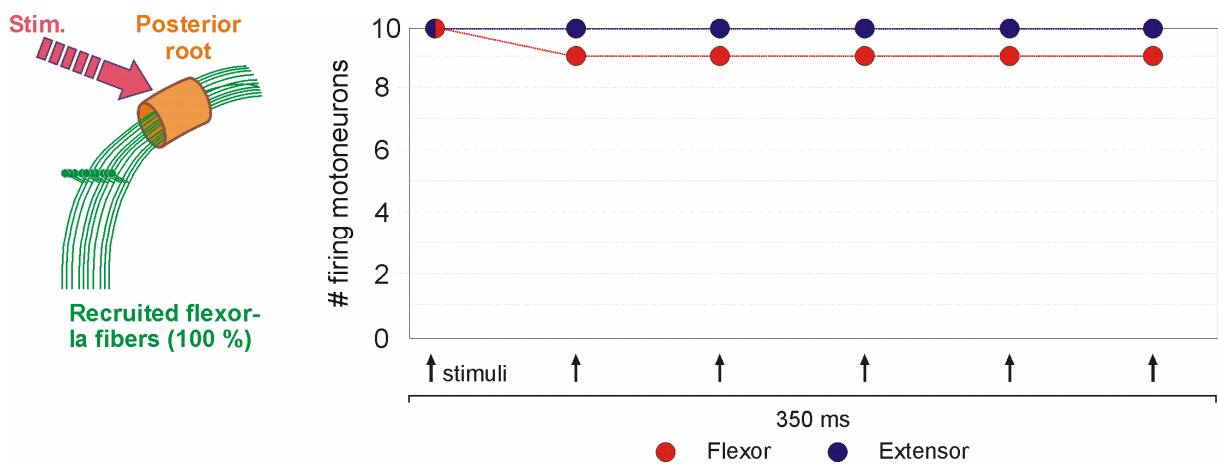
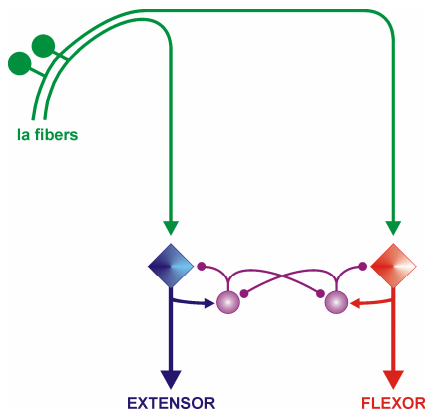


Figure 32. Firing patterns of flexor (red) and extensor (blue) motoneuron pools in response to maximum stimulation corresponding to the recruitment of 100% of the respective Ia fibers. The maximum flexor output is reduced to 90% of that in the model not considering recurrent inhibition. No changes were observed in the extensor.

The same model calculated with a simplified approach to the simulation of recurrent inhibition is presented in *Appendix B*.

Model IV: The effect of recurrent inhibition including mutual inhibition between ‘opposite’ Renshaw cells populations on the output of two antagonistic motoneuron pools



The results described above identified Renshaw cells as neural elements efficiently generating simple periodic patterns within a single motoneuron pool. In particular, no additional inputs originating from antagonistic sources were required to induce the observed response modulations. Hence, the question arises as to whether the activity of two populations of Renshaw cells connected with mutual inhibition may be sufficient to produce simple periodic interactions between two antagonistic motoneuron populations. To approach this question, a network consisting of two symmetric circuits

was first assumed. Under such conditions, both circuits had symmetric numbers of interconnections that were designed in separate simulation runs as to be either associated with the flexor or the extensor. Each of the circuits was designed similarly to the network employed in *Model III*, but additionally contained interconnections between ‘opposite’ Renshaw cells. Subsequently, the network was modified as to include one flexor and one extensor circuit and hence asymmetric numbers of interconnections between the modeled neuron populations.

Model IV produced two main findings:

- (i) If two symmetric reflex circuits with equal parameter settings (either flexor or extensor ones) were assumed, the system output was generally characterized by in-phase-modulations of the antagonistic circuits.
- (ii) In case of two asymmetric flexor and extensor reflex circuits the system revealed a strong tendency towards reciprocal actions.

Coming back to the model considering two symmetric motor pools, some minor differences were observed, depending on whether two flexors circuits (Figure 33) or two extensors circuits (Figure 34) were considered. In a first approach, 30% of the respective Ia fibers were recruited (corresponding to the common threshold of the flexor circuits and 1.5 times that of the extensor circuits). Different simulation runs were carried out with the compositions of the active afferents being different. As for two flexor circuits, three of the four examples tested with different afferents contributing to the 30%-population showed in-phase modulations of the produced outputs (Fig. 33a, b), and constant outputs in the remaining example (Fig. 33c). At the same time, simple in-phase modulations were observed in 100% of all cases if two extensor circuits were assumed. An interesting common feature of this model (irrespective of whether two flexor or two extensor reflex circuits were considered for the calculation) was that the modulations appeared more

pronounced the fewer of the recruited Ia fibers were part of the respective major innervation zones (cf. Fig. 33b, Fig. 34b, d).

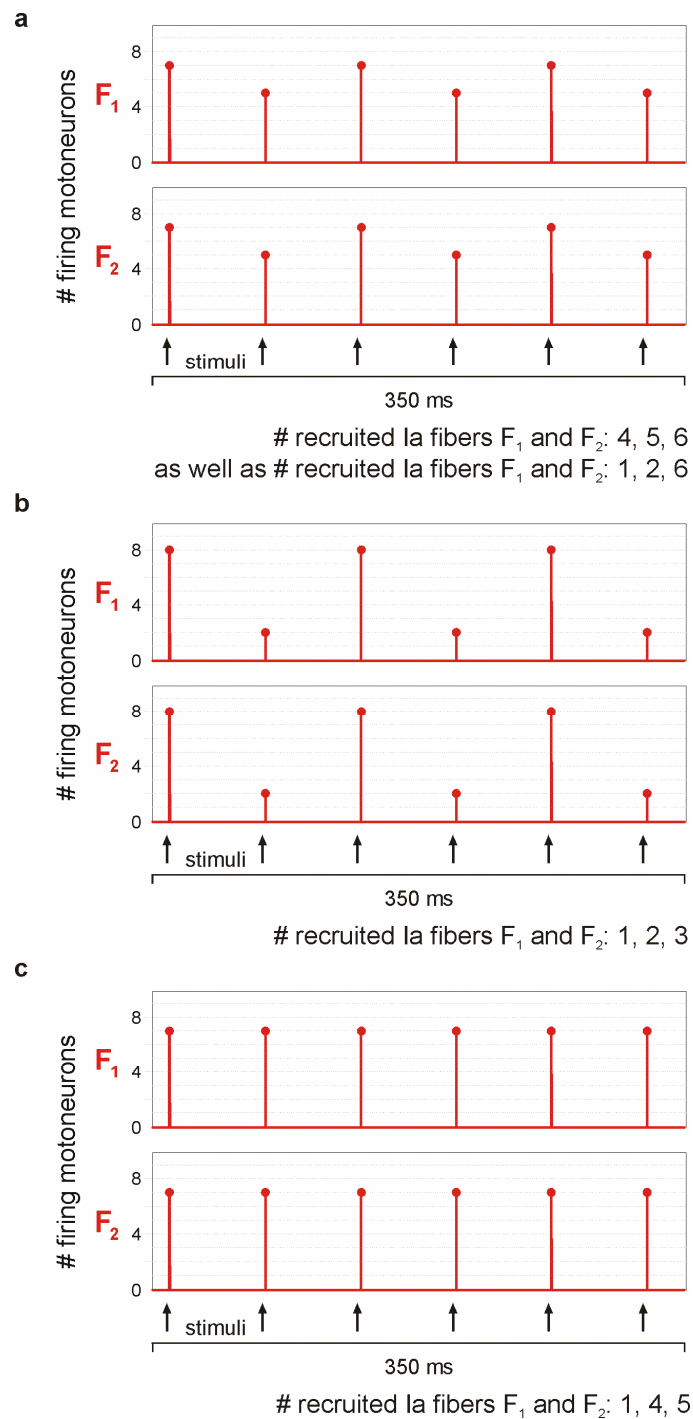
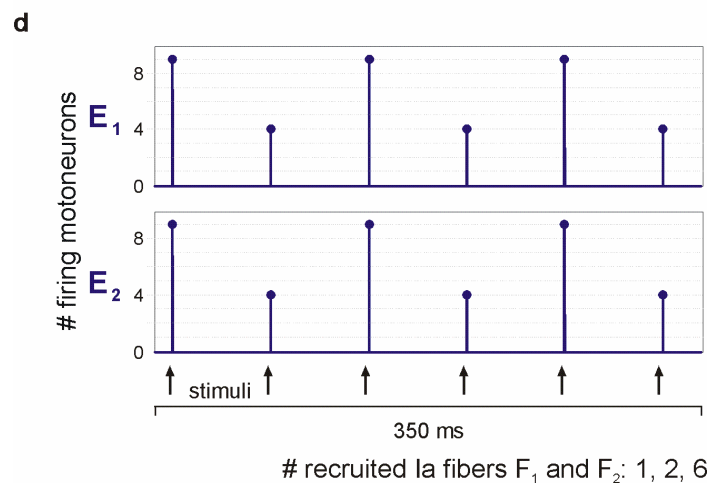
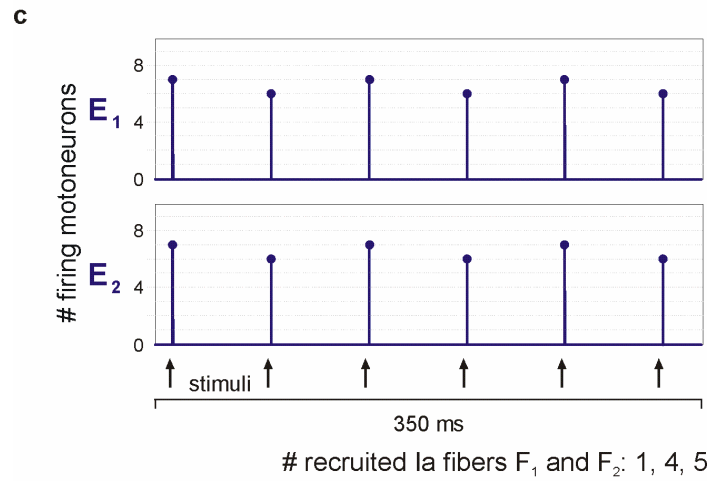
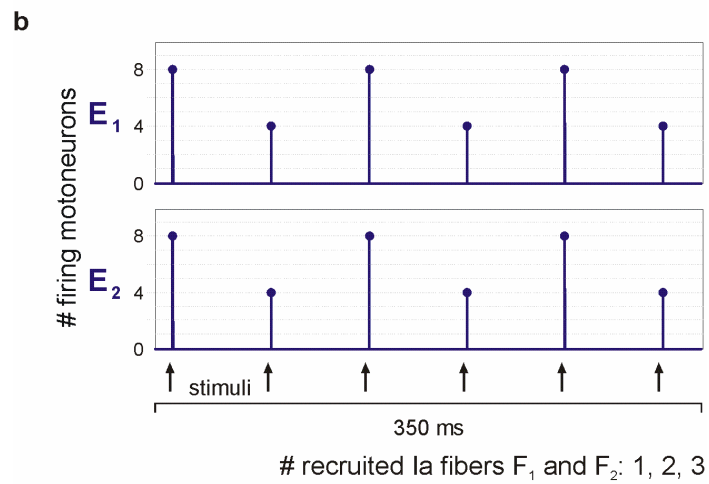
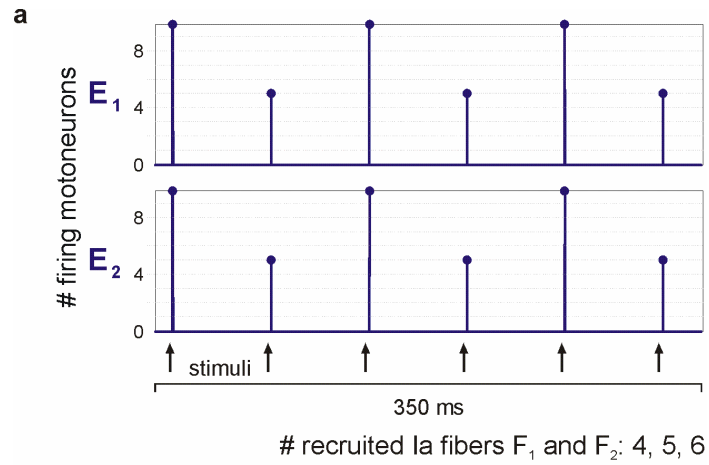


Figure 33. Firing patterns of a model considering two symmetric antagonistic circuits designed both as ‘flexors’ (F_1 and F_2) in response to stimulation at common threshold intensity (i.e., 30% of the two Ia fiber populations recruited). The general result observed in the majority (75%) of all tested cases was characterized by in-phase modulations of the outputs produced by the antagonistic motoneuron populations. Examples from top to bottom differ in the selection of the particularly recruited Ia fibers (i.e., with respect to the major innervation zone, fibers 4-7) that contributed to the 30%-afferent population.



◀ **Figure 34.** Firing patterns of a model considering two symmetric antagonistic motor pools designed with extensor connectivities (E_1 and E_2) in response to stimulation at 1.5 times the common threshold intensity (i.e., 30% of antagonistic Ia fibers recruited). In 100% of all tested cases, in-phase modulations of the antagonistic motoneuron populations occurred. Examples from top to bottom differ in the selection of the particularly recruited Ia fibers (i.e., with respect to the major innervation zone, fibers 4-7).

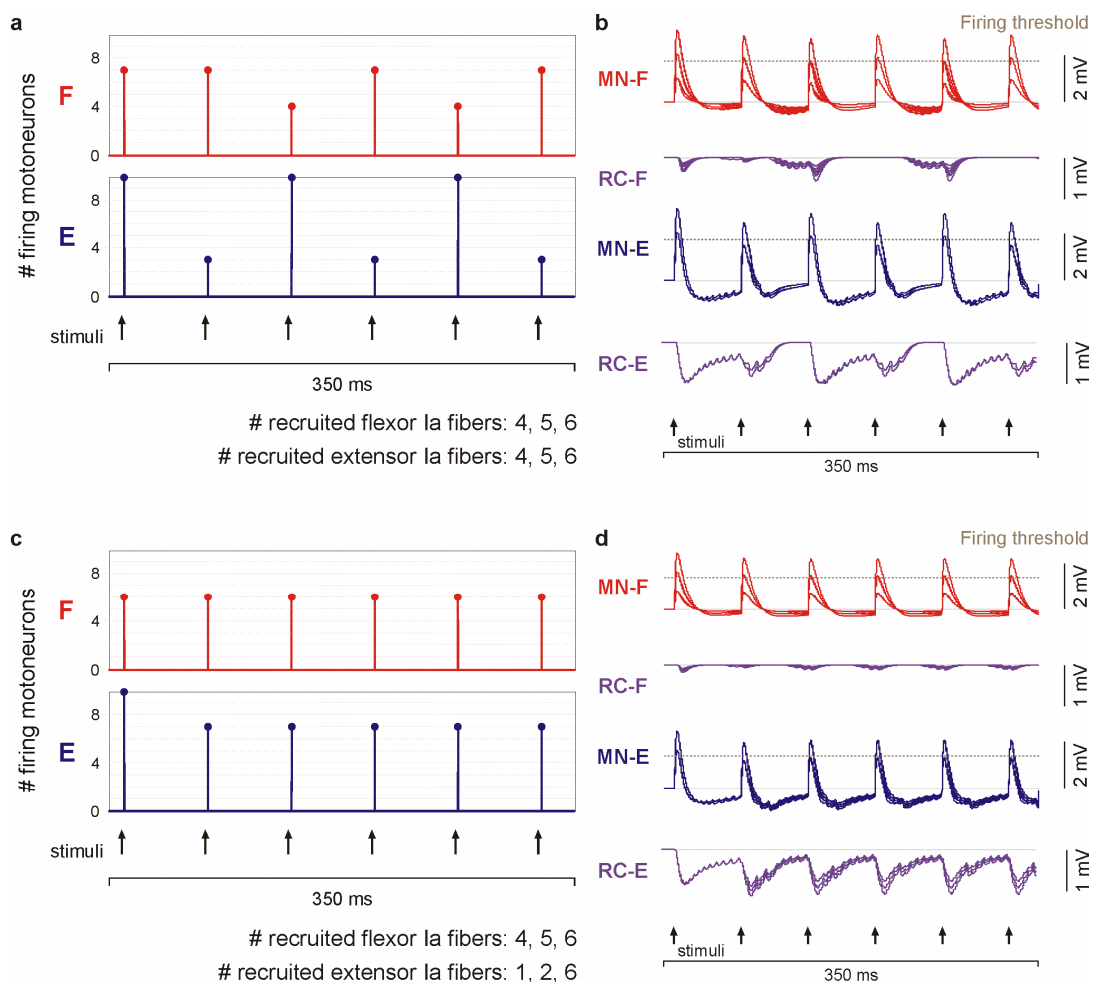
In the network model composed of one flexor and one extensor circuit, the simple periodic pattern most frequently observed was characterized by reciprocal interactions. In few cases, a pattern was produced that featured an attenuated excitability of one of the two motoneuron populations following every second stimulus application. In few cases, a pattern was produced with alternation of large and small responses in a single motor pool. The output of the antagonistic motor pool, at the same time, was completely constant. No cases with in-phase modulations as generated by the symmetric network were observed.

At common threshold intensity of the network (i.e., recruitment of 30% of flexor and extensor Ia fibers, respectively), 50% of all tested examples featured reciprocal motor patterns (Figure 35). In particular, the generation of a particular motor pattern could be directly linked to the activation of specific Ia fibers associated with the extensor: if at least two third of them were part of the extensor major innervation zone, then the output was always reciprocally modulated (Fig. 35*a, b*). Thus, stronger synaptic connections along with an effective generation of PSPs (stronger excitatory drive) of one afferent population with respect to the antagonistic one favored the generation of reciprocal motor outputs. In all other cases, the output was never patterned (Fig. 35*c, d*). With other words, the activity of the dominant (with respect to the relatively larger numbers of internal interconnections) extensor circuit was the determining factor in the generation of particular motor outputs in the two antagonists.

Whenever reciprocal interactions were induced, the extensor motor pool featured stable output modulations starting with the application of the first pulse, i.e., a strong activation of motoneurons by the first pulse, and a weaker one by the subsequent one. The flexor motoneurons, on the other hand, fired in relatively large numbers to the first two stimuli and featured modulated outputs thereafter. This finding can be explained by the effective activity of extensor Renshaw cells following the intense monosynaptic activation of homonymous motoneurons by Ia fibers following the first stimulus. The Renshaw cells would in turn not only reduce the motoneuron excitability, but would also inhibit antagonistic cells of the same type. Consequently, while the output of the extensor motoneuron pool would be moderate in response to the next stimulus, that of the flexor circuit – not affected by recurrent inhibition – would not be reduced. The smaller number of extensor motoneurons would recruit fewer Renshaw cells, while this situation would be just opposite in the flexor circuit, eventually leading to the observed reciprocal network

behavior. A representative example illustrating the emergence of such periodic reciprocal pattern is given in Figure 35a.

Constant motor outputs of the antagonistic circuits were observed if the majority of the recruited extensor Ia fibers were not associated with the major innervation zone, i.e., under conditions when the excitatory drive provided by Ia fibers projecting on extensor motoneurons was somewhat less effective (Fig. 35b). The underlying mechanisms might be explained as follows: In response to the first stimulus, 100% of all extensor motoneurons were recruited. These would in turn activate a considerable subset of Renshaw cells. The reduced number of motoneurons firing in response to the next stimulation pulse would still transsynaptically activate a considerable subpopulation of homonymous Renshaw cells that would have similar effects on the motoneuron excitability as the recurrent inhibitory event following the preceding stimulus. Regarding the flexor, the recurrent inhibition of Renshaw cells exerted by the extensor would be at any time as strong as to almost fully suppress their activity. Hence, the flexor motoneuron output would be less subjected to their inhibitory inputs. A stable state of activity would be achieved.

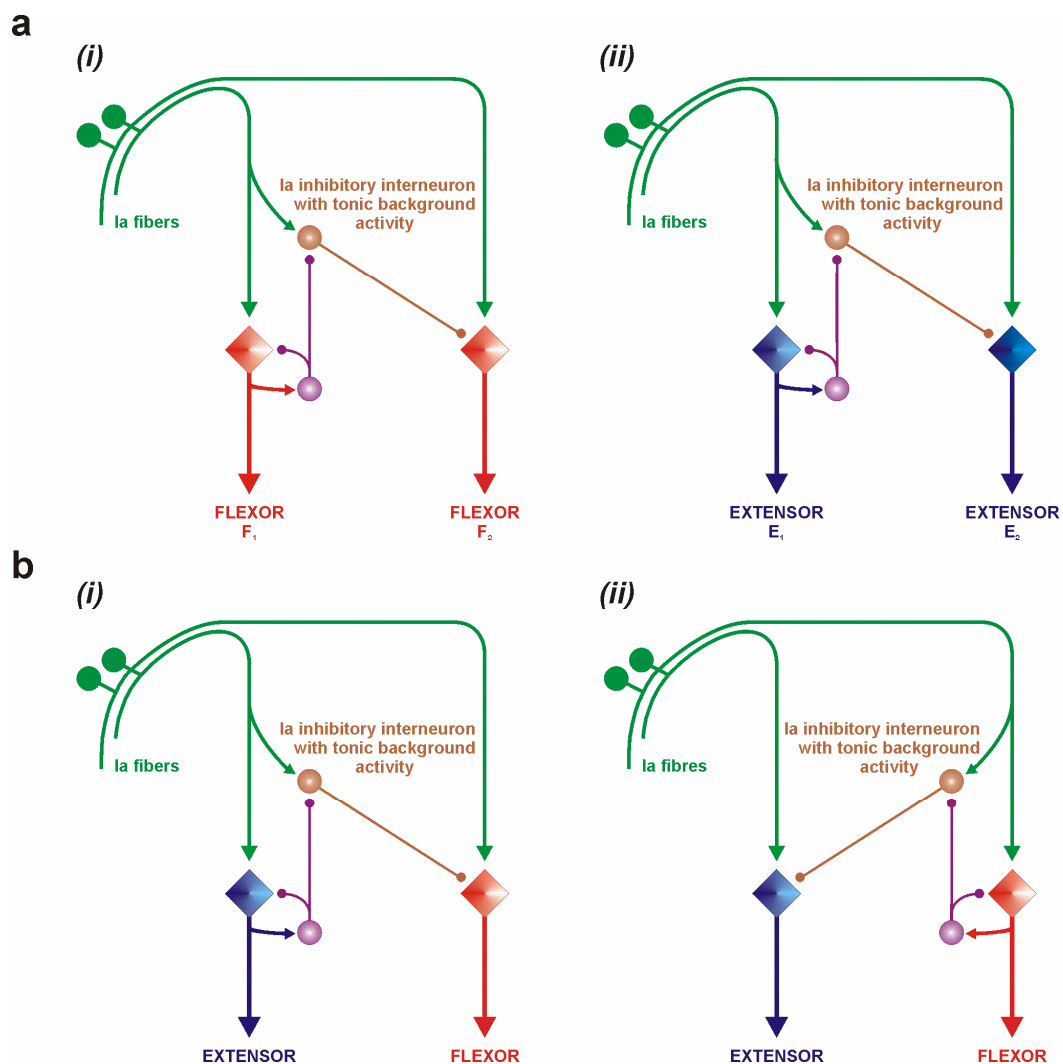


◀ **Figure 35.** Firing patterns of a model considering two asymmetric antagonistic systems designed as flexor (*F*) and extensor (*E*) circuits, respectively. The applied stimulation intensity corresponded to the system's common threshold (i.e., attained if 30% of each population of Ia fibers were recruited). **a** Numbers of flexor and extensor motoneurons firing in response to consecutively applied stimuli feature reciprocal modulations. **b** Reciprocity was mainly due to the strong recurrent inhibition exerted by extensor Renshaw cells on homonymous motoneurons and antagonistic cells of the same type. **c** Unmodulated motor outputs were observed, if the majority of the recruited extensor Ia fibers were not part of the major innervation zone of the extensor. **d** Under such conditions, the totally induced recurrent inhibition via extensor Renshaw cells was too weak as to considerably decrease the excitability of homonymous motoneurons, but still effectively suppressed antagonistic Renshaw cells. MN-F, MN-E, denoting total postsynaptic potentials of flexor and extensor motoneuron pools, respectively; RC-F, RC-E, the activity of antagonistic Renshaw cells.

Increasing the number of recruited extensor Ia fibers to 40% of the total population, but leaving the corresponding value for the flexor Ia fibers unchanged at 30%, 20 simulation runs resulted exclusively in constant motor outputs. If the applied stimulation was assumed to be more effective in recruiting flexor (40% or 60% of the respective fibers being recruited) than extensor Ia fibers (30%), the results were completely different. Reciprocal modulations were observed in 50% of all tested examples (irrespective of whether 40% or 60% of all flexor Ia fibers were recruited) and were hence the commonly induced pattern. Constant motor outputs were observed in 45% of all cases assuming 40% of flexor Ia fiber recruitment and in 40% of the examples assuming the higher stimulation effects. In both cases, one example featured constant outputs in the flexor, but modulated outputs in the extensor.

Model V: The effect of recurrent facilitation

The networks elaborated above were isolated from the effects of Ia inhibitory interneurons. When taking into account the efficacy of Renshaw cells in inhibiting homonymous Ia interneurons along with their ability to induce patterned motor outputs, one can assume recurrent facilitation (cf. *Introduction*) to be an additional promising candidate-mechanism leading to the generation of simple periodic patterns. This hypothesis was approached in several steps (Figure 36), similar to those in *Model IV*: First, two symmetric reflex circuits (either with flexor or extensor characteristics) were assumed (Fig. 36a (i), (ii)). The motoneurons of one of the two circuits made synaptic contacts to a population of Renshaw cells which in turn exerted inhibitory actions back on the motoneurons and on homonymous Ia inhibitory interneurons. The antagonistic motoneuron population, on the other hand, received excitatory drive transmitted by Ia fibers and was affected by reciprocal inhibition. Second, the two circuits of the network were asymmetrically designed as flexor and extensor (Fig. 36b). The effect of recurrent facilitation, i.e., the inhibition of extensor (Fig. 36b (i)) and flexor (Fig. 36b (ii)) Ia interneuron pools was tested in separate trials.



◀ **Figure 36.** Organization of model network testing the effect of recurrent facilitation on the produced motor output. **a** First, two symmetric circuits (either (i), two flexors F_1 and F_2 ; or (ii), two extensors E_1 and E_2) were assumed. **b** Second, the symmetry was replaced by introducing a flexor and an extensor circuit. The effect of recurrent facilitation exerted by (i) extensor or (ii) flexor Renshaw cells was tested in different simulation runs.

As for the symmetric network (two flexor or two extensor circuits), three cases (all of them tested at threshold intensity) were assumed that varied in the selection of the particularly recruited Ia fibers: (i) F_1 and F_2 (E_1 and E_2 , respectively), all recruited Ia fibers were part of the corresponding major innervation zones; (ii) F_1 (E_1 , respectively), all recruited Ia fibers were part of the major innervation zone, and F_2 (E_2 , respectively), all recruited Ia fibers were located outside the major innervation zone; and (iii) F_1 and F_2 (E_1 and E_2 , respectively), all recruited Ia fibers were outside the major innervation zones.

As a common finding, reciprocal motor outputs were always generated in cases with all of the recruited Ia fibers belonging to the major innervation zones (Figure 37). Otherwise, the outputs were constant. A difference between either two flexor or two extensor circuits, however, could be found in the initial phases of the simple periodic patterns: If two flexor circuits were assumed, the generated output resembled that observed in *Model IV* and displayed in Figure 35a; while one of the two motoneuron populations featured modulations as from the first stimulus application, the other one fired in relatively large numbers in response to the first two pulses and only afterwards featured response modulations (Fig. 37a). At the same time, if two extensor circuits were assumed, both motoneuron pools immediately produced patterned outputs (Fig. 37b). This difference can be explained by the relatively stronger inhibitory effect of the tonic background activity exerted by extensor Ia interneurons than by the flexor-associated ones. Consequently, recurrent facilitation mediated via extensor Renshaw cells would have a comparatively bigger effect and would lead to a considerable disinhibition of antagonistic motoneurons. The latter would in turn fire in large number in response to the successive second stimulation pulse.

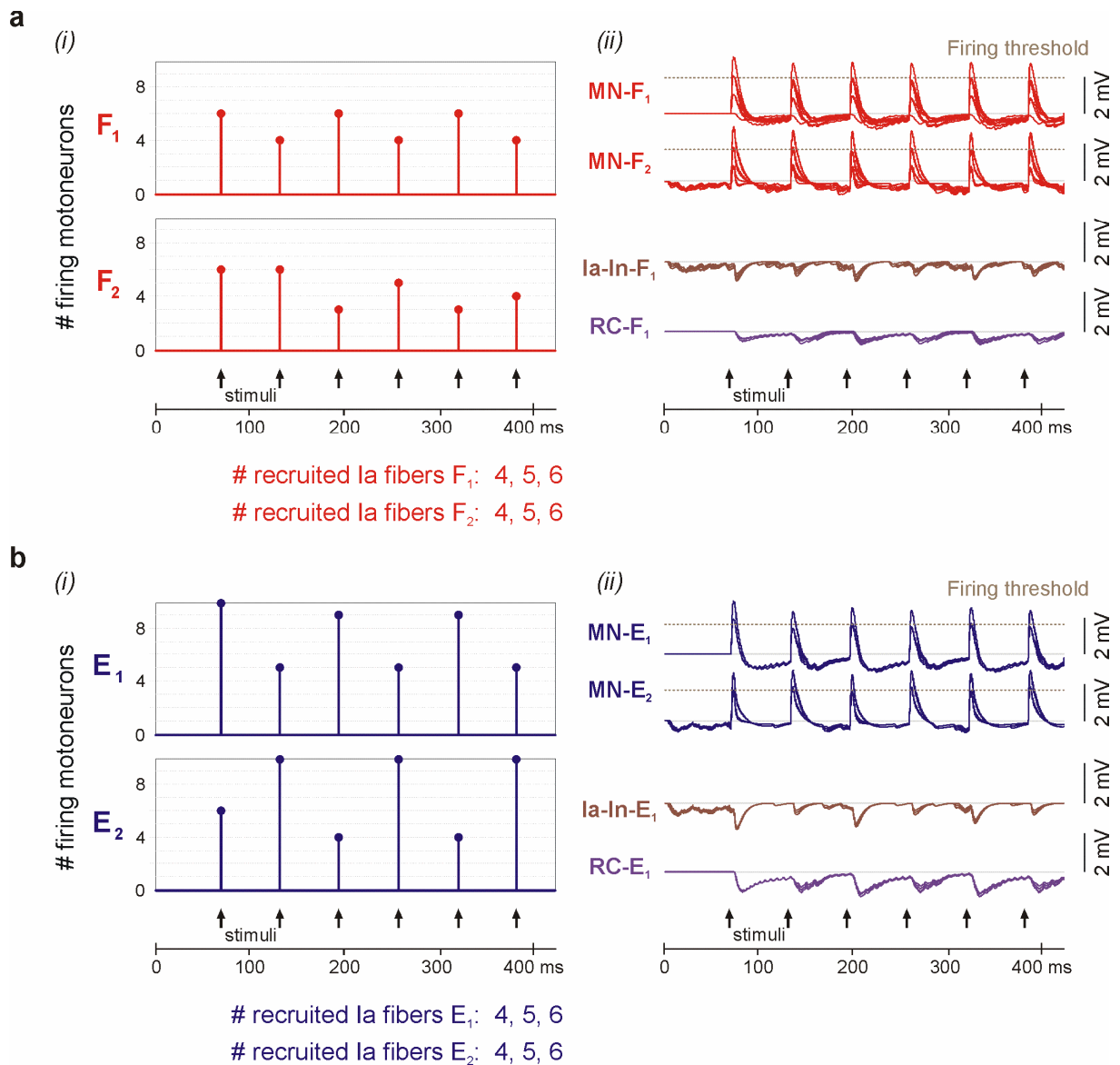


Figure 37. Firing patterns of a model including two symmetric antagonistic circuits as well as recurrent facilitation. Modulations of the system output were induced if both motoneuron populations were exclusively excited by Ia fibers within the respective major innervation zones. **a** Example derived from a network consisting of two flexor circuits F_1 and F_2 . (i) As can be seen in the sketch illustrating the numbers of motoneurons firing in response to successive stimuli, reciprocal interaction is established with the second stimulation pulse. (ii) Total postsynaptic potentials of both flexor motoneuron populations MN- F_1 and MN- F_2 along with the activity of Ia inhibitory interneurons and Renshaw cells revealed the underlying mechanisms producing the patterned outputs. **b** Same example as in *a*, but derived from a network made up of two extensor circuits E_1 and E_2 . Here, reciprocal interactions are initiated following the first stimulus.

If the antagonistic circuits were asymmetrically designed including flexor as well as extensor circuits, the model did not produce periodic output patterns in 11 out of 20 simulation runs. There were some differences between the two models whether they included extensor (cf. Fig. 37*b* (i)) or flexor (cf. Fig. 37*b* (ii)) interneuronal populations. Whenever periodically modulated motor outputs were produced in the former case (i.e., extensor interneurons considered), they were rather stable throughout the whole simulations (Figure 38). At the same time, the results obtained for the second model (i.e., flexor interneurons considered) revealed less steady reciprocal patterns (Figure 39). This finding could be probably due to the smaller number of interconnections between Renshaw cells and Ia interneurons in the flexor which would lead to a less pronounced effect of recurrent facilitation. Modulations in a single motoneuron pool as well as constant outputs of the flexor and the extensor circuits, on the other hand, were stably elicited. Table 3 summarizes all tested examples and induced motor patterns.

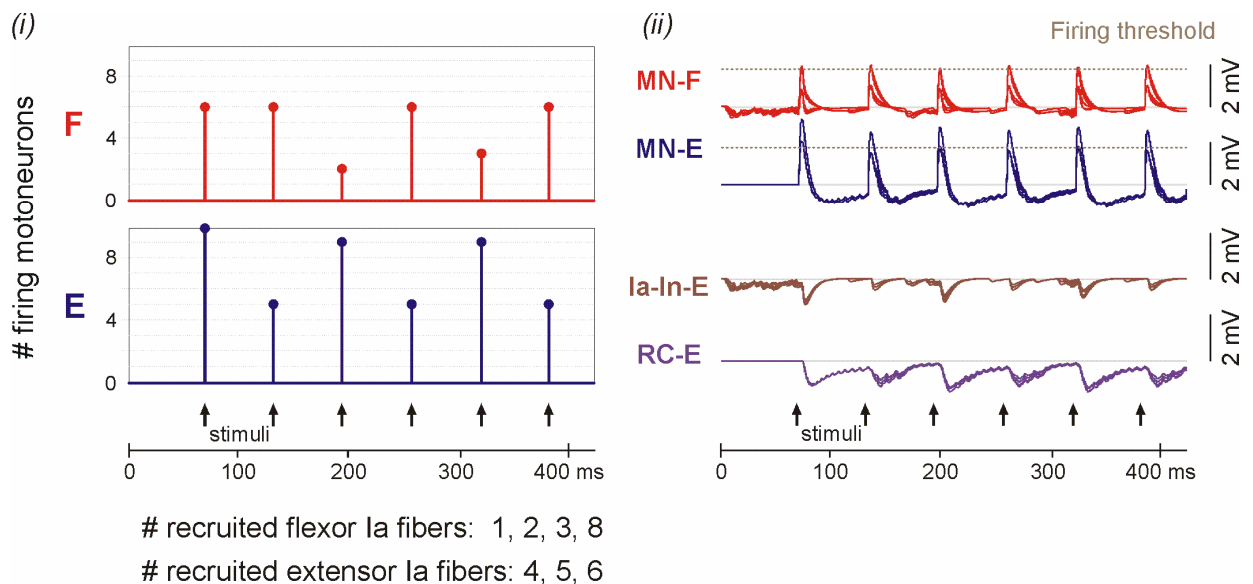


Figure 38. Stable reciprocal patterns elicited by a model including extensor Ia inhibitory interneurons and Renshaw cells. (i) Numbers of flexor (*F*) and extensor (*E*) motoneurons firing in response to successive stimuli along with (ii), total postsynaptic potentials of flexor (*MN-F*) and extensor (*MN-E*) motoneuron pools as well as of extensor Ia interneurons (*Ia-In-E*) and Renshaw cells (*RC-E*).

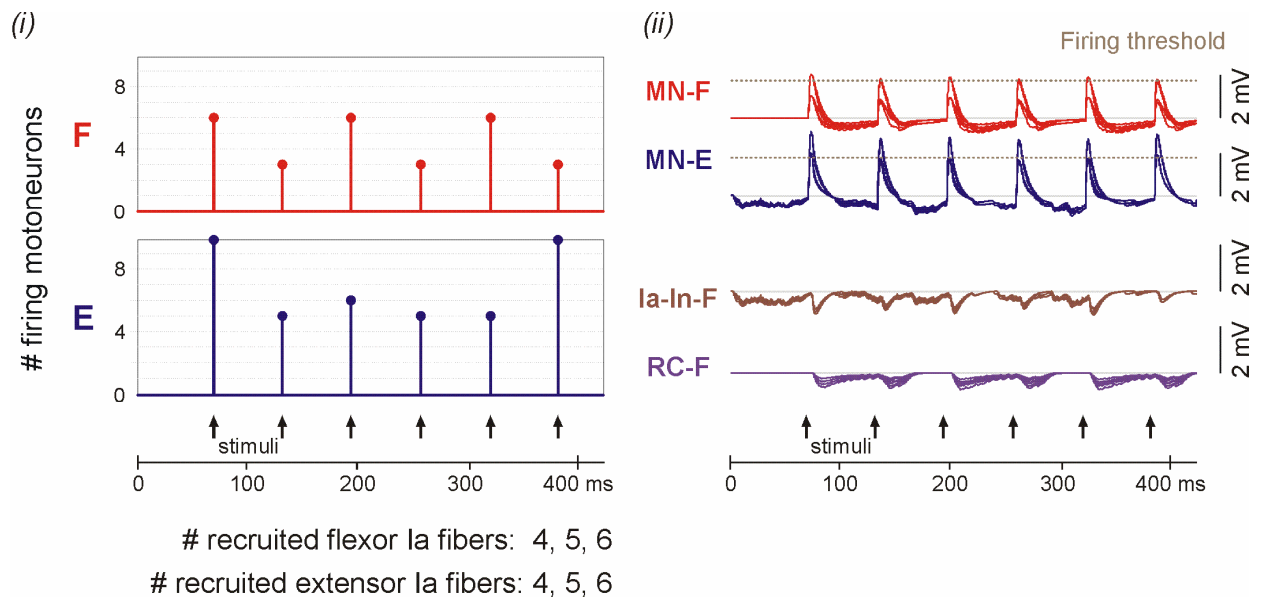
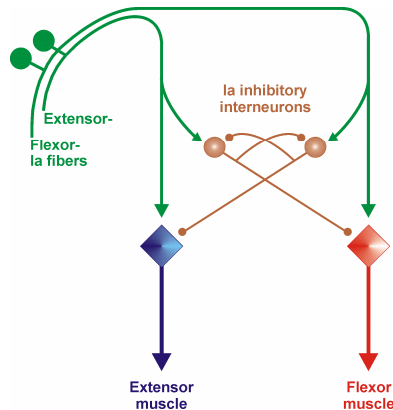


Figure 39. Reciprocal interactions between antagonistic flexor (F) and extensor (E) motoneuron pools of a model including flexor interneuronal populations. Note the fluctuations of extensor motoneuron recruitment as illustrated in (i). Total postsynaptic potentials of flexor ($MN-F$) and extensor ($MN-E$) motoneuron pools as well as of flexor Ia interneurons ($Ia-In-F$) and Renshaw cells ($RC-F$) are displayed in (ii).

Table 3. The effect of recurrent facilitation on the firing patterns of a network composed of flexor and extensor monosynaptic circuits.

A Extensor Renshaw cells and Ia interneurons included in the model network			
# recruited flexor Ia fibers	# recruited extensor Ia fibers	# flexor motoneurons firing in response to successive stimuli	# extensor motoneurons firing in response to successive stimuli
4, 5, 6	4, 5, 6	6-6-2-6-3-6	10-5-9-5-9-5
4, 5, 6	1, 2, 3	1-1-1-1-1-1	10-4-4-4-4-4
4, 5, 6	4, 5, 6, 7	6-6-6-6-6-6	10-10-10-10-10-10
4, 5, 6	1, 2, 3, 8	1-1-1-1-1-1	10-7-7-7-7-7
4, 5, 6, 7	4, 5, 6	6-6-6-6-6-6	10-5-9-5-9-5
1, 2, 3, 8	4, 5, 6	6-6-2-6-3-6	10-5-9-5-9-5
1, 2, 4, 5, 6, 7	4, 5, 6, 7	4-6-6-6-6-6	10-10-10-10-10-10
1, 2, 3, 8, 9, 10	4, 5, 6, 7	4-6-6-6-6-6	10-10-10-10-10-10
1, 2, 4, 5, 6, 7	1, 2, 3, 8	1-1-1-1-1-1	10-7-7-7-7-7
1, 2, 3, 8, 9, 10	1, 2, 3, 8	1-1-1-1-1-1	10-7-7-7-7-7
B Flexor Renshaw cells and Ia interneurons included in the model network			
4, 5, 6	4, 5, 6	6-3-6-3-6-3	10-5-6-5-5-10
4, 5, 6	1, 2, 3	8-1-1-1-1-1	4-4-4-4-4-4
4, 5, 6	4, 5, 6, 7	6-3-6-3-6-3	10-10-10-10-10-10
4, 5, 6	1, 2, 3, 8	8-1-1-1-1-1	7-7-7-7-7-7
4, 5, 6, 7	4, 5, 6	6-3-6-3-6-3	10-5-6-5-5-10
1, 2, 3, 8	4, 5, 6	6-3-6-3-6-3	10-5-6-5-5-10
1, 2, 4, 5, 6, 7	4, 5, 6, 7	6-3-6-3-6-3	10-10-10-10-10-10
1, 2, 3, 8, 9, 10	4, 5, 6, 7	6-3-6-3-6-3	10-10-10-10-10-10
1, 2, 4, 5, 6, 7	1, 2, 3, 8	8-1-1-1-1-1	7-7-7-7-7-7
1, 2, 3, 8, 9, 10	1, 2, 3, 8	8-1-1-1-1-1	7-7-7-7-7-7

Model VI: The effect of mutual reciprocal Ia inhibition



Before studying the complete the model, a network neglecting the influence of Renshaw cells, but considering populations of antagonistic Ia interneurons as well as mutual inhibition between these cells was tested. Again, the complexity of this model was stepwise increased by assuming first two ‘equal’ network circuits (i.e., two flexors or two extensors), and second, by introducing asymmetry to the model by designing one of the two circuits as flexor and the one other as extensor.

Except for the network composed of two flexor circuits, the majority of the simulated networks did not yield in simple periodic output patterns in the antagonistic motor pools. In the former case, most of the tested examples featured modulations in the output of one of the two motoneuron populations only, and constant outputs in the antagonistic one (Figure 40a). In a single case, a reciprocal pattern was detected (Fig. 40b). All other examples featured unstable outputs produced by one of the motoneuron populations, and either modulated or non-patterned outputs in the antagonistic one (Fig. 40c). As opposed to that, the outputs produced by two antagonistic extensor circuits were always constant (Fig. 40d). With other words, constant numbers of However, these numbers of motoneurons firing in response to the successively applied stimuli could be different in the two motoneuron populations considered.

If one of the antagonistic motor pools was designed as flexor and the other one as extensor, the results were similar to those obtained for two extensor circuits. The most commonly observed outputs were constant (Figure 41). In exceptional cases, they featured some instability affecting the output of one motoneuron population, whereas that of the antagonistic one was unmodulated.

Figure 40. Motor patterns elicited in a network composed of two symmetric circuits (*a-c*, two flexors; *d*, two extensors) and considering mutual reciprocal Ia inhibition. **a** The pattern most frequently evoked in case of two antagonistic flexor motor pools was characterized by modulated outputs in one, and unmodulated stable outputs in the antagonistic motoneuron population. **b** In one case, a reciprocally modulated pattern was observed. **c** All other examples revealed either constant or periodically modulated outputs in one motoneuron pool, with unstable outputs in the antagonistic one. **d** In case of a network composed of two extensor circuits, the output was always stable and unmodulated. ►

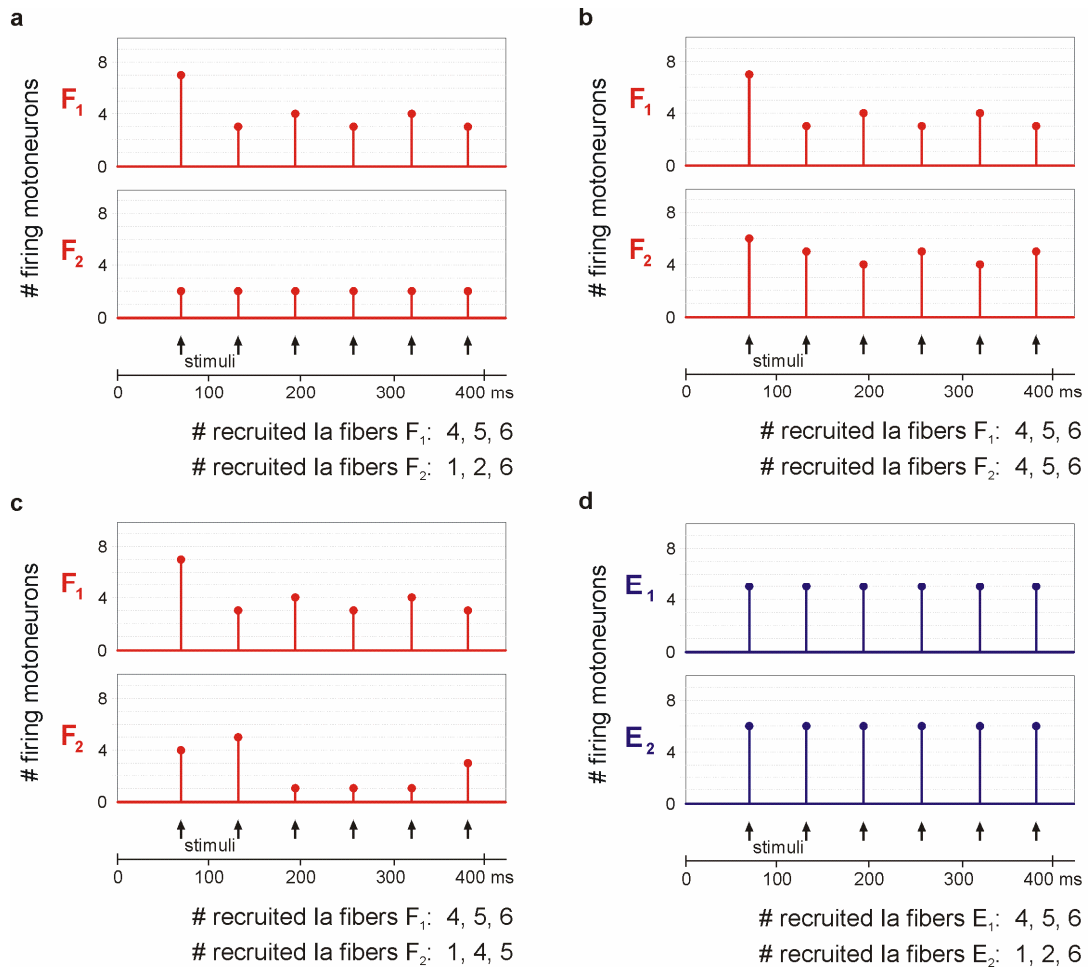
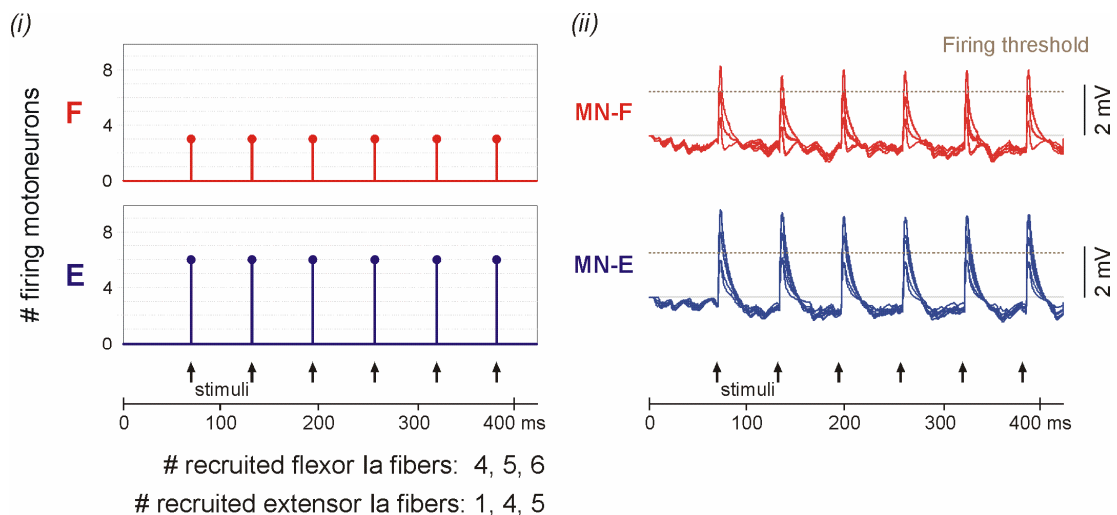
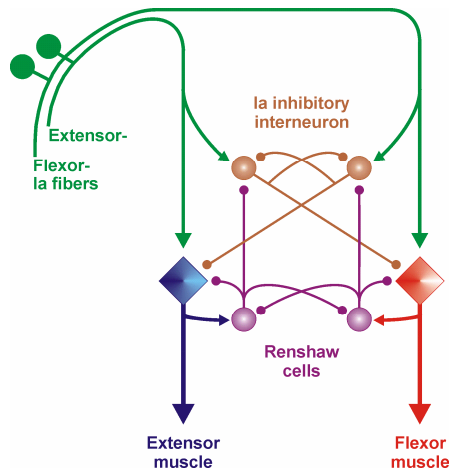


Figure 41. Networks composed of flexor and extensor monosynaptic circuits connected by mutual reciprocal Ia inhibition most frequently generated constant motor outputs. (i) illustrates the numbers of motoneurons of each pool firing in response to successive stimuli. (ii) shows total postsynaptic potentials at the motoneuronal level composed of excitatory drive provided by Ia afferent fibers and inhibitory actions exerted by Ia interneurons. ▼



Model VII: The complete network model



The network model integrating the operation of all neuronal populations produced simple periodic patterns only in exceptional cases. Moreover, all generated periodic patterns featured anti-phase alternation of the responses in the antagonistic motor pools.

A new feature of the model network was the generation of motor outputs with considerable variations in the numbers of motoneurons responding to successive stimuli. Networks consisting of two symmetric flexor circuits resulted in such motoneuron firings (Figure 42).

The applied stimulus intensity in the illustrated example was assumed to correspond to the common threshold and all of the recruited Ia fibers were part of the major innervation zones. Under otherwise same conditions, but when assuming two symmetric extensor circuits, the produced motor outputs featured near-perfect reciprocity (Figure 43). In particular, the pattern was established as with the first stimulus application.

Figure 42. Firing patterns of the complete network model with two symmetrical flexor circuits. **a** Variable numbers of motoneurons associated with the antagonistic motor pools fired in response to successive stimuli. **b** shows the total postsynaptic potentials at motoneuronal levels ($MN-F_1$ and $MN-F_2$, red) as the sum of excitatory and various inhibitory inputs. **c** and **d** illustrate the activities of Ia interneurons ($Ia-In-F_1$ and $Ia-In-F_2$, brown) and Renshaw cells ($RC-F_1$ and $RC-F_2$, violet) associated with the two motor pools. Renshaw cells received inhibitory input only from antagonistic cells of the same type, Ia interneurons were affected by their antagonistic counterparts as well as by homonymous Renshaw cells. ►

Figure 43. Firing patterns of two symmetrically designed extensor circuits. **a** A stable reciprocal pattern was elicited as with the application with the first stimulus. **b** shows the total postsynaptic potentials at motoneuronal levels ($MN-E_1$ and $MN-E_2$, blue) as the sum of excitatory and various inhibitory inputs. **c** and **d** illustrate the activities of Ia interneurons ($Ia-In-E_1$ and $Ia-In-E_2$, brown) and Renshaw cells ($RC-E_1$ and $RC-E_2$, violet), respectively. ►►

Figure 42.

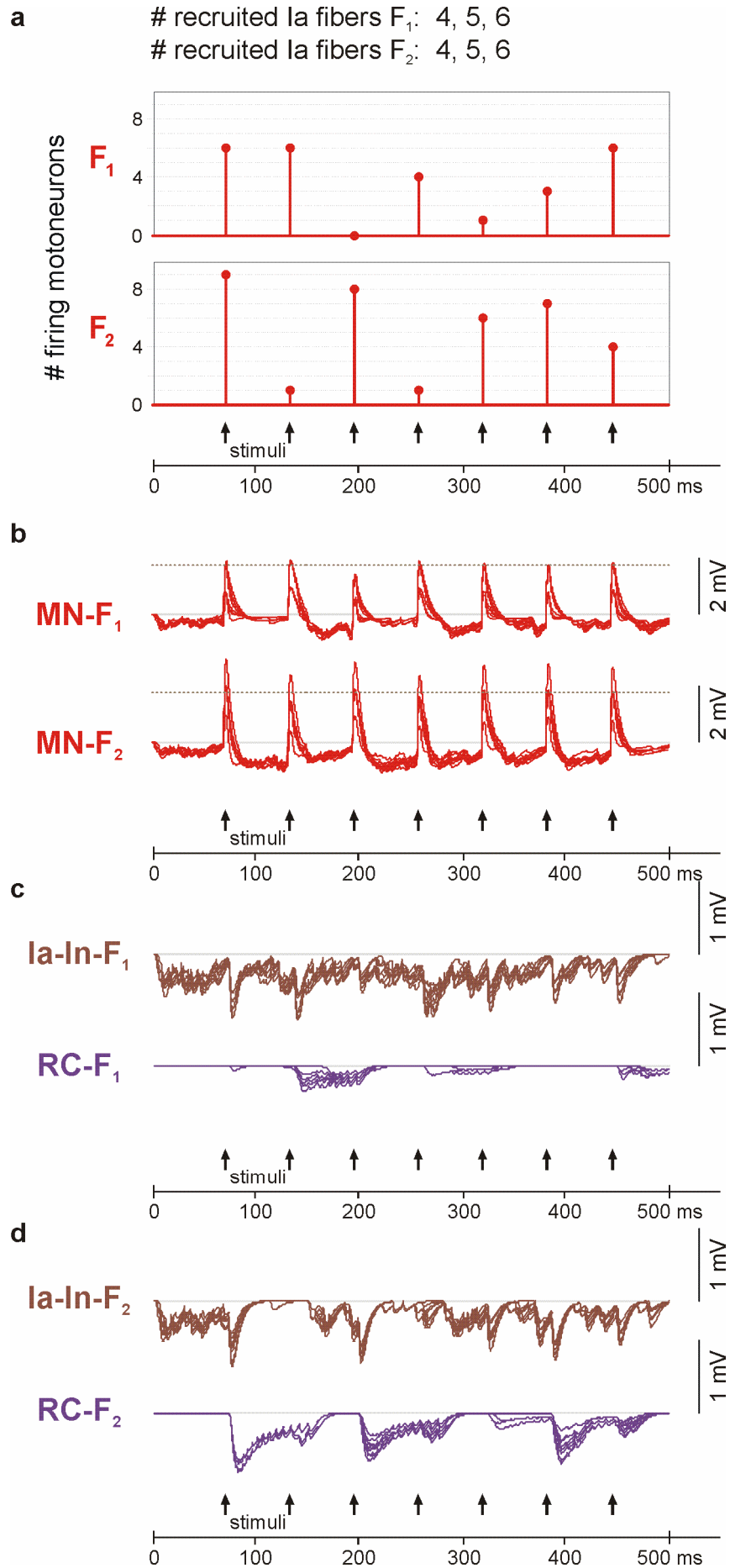
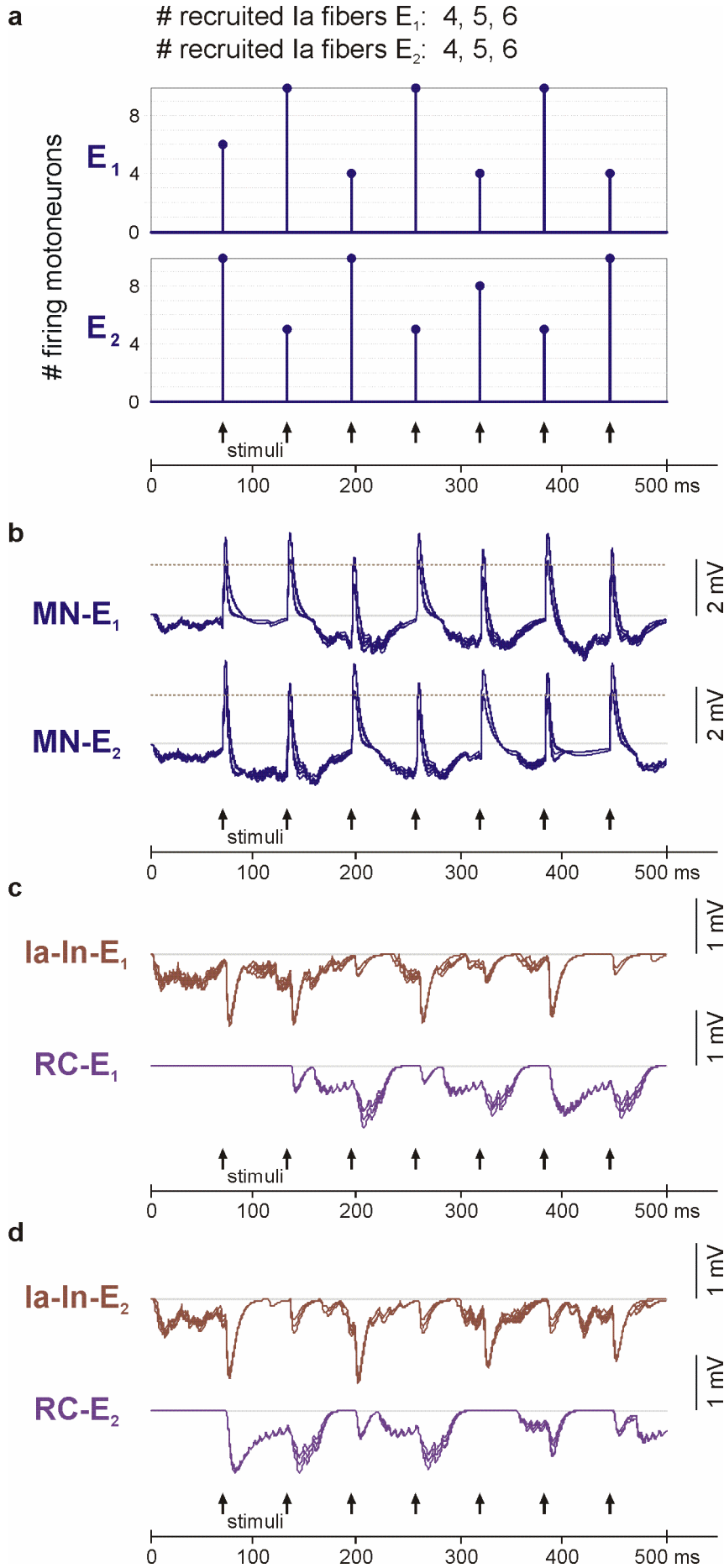


Figure 43.



The complete network model with flexor and extensor connectivities did not produce simple periodic patterns with anti-phase alternation of the responses in the antagonistic motor pools (Figures 44, 45, and 46). The output of the extensor motoneuron population featured only minor variations in most simulation runs, irrespective of the applied stimulation intensities and the activation of particular Ia fibers with respect to the major innervation zone. Recruitment of motoneurons within the extensor pools was further characterized by high efficacy, with 100% of the population firing in most cases. On the other hand, the outputs of the flexor motoneuron population were subject to stronger inhibitory influences that could even lead to complete suppression in a random sequence in response to the repetitive stimulus application. Otherwise, the flexor-output did not modulate with the simple patterns either. Only with the maximum afferent input the flexor motoneuron pool would be recruited to a degree that 80% of the motoneurons would fire.

The PSPs generated by the Renshaw cells in their target motoneurons as well as in the antagonistic neurons of the same type played a major role in shaping the motor outputs with simple periodic patterns. In the asymmetric complete network model, ongoing tonic background activity of Ia inhibitory interneurons was imposed upon the whole network system – even before the first stimulus was applied –, thereby reducing Renshaw cell activities. Due to the strong effect of flexor motoneurons suppression by the antagonistic Ia interneurons, the role of flexor Renshaw cells was particularly knocked out at moderate afferent inputs delivered to the system. Stronger stimulation, required to overcome this inhibition, resulted in constant motor outputs as was also experienced from the simulation results of the reduced models.

Figures 44-46. Firing patterns of a network model composed of two asymmetric circuits with flexor and extensor connectivities. The three representative results differ in the number of the activated afferents delivering input to the circuits as well as the composition of the specific fibers active. **a** Numbers of motoneurons of the two antagonistic populations firing in response to successive stimuli. **b** shows the total postsynaptic potentials at motoneuronal levels (*MN-F*, red; and *MN-E*, red) as the sum of excitatory and various inhibitory inputs. **c** and **d** illustrate the PSPs produced by the activities of Ia interneurons (*Ia-In-F* and *Ia-In-E*, brown) and Renshaw cells (*RC-F* and *RC-E*, violet) associated with the two motor pools. Renshaw cells received inhibitory input only from antagonistic cells of the same type, Ia interneurons were affected by their antagonistic counterparts as well as by homonymous Renshaw cells. ►

Figure 44.

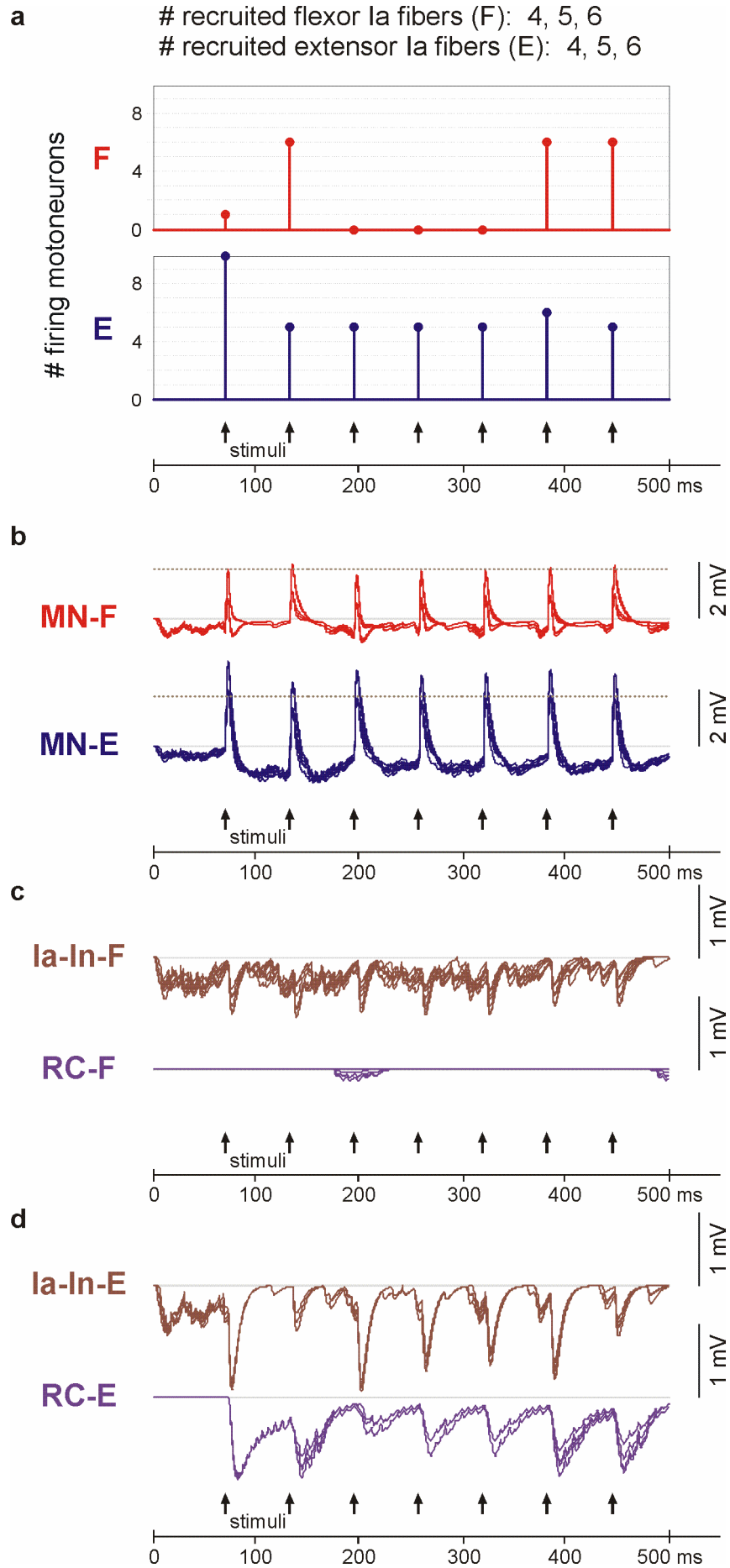


Figure 45.

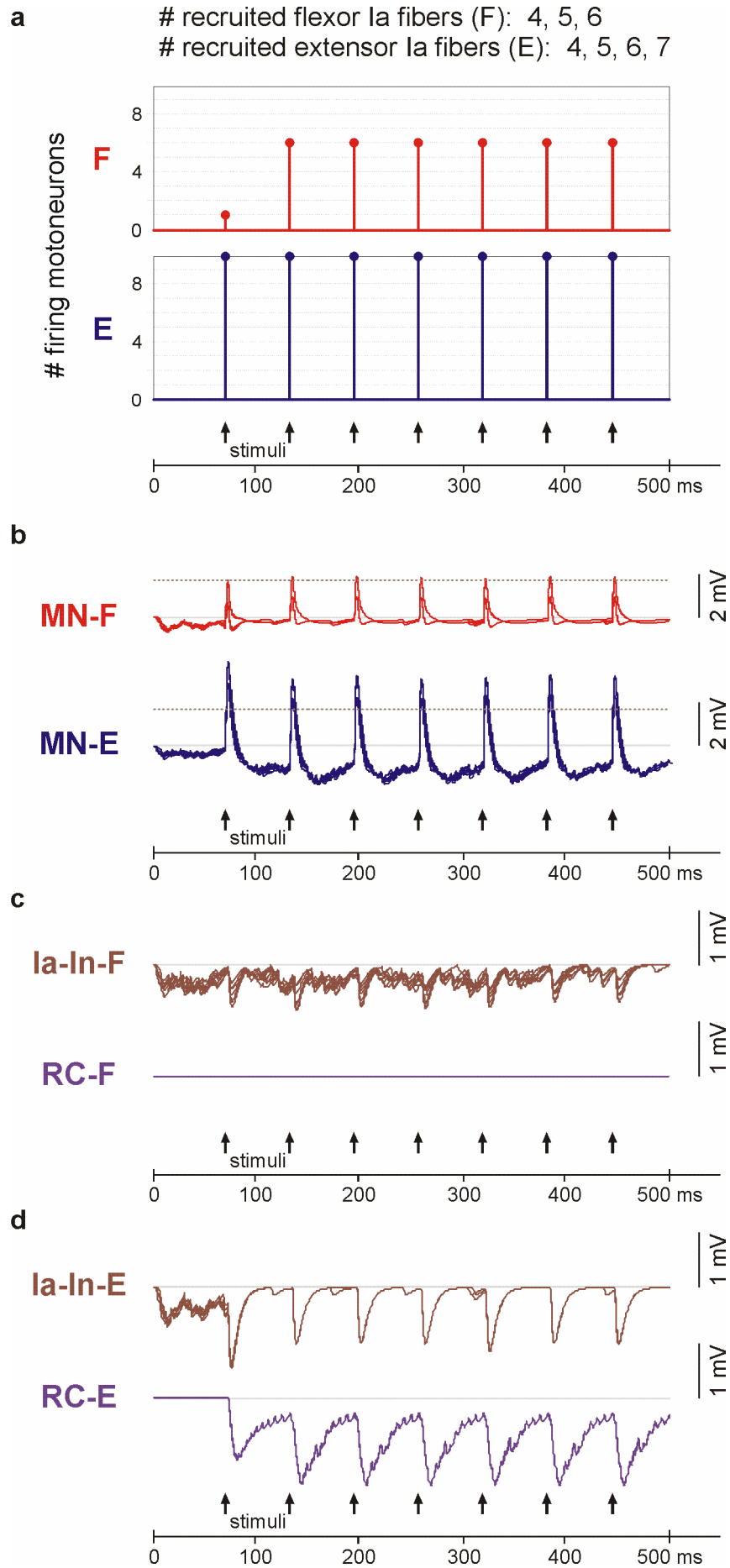
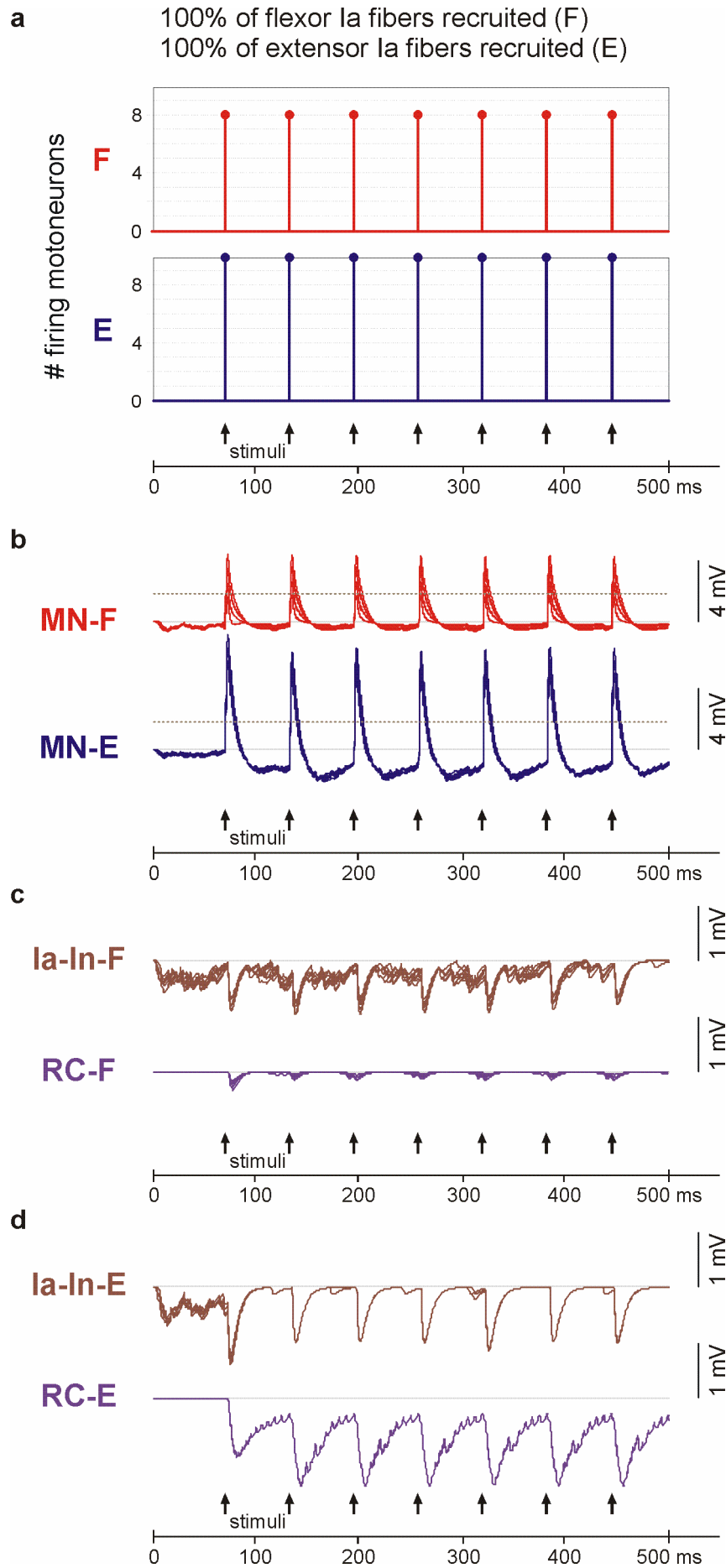


Figure 46.



Conclusions

Unexpected results were derived from the models that integrated different interneuronal populations and connectivities at the spinal cord level with the aim to re-produce the electrophysiological finding of anti-phase alternations of responses in antagonistic motor pools. The generation of simple periodic patterns did not particularly depend on the activity of Ia inhibitory interneurons with their main role in conveying mutual reciprocal inhibition also during simple reflex activities. It was rather recurrent inhibition mediated by Renshaw cells and mutual inhibition between Renshaw cells of antagonistic motoneurons that led to robust simple periodic patterns in most of the simulation runs. Specifically, asymmetric network models, i.e., two antagonistic circuits with different numbers of connectivities between neuron populations corresponding to 'flexor' and 'extensor' circuits, most readily resulted in out-of-phase attenuation of the two motor outputs. With the cancellation of the effect of Renshaw cells by including also the actions of Ia interneuronal populations, the complete network model lost the capacity of producing stable periodic patterns.

The hypothesis of the present study was fulfilled in that the generation of periodic patterns was accomplished by a relatively simple network model. In particular, the model considered only monosynaptic excitation via Ia afferent fibers and disynaptic inhibition mediated by last order interneurons located in the laminae VII of the spinal gray matter and thus in close vicinity to the motor nuclei. Specifically, none of the included nerve cells had cellular properties of CPG-related neurons that could lead to the generation of oscillation. It was rather the patterns of interconnections between the neuronal populations as well as the different time courses and durations of synaptic actions that led to the simplest expression of rhythmicity produced by the central nervous system, i.e., modulations with a period covering only two successive responses. On the contrary, more complex model assumptions, like spontaneous background activities and numerous populations of active neurons, decreased the probability to produce robust periodic patterns.

It is important to note that an 'appropriate stimulation code' was required to set the model network into action to produce the simple periodic patterns. In particular, the applied stimulation frequencies had to be within a certain range so that the central effects following an incoming afferent volley would still influence actions elicited by a successive stimulus. Except for the ongoing background activity of Ia interneurons, the longest lasting stimulation related PSPs (approximately 100 ms assumed) were due to the Renshaw cells. By applying frequencies of 16 Hz, the mechanism of temporal summation became effective. The relevant electrophysiological finding showing that only a small range of moderate stimulus intensities would effectively lead to the generation of simple periodic patterns was re-produced by the present model. Simple periodic patterns were destroyed in the model network at stimulation intensities above approximately 1.5 times the threshold. Under such conditions, the large number of activated Ia fibers produce a strong excitatory drive of the homonymous motoneurons. The membrane potentials of each motoneuron are elevated effectively above the threshold level so that they would not fall below this level

even with inhibitory actions being superimposed. Therefore, the excitatory actions exerted by large Ia afferent populations would compensate the modulating influences by the last order interneurons. Another mechanism of canceling the modulations of motor outputs is the growing mutual inhibition between antagonistic Renshaw cells with the increasing numbers of firing motoneurons. It should be noted that the stimulation intensity was defined in the present model by the percentage of recruited Ia afferent fibers. There was no linear relation assumed between the number of afferents recruited and the applied stimulus intensity in volts (e.g. if the recruitment of 30% of Ia afferents was required to induce motoneuron firing, this 'intensity' did not necessarily correspond to the application of stimuli at 3V). The non-linear relation between stimulation intensities and the recruitment of afferents relies amongst others on different thresholds of Ia fibers with different diameters, locations at various distances to the stimulation source as well as the orientation of their trajectories with respect to the applied electric field (Rattay, 1987; Rattay et al., 2000). The relevance of the efficacy of synaptic transmission between Ia afferents and motoneurons can be further deduced from the strong influence of the assumed major innervation zones on the results. Thereby, the rationale of assuming such zones was to consider differences in the efficacy of Ia afferent fibers in producing monosynaptic EPSPs. The influence of enhanced EPSPs produced by specific Ia fibers had a stronger impact on the flexor circuits since it compensated for the smaller numbers of synaptic contacts on motoneurons per Ia fiber.

In summary, it can be concluded from the modeling study that a relatively simple network can produce rhythmic outputs closely resembling the neurophysiological finding of periodic modulations of successively elicited PRM reflexes. The transition of the independent, segmental PRM reflexes elicited by 2.1 Hz stimulation to reflex interactions at 16 Hz could be clearly demonstrated. While the segmental circuits of each motoneuron pool had the capacity to produce alternating motor outputs independently from each other at 16 Hz (*Model III*), the generation of reciprocally alternating patterns required the incorporation of interconnections between the segmental circuits (*Models IV & V*).

The present modeling study thus provides strong evidence for the frequency-dependent activation of segmental circuits that do not operate in isolation, but exert actions on each other. Inter-segmental coordination of segmental activity can be regarded as a major element of spinal motor control of complex motor patterns, like posture and locomotion.

Appendix A - Determination of parameter settings

Same parameter settings are considered for the calculation of PSPs in the flexor and the extensor circuit.

I. monosynaptic EPSP produced in motoneurons by Ia fibers

$$EPSP_{MN,e}(t) = \omega_{MN,e} \cdot \exp[(\tau_{MN,e,d} \cdot t) - \exp(\tau_{MN,e,r} \cdot t)],$$

$$EPSP_{MN,AHP}(t) = \omega_{MN,AHP} \cdot \exp[(\tau_{MN,AHP,d} \cdot t) - \exp(\tau_{MN,AHP,r} \cdot t)]$$

with $0 \leq t \leq t_{end}/10$ (in steps of 0.1 ms), and

δ_{MN}	10; 70	delay [ms] after stimulus application after which an EPSP is produced in a motoneuron If Ia interneurons are incorporated in the network, this delay is set to 70 ms to ensure an established state of tonic background Ia interneuron discharges before the first action occurs at the motoneuronal level.
$\omega_{MN,e}$	1.505	scaling factors of the excitatory potential phase
$\omega_{MN,AHP}$	0.805	scaling factor of the AHP phase
$\tau_{MN,e,r}$	-0.98	time constant for rising phase of excitatory potential phase
$\tau_{MN,AHP,r}$	-0.15	time constant for rising phase of AHP potential phase
$\tau_{MN,e,d}$	-0.1	time constant for decaying phase of excitatory potential phase
$\tau_{MN,AHP,d}$	-0.5	time constant for decaying phase of AHP potential phase

II. disynaptic IPSP mediated by Ia interneurons

$$IPSP(t) = \omega_{IPSP} \cdot [\exp(\tau_{IPSP,d} \cdot t) - \exp(\tau_{IPSP,r} \cdot t)]$$

with $0 \leq t \leq t_{end}/10$ (in steps of 0.1 ms), and

δ_{IPSP}	2	delay [ms] with respect to the monosynaptic generation of an EPSP after which the IPSP arrives at the motoneuron
ω_{IPSP}	0.3	scaling factor
$\tau_{IPSP,r}$	-0.15	time constant for rising phase
$\tau_{IPSP,d}$	-0.5	time constant for decaying phase

III. Recurrent inhibition mediated by Renshaw cells

$$IPSP_{RC}(t) = \omega_{RC} \cdot [\exp(\tau_{RC,d} \cdot t) - \exp(\tau_{RC,r} \cdot t)]$$

with $0 \leq t \leq t_{end}/10$ (in steps of 0.1 ms), and

δ_{RC}	4	delay [ms] with respect to the monosynaptic generation of an EPSP after which recurrent inhibition arrives at the target cell (2 ms delay from motoneuron to Renshaw cell + 2 ms delay from Renshaw cell to target cell)
$V_{enhance}$	0.12	enhancement [mV] of V_{rest} of a Renshaw cell due to a single excitatory input
ω_{RC}	0.5	synaptic weight
$\tau_{IPSP,r}$	-0.25	time constant for rising phase
$\tau_{IPSP,d}$	-0.3	time constant for decaying phase

Appendix B – Supplementary results

ad Model I: Ia afferent fibers monosynaptically projecting on homonymous motoneurons

Recruitment curves were calculated for the same model as described above, but *without* considering major innervation zones, i.e., with all of the Ia afferents producing EPSPs of same amplitude within a motoneuron (Fig. Appendix B.1a).

As could be expected, the initial slopes of the resulting curves (Fig. Appendix B.1b) were steeper than in the example that incorporated a difference in the EPSP magnitudes generated by the various Ia afferents. Still, the same percentage of Ia afferents had to be recruited in both the flexor and the extensor circuit to reach the plateau of 100% of motoneurons firing (i.e., 40% in the flexor and 60% in the extensor, respectively). Differently to the model above, the common threshold of the flexor was already attained if 20% of all corresponding Ia fibers were recruited.

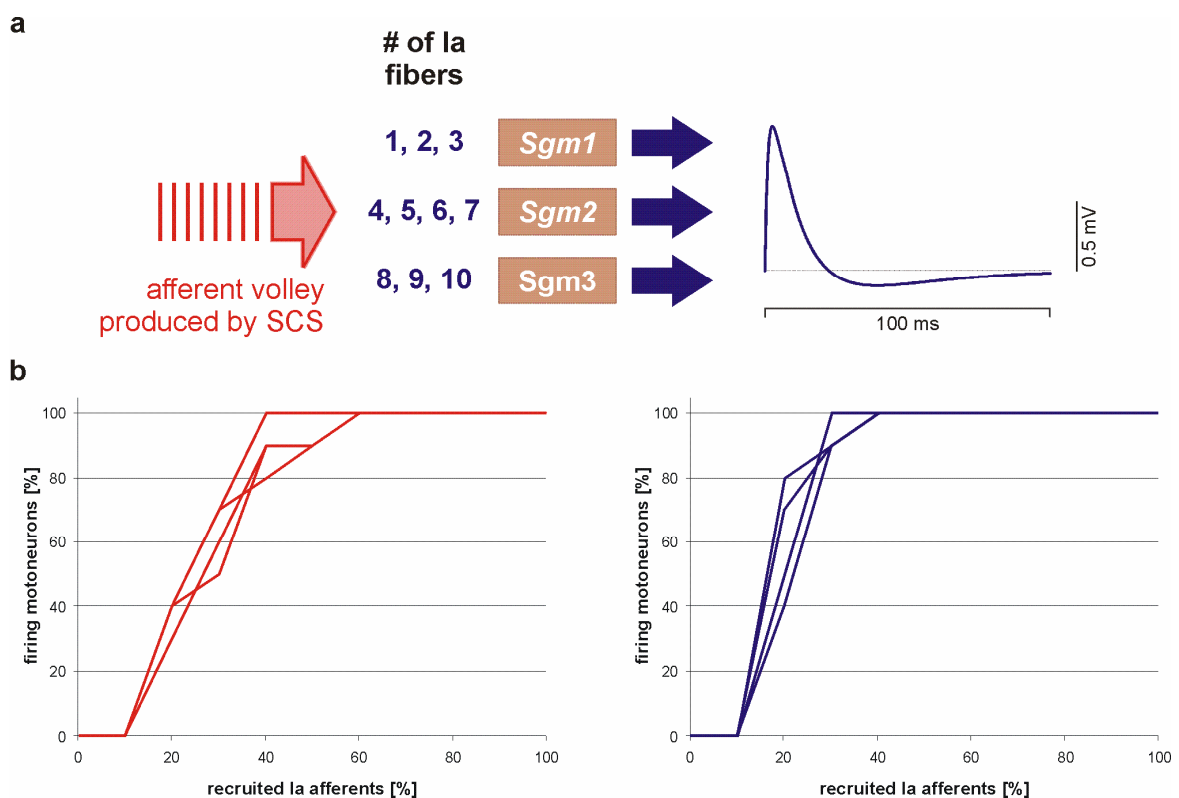


Figure Appendix B.1. Recruitment curves of motoneuron populations activated by Ia afferent volleys. **a** The model utilized here did not consider major innervation zones, i.e., EPSPs featured same amplitudes irrespective of the particularly recruited Ia fibers which had triggered them. **b** Recruitment curves of flexor (red) and extensor (blue) motoneurons. Note the steep initial slope and the lowered common threshold in case of the flexor as compared to the example given above.

ad Model III: *The effect of recurrent inhibition within a single motoneuron pool*

In addition to the rather detailed description of Renshaw cell bursts made up of individual spikes fired at specific rates, a second, naïve approach towards the simulation of recurrent inhibition was implemented.

The simplified version was based on the assumption that, if only a single motoneuron pool was considered (i.e., either flexor or extensor), the bursting behavior of a population of Renshaw cells could not be influenced by antagonistic cells of the same type. Hence, when set into action, a Renshaw cell would always exert the same inhibitory action on the target cells, in terms of amplitude and time course. Therefore, rather than checking after the initiation of the activity within a particular Renshaw cell at each step of the calculation (corresponding to 0.1 ms) whether its membrane potential was still above threshold – a prerequisite for a consecutive spike to be initiated – the resulting inhibitory event was described by a single alpha function:

$$IPSP_{RC,simplified}(t) = \omega_{RC,simplified} \cdot [\exp(\tau_{RC,simplified,d} \cdot t) - \exp(\tau_{RC,simplified,r} \cdot t)]$$

with

$0 \leq t \leq t_{end}/10$ (in steps of 0.1 ms), $\omega_{RC,simplified} = 0.23$ denoting the synaptic weight, and $\tau_{RC,simplified,r} = -0.03$ and $\tau_{RC,simplified,d} = -0.1$ the time constants for the rising and decaying phases, respectively. All parameter settings were chosen as to allow for time courses of the calculated potentials resembling those made up of individual shorter lasting IPSPs as with the ‘complex’ approach. Figure Appendix B.2 illustrates an example of a (long lasting) IPSP induced by a single Renshaw cell in a target motoneuron computed by the simplified approach.

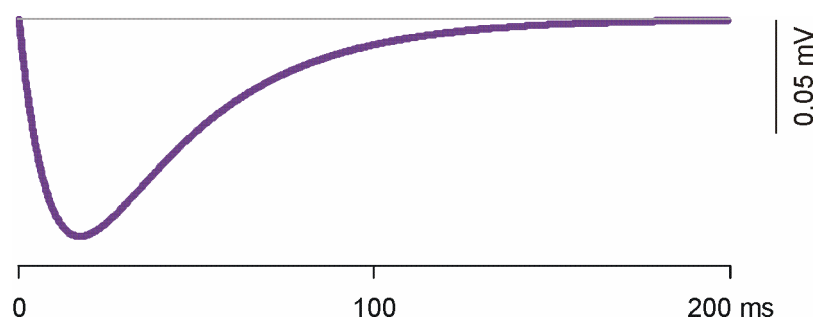


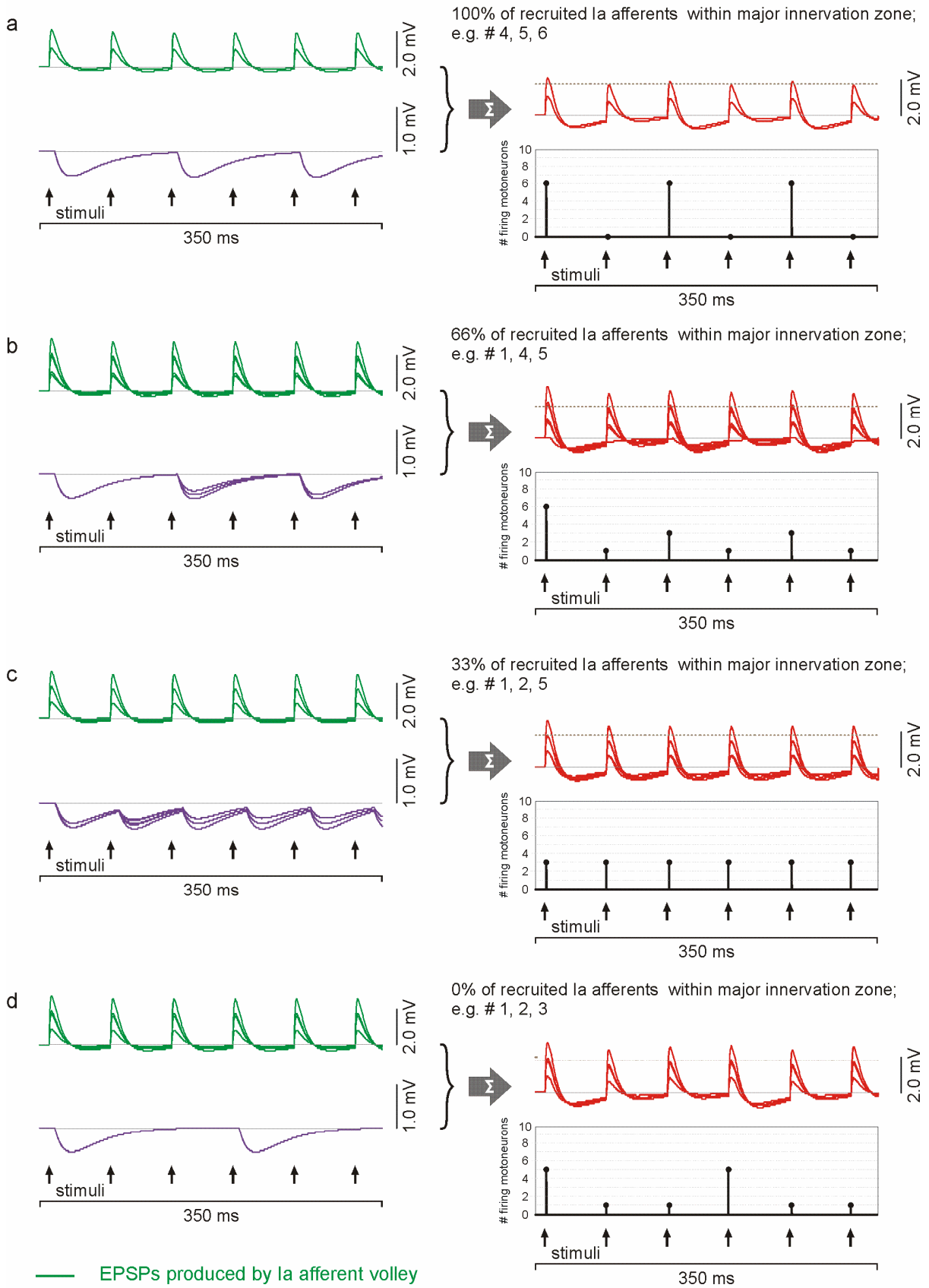
Figure Appendix B.2. IPSP exerted by a single Renshaw cell on a target motoneuron. Recurrent inhibition is calculated as a single long lasting inhibitory postsynaptic potential of relatively large amplitude.

The simulations computed with this approach produced very interesting results. In particular, all types of simple periodic patterns that had been observed in single muscle groups during the neurophysiological recordings could be reproduced. Furthermore, the specific types of the produced motor patterns could be unequivocally related to the recruitment of particular Ia fibers in terms of their location with respect to the major innervation zone.

Regarding a flexor circuit (Figure Appendix B.3), simple periodic patterns covering two successive responses were observed at the common threshold intensity (i.e., 30% of Ia fibers recruited) if all (Fig. Appendix B.3a) or two thirds (Fig. Appendix B.3b) of the Ia afferents activated by the stimulation were associated with the major innervation zone. The difference was, however, that the former case (i.e., all recruited fibers within the major innervation zone) always yielded full suppression of every second response. With other words, the strongest possible input at this stimulus intensity applied to the motoneurons via the Ia fibers sufficiently recruited a considerable subpopulation of Renshaw cells that was in turn capable of exerting a maximum inhibition on the motoneurons. At the same time, the slightly weaker excitatory drive produced by a subset of Ia fibers with 66% of them associated with the major innervation zone would activate fewer motoneurons which would hence make fewer Renshaw cells fire. If the majority (two thirds) of the recruited Ia fibers were associated with segments outside the major innervation zone (Fig. Appendix B.3c), the resulting motor output did not feature any modulations at all, but a constant, rather low number of motoneurons firing in response to each of the successively applied stimuli. An interesting result was found when testing the case with none of the activated Ia fibers belonging to the major innervation zone (Fig. Appendix B.3d); under such conditions, a periodic pattern covering three successive responses was detected that was also sometimes, though seldom, recorded in the subjects participating to the neurophysiological study presented in this thesis. This type of modulation featured a rather large number of motoneurons firing in response to the first stimulus application, but fewer to the two successive pulses. This might be due to the strong inhibitory action of Renshaw cells induced by the first pulse; the former would strongly decrease the motoneuron excitability at times when the second pulse is applied and would still have some minute effects on the motoneuron excitability during the application of the third pulse. As a consequence of the latter case, EPSPs would be produced in most of the motoneurons with peak amplitudes just below the firing threshold. Eventually, the subsequent stimulus would be transmitted to the motoneurons, the latter already back in their resting states.

At higher stimulus intensities corresponding to two times the common threshold or the recruitment of 60% of Ia fibers, the general observation was a replacement of the simple periodic patterns by constant motor outputs (Figure Appendix B.4). An exception was only found in one case: If one sixth of the recruited Ia afferents was part of the major innervation zone, the elicited patterned output was the one covering three successive responses.

recruited Ia afferents: 30%



- EPSPs produced by Ia afferent volley
- recurrent inhibition
- sum of potentials arriving at motoneurons
- firing threshold

◀ **Figure Appendix B.3.** Simple periodic patterns within the flexor motoneuron pool generated by recurrent inhibition, calculated with the simplified definition of inhibitory actions exerted by Renshaw cells. Displayed are excitatory postsynaptic potentials induced by Ia fibers (green) along with recurrent inhibition mediated via Renshaw cells (violet), which sum up to result to a total membrane potential of motoneurons (red). **a** The pattern evoked if all of the recruited Ia fibers were associated with the major innervation zone was characterized by the full suppression of every second response. **b** A similar pattern was observed, if two third of the activated Ia fibers were part of this particular zone. However, the suppression of every second response was less pronounced than that in *a*. **c** The activity of a subset of Ia fibers with a majority of two third located outside the major innervation zone would lead to a periodic pattern covering three responses. **d** Unmodulated output was elicited if none of the recruited Ia fibers was part of the major innervation zone.

The simulation of the network behavior for the extensor motoneuron pool produced similar results (Figure Appendix B.5). The only difference compared to the flexor was that the exclusive activation of Ia afferents within the major innervation zone would here generate unpatterned, constant outputs (Fig. Appendix B.5*a*). At the same time, the recruitment of a combination of Ia afferents with one third of them outside the major innervation zone led to the full suppression of every second response (Fig. Appendix B.5*b*). Note that the applied intensity associated with the recruitment of 30% of all Ia fibers corresponded to 1.5 times the common threshold in case of the extensor. All other results were qualitatively the same as in the flexor: No modulations were induced if two thirds of the recruited Ia fibers were outside the major innervation zone (Fig. Appendix B.5*c*); the type of periodic pattern covering three successive responses was observed if the stimuli activated only Ia fibers that were not associated with the major innervation zone (Fig. Appendix B.5*d*).

The recruitment of 60% of all extensor Ia fibers (Fig. Appendix B.6) constantly produced maximum outputs in the motoneuron population, i.e., all of the motoneurons responded to each of the incoming monosynaptic Ia volleys. The only exception occurred when all recruited Ia fibers were located outside the major innervation zone; under these circumstances, the resulting output was still unmodulated, but fewer motoneurons were caused to fire by the individual pulses.

Figure Appendix B.4. Output generated within the flexor motoneuron pool (red) with stimulation at intensities of two times the common motor threshold, considering excitatory input exerted by Ia fibers (green) and recurrent inhibition (violet). The common finding was a constant output under such stimulation conditions, with an exception featuring a simple periodic pattern covering three successive responses. Examples from top to bottom differ in the combination of activated Ia fibers with respect to their location within or outside the major innervation zone. ▶

recruited Ia afferents: 60%

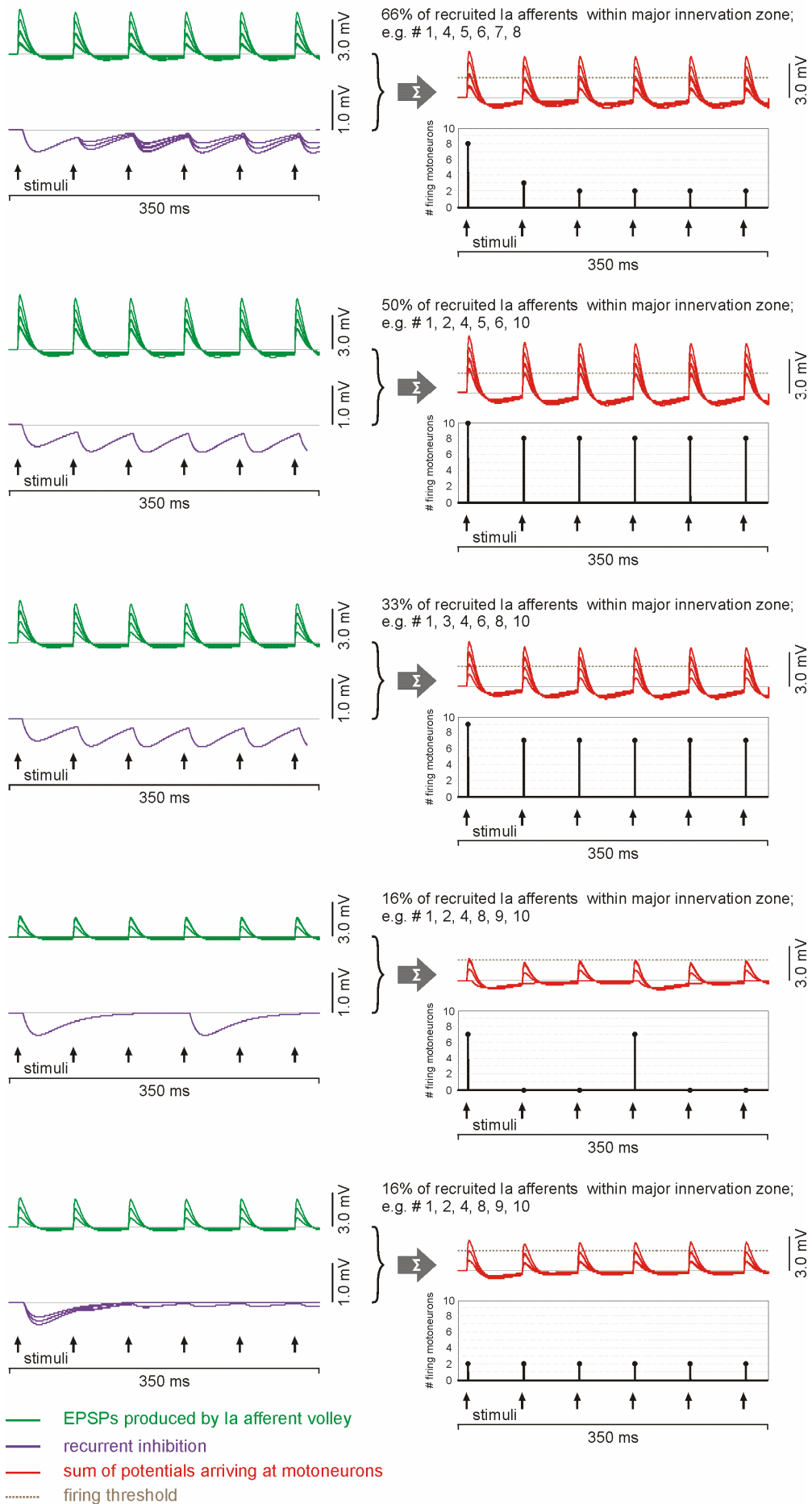


Figure Appendix B.5. Simple periodic patterns within the extensor motoneuron pool at stimulation intensities corresponding to 1.5 times the common threshold. The illustrated postsynaptic potentials are excitatory ones mediated by Ia fibers (green) and inhibitory ones exerted by Renshaw cells (violet). Total membrane potentials of the extensor motoneurons are shown in blue color. **a** Differently to the flexor, the exclusive activation of Ia fibers within the major innervation zone led to unpatterned, constant outputs. **b** Full suppression of every second response was achieved if the majority (66%), but not all of the recruited Ia fibers were part of the main innervation zone. Qualitatively same results as in the flexor were obtained if **c**, two third of the recruited Ia fibers did not belong to the main innervation zone, leading to a simple pattern covering three successive responses; and **d**, none of the activated Ia afferents were part of the major innervation zone. The output was then constant. ►

Figure Appendix B.6. Output generated within the extensor motoneuron pool (red) if 60% of all Ia fibers were recruited by the stimulation. EPSPs produced by the latter are displayed in green color, the influence of recurrent inhibition in violet. The resulting total membrane potential of the motoneurons is given in blue color. All outputs generated at such stimulus intensities were constant. Generally, the whole population of extensor motoneurons fired to each pulse. An exception was only found if the weakest possible excitatory input was assumed (provided by the input of Ia fibers exclusively outside the major innervation zone), leading to the simple periodic pattern covering three successive responses. ►►

Figure Appendix B.5.

recruited Ia afferents: 30%

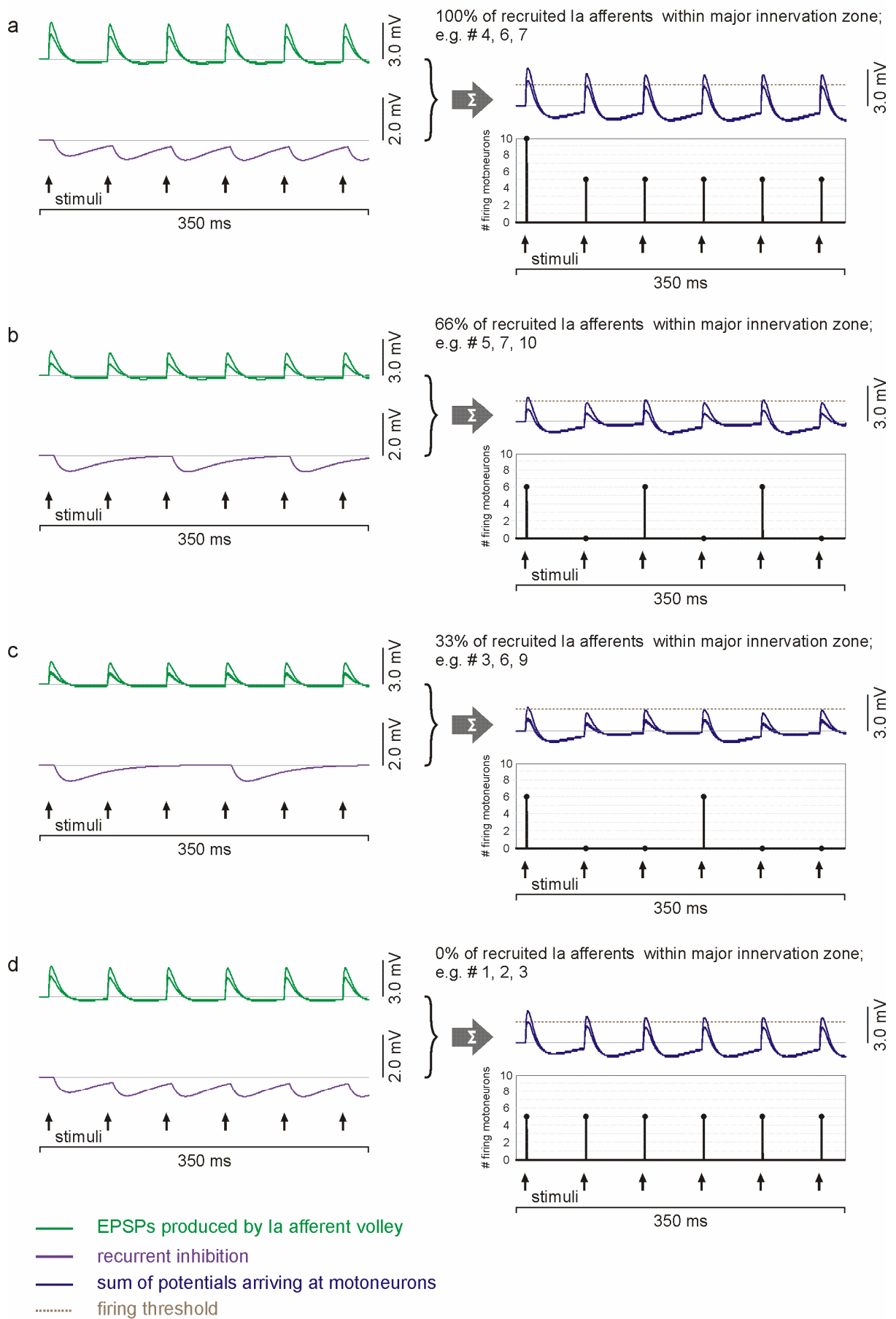
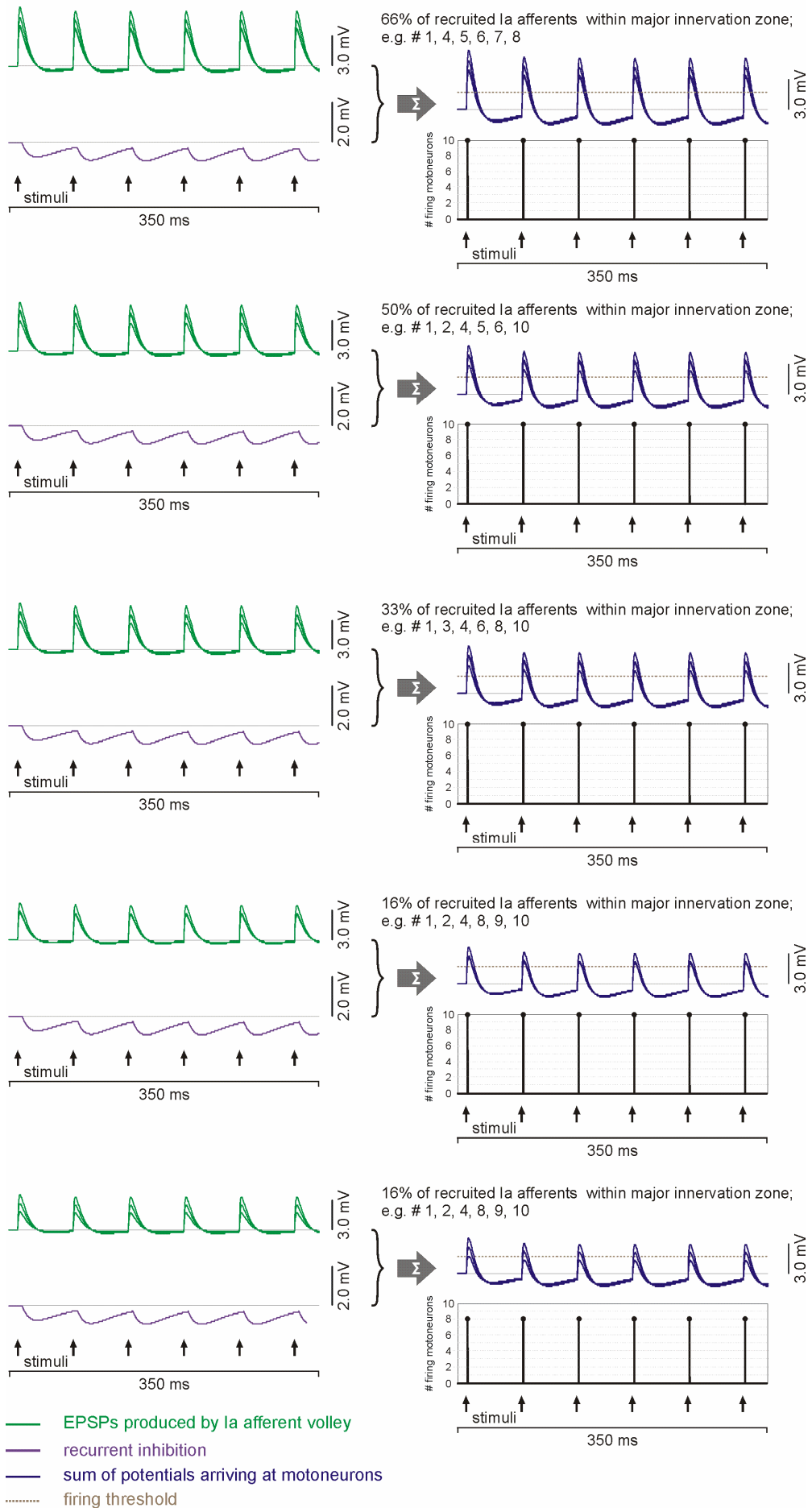


Figure Appendix B.6.

recruited Ia afferents: 60%



At maximum stimulation (i.e., 100% of Ia fibers being recruited), the results here were the same as with the more detailed calculation of recurrent inhibition; due to the inhibitory actions exerted by Renshaw cells, the output of the flexor motoneuron pool was reduced by 10% as compared to the model without considering recurrent inhibition. The output of the extensor motoneuron population, on the other hand, remained constant at the maximum level (i.e., 100% of motoneurons firing). The corresponding potentials leading to these results are given in Figure Appendix B.7.

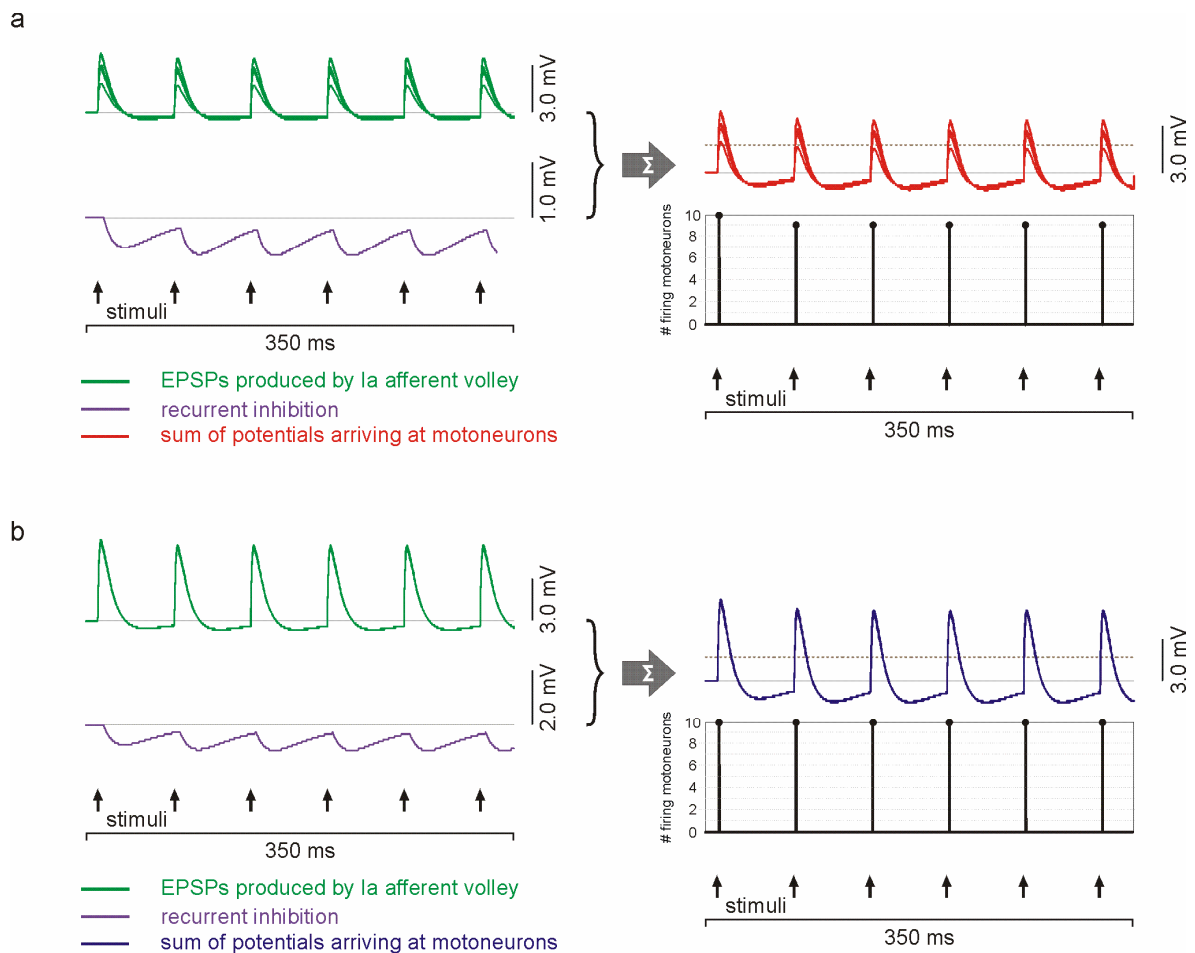


Figure Appendix B.7. Firing patterns of flexor (**a**, red) and extensor (**b**, blue) motoneuron pools induced by maximum stimulation (i.e., 100% of the respective Ia fibers being recruited). As with the more complex description of recurrent inhibition given above, the maximum flexor output is here reduced to 90% of that in the model not considering Renshaw cells. Again, no changes in the maximum extensor output could be detected.

Appendix C – Matlab codes

```

% program reading stimuli

function x = read_stimuli(t)

global vAP

offset = 0;
duration = 1;

f=0.0016;    % 16 Hz

i_max = 200;

cyc_period = 1/f;

x = 0;
i = 0;

while (i <= i_max),
    ic = i*cyc_period;
    if (t >= offset + ic) & (t < offset + duration + ic)
        x = vAP;
    end
    i = i + 1;
end

```

```

% main program PSP

clear all

global vAP

%%%%%%%%%%%%%%%%%%%%%%%%%%%%%%%%%%%%%%%%%%%%%%%%%%%%%%%%%%%%%%%%%%%%%%%%

nr_Ia_aff=10;

number_recruited_Ia_aff_F=3;
number_recruited_Ia_aff_E=4;

recruited_Ia_aff_F=[4 5 6]
recruited_Ia_aff_E=[4 5 6 7]

population_MN_F=10;
population_MN_E=10;

population_Ia_In_F=10;
population_Ia_In_E=10;

population_RC_F=10;
population_RC_E=10;

nr_projections_Ia_aff_MN_F=6;

```

```

% delays:

d1_f=700;
d3_f=20;
d5_f=20;

d1_e=700;
d3_e=20;
d5_e=20;

% synaptic weights:

w1_f=1.505;
w1_f_hyp=-0.805;
w3_f=0.3;
w6_f=0.5;

w1_e=1.505;
w1_e_hyp=-0.805;
w3_e=0.3;
w6_e=0.5;

% exponential decay/rise

tau1_f_r=-0.98;
tau1_f_d=-0.1;
tau1_f_r_hyp=-0.04;
tau1_f_d_hyp=-0.07;
tau3_f_r=-0.15;
tau3_f_d=-0.5;
tau6_f_r=-0.25;
tau6_f_d=-0.3;

tau1_e_r=-0.98;
tau1_e_d=-0.1;
tau1_e_r_hyp=-0.04;
tau1_e_d_hyp=-0.07;
tau3_e_r=-0.15;
tau3_e_d=-0.5;
tau6_e_r=-0.25;
tau6_e_d=-0.3;

% EPSPs/IPSPs

t0=0:0.1:ceil(tend+1)/10;
PSP1_f=(w1_f*(exp(tau1_f_d*t0)-exp(tau1_f_r*t0)));
PSP1_f_hyp=(-w1_f_hyp*(exp(tau1_f_d_hyp*t0)-exp(tau1_f_r_hyp*t0)));
PSP3_f=(w3_f*(exp(tau3_f_d*t0)-exp(tau3_f_r*t0)));
PSP6_f=(w6_f*(exp(tau6_f_d*t0)-exp(tau6_f_r*t0)));

PSP1_e=(w1_e*(exp(tau1_e_d*t0)-exp(tau1_e_r*t0)));
PSP1_e_hyp=(-w1_e_hyp*(exp(tau1_e_d_hyp*t0)-exp(tau1_e_r_hyp*t0)));
PSP3_e=(w3_e*(exp(tau3_e_d*t0)-exp(tau3_e_r*t0)));
PSP6_e=(w6_e*(exp(tau6_e_d*t0)-exp(tau6_e_r*t0)));

for i=length(PSP1_f)+1:tend+1
    PSP1_f(i)=0;
    PSP1_f_hyp(i)=0;
    PSP3_f(i)=0;

```

```

PSP6_f(i)=0;
PSP1_e(i)=0;
PSP1_e_hyp(i)=0;
PSP3_e(i)=0;
PSP6_e(i)=0;
end

for i=10:length(PSP1_f)
    if PSP1_f(i)<0.02 & PSP1_f(i)>0
        count1f(i)=i;
        count1f=nonzeros(count1f);
    end
    if PSP1_e(i)<0.02 & PSP1_e(i)>0
        count1e(i)=i;
        count1e=nonzeros(count1f);
    end
end

counter1f=count1f(length(count1f))-count1f(1);
counter1e=count1e(length(count1e))-count1e(1);

PSP1_f_help=zeros(tend+1,1);
PSP1_f_help(count1f(1)-355:length(PSP1_f))=PSP1_f_hyp(1:length(PSP1_f_hyp)-count1f(1)+356);
PSP1_f_final=PSP1_f+PSP1_f_help;
PSP1_e_help=zeros(tend+1,1);
PSP1_e_help(count1e(1)-355:length(PSP1_e))=PSP1_e_hyp(1:length(PSP1_e_hyp)-
count1e(1)+356);
PSP1_e_final=PSP1_e+PSP1_e_help;

%%%%%%%%%%%%%%%%%%%%%%%%%%%%%%%%%%%%%%%%%%%%%%%%%%%%%%%%%%%%%%%%%%%%%%%%

% connections between neurons of one type to neurons of a different type

for i=1:population_MN_F
    Ia_aff_MNF=randperm(nr_Ia_aff);
    Ia_aff_MN_F(1:nr_Ia_aff,i)=Ia_aff_MNF;
    RC_F_MNF=randperm(population_RC_F);
    RC_F_MN_F(1:population_RC_F,i)=RC_F_MNF;
    Ia_In_E_MNF=randperm(population_Ia_In_E);
    Ia_In_E_MN_F(1:population_Ia_In_E,i)=Ia_In_E_MNF;
end

for i=1:population_RC_F
    MN_F_RCF=randperm(population_MN_F);
    MN_F_RC_F(1:population_MN_F,i)=MN_F_RCF;
    RC_F_RCE=randperm(population_RC_F);
    RC_F_RC_E(1:population_RC_F,i)=RC_F_RCE;
end

for i=1:population_MN_E
    Ia_aff_MNE=randperm(nr_Ia_aff);
    Ia_aff_MN_E(1:nr_Ia_aff,i)=Ia_aff_MNE;
    RC_E_MNE=randperm(population_RC_E);
    RC_E_MN_E(1:population_RC_E,i)=RC_E_MNE;
    Ia_In_F_MNE=randperm(population_Ia_In_F);
    Ia_In_F_MN_E(1:population_Ia_In_F,i)=Ia_In_F_MNE;
end

```

```

for i=1:population_RC_E
    MN_E_RCE=randperm(population_MN_E);
    MN_E_RC_E(1:population_MN_E,i)=MN_E_RCE;
    RC_E_RCF=randperm(population_RC_E);
    RC_E_RC_F(1:population_RC_E,i)=RC_E_RCF;
end

for i=1:population_Ia_In_E
    Ia_aff_Ia_InE=randperm(nr_Ia_aff);
    Ia_aff_Ia_In_E(1:nr_Ia_aff,i)=Ia_aff_Ia_InE;
    Ia_In_F_Ia_InE=randperm(population_Ia_In_F);
    Ia_In_F_Ia_In_E(1:population_Ia_In_F,i)=Ia_In_F_Ia_InE;
    RC_E_Ia_InE=randperm(population_RC_E);
    RC_E_Ia_In_E(1:population_RC_E,i)=RC_E_Ia_InE;
end

for i=1:population_Ia_In_F
    Ia_aff_Ia_InF=randperm(nr_Ia_aff);
    Ia_aff_Ia_In_F(1:nr_Ia_aff,i)=Ia_aff_Ia_InF;
    Ia_In_E_Ia_InF=randperm(population_Ia_In_E);
    Ia_In_E_Ia_In_F(1:population_Ia_In_E,i)=Ia_In_E_Ia_InF;
    RC_F_Ia_InF=randperm(population_RC_F);
    RC_F_Ia_In_F(1:population_RC_F,i)=RC_F_Ia_InF;
end

project_Ia_aff_MN_F=Ia_aff_MN_F(1:nr_projections_Ia_aff_MN_F,:);
project_Ia_aff_MN_F=sort(project_Ia_aff_MN_F);
project_Ia_aff_MN_E=Ia_aff_MN_E(1:nr_projections_Ia_aff_MN_E,:);
project_Ia_aff_MN_E=sort(project_Ia_aff_MN_E);

project_Ia_aff_Ia_In_E=Ia_aff_Ia_In_E(1:nr_projections_Ia_aff_Ia_In_E,:);
project_Ia_aff_Ia_In_E=sort(project_Ia_aff_Ia_In_E);
project_Ia_aff_Ia_In_F=Ia_aff_Ia_In_F(1:nr_projections_Ia_aff_Ia_In_F,:);
project_Ia_aff_Ia_In_F=sort(project_Ia_aff_Ia_In_F);

project_MN_F_RC_F=MN_F_RC_F(1:nr_projections_MN_F_RC_F,:);
project_MN_F_RC_F=sort(project_MN_F_RC_F);
project_MN_E_RC_E=MN_E_RC_E(1:nr_projections_MN_E_RC_E,:);
project_MN_E_RC_E=sort(project_MN_E_RC_E);

project_RC_F_MN_F=RC_F_MN_F(1:nr_projections_RC_F_MN_F,:);
project_RC_F_MN_F=sort(project_RC_F_MN_F);
project_RC_E_MN_E=RC_E_MN_E(1:nr_projections_RC_E_MN_E,:);
project_RC_E_MN_E=sort(project_RC_E_MN_E);

project_RC_F_RC_E=RC_F_RC_E(1:nr_projections_RC_F_RC_E,:);
project_RC_F_RC_E=sort(project_RC_F_RC_E);
project_RC_E_RC_F=RC_E_RC_F(1:nr_projections_RC_E_RC_F,:);
project_RC_E_RC_F=sort(project_RC_E_RC_F);

project_RC_F_Ia_In_F=RC_F_Ia_In_F(1:nr_projections_RC_F_Ia_In_F,:);
project_RC_F_Ia_In_F=sort(project_RC_F_Ia_In_F);
project_RC_E_Ia_In_E=RC_E_Ia_In_E(1:nr_projections_RC_E_Ia_In_E,:);
project_RC_E_Ia_In_E=sort(project_RC_E_Ia_In_E);

project_Ia_In_E_MN_F=Ia_In_E_MN_F(1:nr_projections_Ia_In_E_MN_F,:);
project_Ia_In_E_MN_F=sort(project_Ia_In_E_MN_F);
project_Ia_In_F_MN_E=Ia_In_F_MN_E(1:nr_projections_Ia_In_F_MN_E,:);
project_Ia_In_F_MN_E=sort(project_Ia_In_F_MN_E);

```

```

project_Ia_In_E_Ia_In_F=Ia_In_E_Ia_In_F(1:nr_projections_Ia_In_E_Ia_In_F,:);
project_Ia_In_E_Ia_In_F=sort(project_Ia_In_E_Ia_In_F);
project_Ia_In_F_Ia_In_E=Ia_In_F_Ia_In_E(1:nr_projections_Ia_In_F_Ia_In_E,:);
project_Ia_In_F_Ia_In_E=sort(project_Ia_In_F_Ia_In_E);

%%%%%%%%%%%%%%%%%%%%%%%%%%%%%%%%%%%%%%%%%%%%%%%%%%%%%%%%%%%%%%%%%%%%%%%%

% matrices:

MN_F=zeros(tend+1,nr_st);
R_F=zeros(tend+1,nr_st);
out_f1=zeros(tend+1,nr_Ia_aff);
outf1=zeros(tend+1,nr_Ia_aff);
out_f3=zeros(tend+1,nr_Ia_aff);
outf3=zeros(tend+1,nr_Ia_aff);
out_f3a=zeros(tend+1,nr_Ia_aff);
outf3a=zeros(tend+1,nr_Ia_aff);
out_f3b=zeros(tend+1,nr_Ia_aff);
outf3b=zeros(tend+1,nr_Ia_aff);
out_f5=zeros(tend+1,nr_Ia_aff);
outf5=zeros(tend+1,nr_Ia_aff);
outf5_MN_F_RC_F=zeros(tend+1,nr_Ia_aff);
outf5_MN_F_RCF=zeros(tend+1,nr_Ia_aff);
out_f6=zeros(tend+1,nr_Ia_aff);
outf6=zeros(tend+1,nr_Ia_aff);
out_f6_MN=zeros(tend+1,nr_Ia_aff);
outf6_MN=zeros(tend+1,nr_Ia_aff);
OUT_R_F=zeros(tend+1,nr_Ia_aff);
OUT_MNF=zeros(tend+1,population_MN_F);
OUT_MN_F=zeros(tend+1,population_MN_F);
outMNF=zeros(tend+1,population_MN_F);
PSP_RC_F=zeros(tend+1,population_RC_F);
PSP_RC_F_total=zeros(tend+1,population_RC_F);
PSP_RCF=zeros(tend+1,population_RC_F);
OUT_RC_F_MN_F=zeros(tend+1,population_MN_F);
OUT_RC_F_MNF=zeros(tend+1,population_MN_F);
out_f6_RC_E=zeros(tend+1,population_RC_E);
out_f6_RCE=zeros(tend+1,population_RC_E);
stim_f5_neu=zeros(tend+1,population_MN_F);
stim_f6_neu=zeros(tend+1,population_RC_F);
OUT_RC_E_RC_F=zeros(tend+1,population_RC_F);
OUT_RC_E_RCF=zeros(tend+1,population_RC_F);
OUT_MN_F_RC_F=zeros(tend+1,population_RC_F);
OUT_MN_F_RCF=zeros(tend+1,population_RC_F);
OUT_Ia_In_F=zeros(tend+1,population_Ia_In_F);
OUT_Ia_InF=zeros(tend+1,population_Ia_In_F);
OUT_RC_F_Ia_In_F=zeros(tend+1,population_Ia_In_F);
OUT_RC_F_Ia_InF=zeros(tend+1,population_Ia_In_F);
OUT_back_Ia_In_F=zeros(tend+1,population_Ia_In_F);
rec_inh_E_to_F=zeros(tend+1,population_Ia_In_E);
input_Ia_In_E_Ia_In_F=zeros(tend+1,population_Ia_In_F);
input_Ia_In_E_Ia_In_F_back=zeros(tend+1,population_Ia_In_F);
OUT_f_back_total=zeros(tend+1,population_Ia_In_F);
OUT_f3_total=zeros(tend+1,population_Ia_In_F);
input_Ia_In_E_MNF_2=zeros(tend+1,population_MN_F);
input_Ia_In_E_MN_F_2=zeros(tend+1,population_MN_F);
out_background_Ia_In_F=zeros(tend+1,population_Ia_In_F);
out_background_Ia_InF=zeros(tend+1,population_Ia_In_F);

```

```

outf3_spont=zeros(tend+1,population_Ia_In_F);
out_f3_spont=zeros(tend+1,population_Ia_In_F);
vin_f1_all=zeros(tend+1,population_MN_F);

MN_E=zeros(tend+1,nr_st);
R_E=zeros(tend+1,nr_st);
out_e1=zeros(tend+1,nr_Ia_aff);
oute1=zeros(tend+1,nr_Ia_aff);
out_e3=zeros(tend+1,nr_Ia_aff);
oute3=zeros(tend+1,nr_Ia_aff);
out_e3a=zeros(tend+1,nr_Ia_aff);
oute3a=zeros(tend+1,nr_Ia_aff);
out_e3b=zeros(tend+1,nr_Ia_aff);
oute3b=zeros(tend+1,nr_Ia_aff);
out_e5=zeros(tend+1,nr_Ia_aff);
oute5=zeros(tend+1,nr_Ia_aff);
oute5_MN_E_RC_E=zeros(tend+1,nr_Ia_aff);
oute5_MN_E_RCE=zeros(tend+1,nr_Ia_aff);
out_e6=zeros(tend+1,nr_Ia_aff);
oute6=zeros(tend+1,nr_Ia_aff);
out_e6_MN=zeros(tend+1,nr_Ia_aff);
oute6_MN=zeros(tend+1,nr_Ia_aff);
OUT_R_E=zeros(tend+1,nr_Ia_aff);
OUT_MNE=zeros(tend+1,population_MN_E);
OUT_MN_E=zeros(tend+1,population_MN_E);
outMNE=zeros(tend+1,population_MN_E);
PSP_RC_E=zeros(tend+1,population_RC_E);
PSP_RC_E_total=zeros(tend+1,population_RC_E);
PSP_RCE=zeros(tend+1,population_RC_E);
OUT_RC_E_MN_E=zeros(tend+1,population_MN_E);
OUT_RC_E_MNE=zeros(tend+1,population_MN_E);
out_e6_RC_F=zeros(tend+1,population_RC_F);
out_e6_RCF=zeros(tend+1,population_RC_F);
stim_e5_neu=zeros(tend+1,population_MN_F);
stim_e6_neu=zeros(tend+1,population_RC_E);
OUT_RC_F_RC_E=zeros(tend+1,population_RC_E);
OUT_RC_F_RCE=zeros(tend+1,population_RC_E);
OUT_MN_E_RCE=zeros(tend+1,population_RC_E);
OUT_MN_E_RC_E=zeros(tend+1,population_RC_E);
OUT_Ia_In_E=zeros(tend+1,population_Ia_In_E);
OUT_Ia_InE=zeros(tend+1,population_Ia_In_E);
OUT_RC_E_Ia_In_E=zeros(tend+1,population_Ia_In_E);
OUT_RC_E_Ia_InE=zeros(tend+1,population_Ia_In_E);
OUT_back_Ia_In_E=zeros(tend+1,population_Ia_In_E);
rec_inh_F_to_E=zeros(tend+1,population_Ia_In_F);
input_Ia_In_F_Ia_In_E=zeros(tend+1,population_Ia_In_E);
input_Ia_In_F_Ia_In_E_back=zeros(tend+1,population_Ia_In_E);
OUT_e_back_total=zeros(tend+1,population_Ia_In_E);
OUT_e3_total=zeros(tend+1,population_Ia_In_E);
input_Ia_In_F_MNE_2=zeros(tend+1,population_MN_E);
input_Ia_In_F_MN_E_2=zeros(tend+1,population_MN_E);
out_background_Ia_In_E=zeros(tend+1,population_Ia_In_E);
out_background_Ia_InE=zeros(tend+1,population_Ia_In_E);
oute3_spont=zeros(tend+1,population_Ia_In_E);
out_e3_spont=zeros(tend+1,population_Ia_In_E);
vin_e1_all=zeros(tend+1,population_MN_E);

help_RC(1)=0;
help_RC(2)=5;

```

```

help_RC(3)=15;
help_RC(4)=30;
help_RC(5)=50;
help_RC(6)=75;
help_RC(7)=105;
help_RC(8)=140;
help_RC(9)=180;
help_RC(10)=225;
help_RC(11)=275;
help_RC(12)=330;
help_RC(13)=390;
help_RC(14)=455;
help_RC(15)=525;
help_RC(16)=600;
help_RC(17)=680;
help_RC(18)=765;
help_RC(19)=855;
help_RC=help_RC';

%%%%%%%%%%

% tonic background activity of Ia interneurons:

Applied_isis_Ia_In_E=zeros(15,population_Ia_In_E);
applied_isis_Ia_In_E=zeros(16,population_Ia_In_E);
tonic_background_Ia_In_E=zeros(tend+1,population_Ia_In_E);
input_Ia_In_E_MNF=zeros(tend+1,population_MN_F);
input_Ia_In_E_MN_F=zeros(tend+1,population_MN_F);

Applied_isis_Ia_In_F=zeros(15,population_Ia_In_F);
applied_isis_Ia_In_F=zeros(16,population_Ia_In_F);
tonic_background_Ia_In_F=zeros(tend+1,population_Ia_In_F);
input_Ia_In_F_MNE=zeros(tend+1,population_MN_E);
input_Ia_In_F_MN_E=zeros(tend+1,population_MN_E);

f_lo=50; % 20 Hz
f_hi=10; % 100 Hz
ISIs_Ia_In_E=[f_lo:1:f_hi]';
isi=randint(1,1,[f_lo,f_hi]);
ISIs_Ia_In_F=[f_lo:1:f_hi]';

for k=1:population_Ia_In_E
    Applied_isis_Ia_In_E(1,k)=randint(1,1,[f_lo,f_hi])*10;
end
for k=1:population_Ia_In_F
    Applied_isis_Ia_In_F(1,k)=randint(1,1,[f_lo,f_hi])*10;
end

for j=2:15
    j;
    for k=1:population_Ia_In_E
        Applied_isis_Ia_In_E(j,k)=Applied_isis_Ia_In_E(j-1,k)+randint(1,1,[f_lo,f_hi])*10;
    end
    for k=1:population_Ia_In_F
        Applied_isis_Ia_In_F(j,k)=Applied_isis_Ia_In_F(j-1,k)+randint(1,1,[f_lo,f_hi])*10;
    end
end

for k=1:population_Ia_In_E

```

```

for i=2:16
    applied_isis_Ia_In_E(i,k)=Applied_isis_Ia_In_E(i-1,k);
    applied_isis_Ia_In_F(i,k)=Applied_isis_Ia_In_F(i-1,k);
end
applied_isis_Ia_In_E(1,k)=abs(applied_isis_Ia_In_E(2,k)-randint(1,1,[f_lo,f_hi])*10)+1;
applied_isis_Ia_In_F(1,k)=abs(applied_isis_Ia_In_F(2,k)-randint(1,1,[f_lo,f_hi])*10)+1;
end

Applied_isis_Ia_In_E;
applied_isis_Ia_In_E;
Applied_isis_Ia_In_F;
applied_isis_Ia_In_F;

%%%%%%%%%%

for u=1:tend+1

    if mod(u,100)==0
        u
    end

    t=u-1;
    x(u)=Stimuli_1(t);
    stim(u)=x(u);

    if (u-d1_f >= 1)
        v=u-d1_f;
        stim_f1(u)=stim(v);
    else
        stim_f1(u)=0;
    end
    vin_f1=stim_f1;

    if (u-d1_e >= 1)
        v=u-d1_e;
        stim_e1(u)=stim(v);
    else
        stim_e1(u)=0;
    end
    vin_e1=stim_e1;

    for k=1:number_recruited_Ia_aff_F
        vin_f1_all(u,recruited_Ia_aff_F(k))=stim_f1(u);
    end
    for k=1:number_recruited_Ia_aff_E
        vin_e1_all(u,recruited_Ia_aff_E(k))=stim_e1(u);
    end

    for j=1:length(applied_isis_Ia_In_E)
        for k=1:population_Ia_In_E
            if applied_isis_Ia_In_E(j,k)==u
                tonic_background_Ia_In_E(u,k)=vAP;
            end
        end
    end

    for j=1:length(applied_isis_Ia_In_F)
        for k=1:population_Ia_In_F
            if applied_isis_Ia_In_F(j,k)==u

```

```

        tonic_background_Ia_In_F(u,k)=vAP;
    end
end
end

%%%%%%%%%%%%%%%%%%%%%%%%%%%%%%%%%%%%%%%%%%%%%%%%%%%%%%%%%%%%%%%%%%%%%%%%

for i=1:nr_projections_Ia_aff_MN_F
% PSPs at MN_F
if vin_f1_all(u,i)>=vAP
    out_f1(1:u-1,i)=0+outf1(1:u-1,i);
    if i==4
        out_f1(u:tend+1,i)=outf1(u:tend+1,i)+PSP1_f_final(1:tend+1-u+1);
        outf1=out_f1;
    elseif i==5
        out_f1(u:tend+1,i)=outf1(u:tend+1,i)+PSP1_f_final(1:tend+1-u+1);
        outf1=out_f1;
    elseif i==6
        out_f1(u:tend+1,i)=outf1(u:tend+1,i)+PSP1_f_final(1:tend+1-u+1);
        outf1=out_f1;
    elseif i==7
        out_f1(u:tend+1,i)=outf1(u:tend+1,i)+PSP1_f_final(1:tend+1-u+1);
        outf1=out_f1;
    else
        out_f1(u:tend+1,i)=outf1(u:tend+1,i)+0.85*PSP1_f_final(1:tend+1-u+1);
        outf1=out_f1;
    end
end
end
for k=1:population_MN_F
    for j=1:length(project_Ia_aff_MN_F(:,1))
        if i==project_Ia_aff_MN_F(j,k)
            OUT_MN_F(u,k)=OUT_MNF(u,k)+out_e1(u,i);
            OUT_MNF=OUT_MN_F;
        end
    end
end
end
for k=1:population_Ia_In_F
    for j=1:length(project_Ia_aff_Ia_In_F(:,1))
        if i==project_Ia_aff_Ia_In_F(j,k)
            OUT_Ia_In_F(u,k)=OUT_Ia_InF(u,k)+out_f1(u,i);
            OUT_Ia_InF=OUT_Ia_In_F;
        end
    end
end
end
end

for i=1:nr_projections_Ia_aff_MN_E
% PSPs at MN_E
if vin_e1_all(u,i)>=vAP
    out_e1(1:u-1,i)=0+oute1(1:u-1,i);
    if i==4
        out_e1(u:tend+1,i)=oute1(u:tend+1,i)+PSP1_e_final(1:tend+1-u+1);
        oute1=out_e1;
    elseif i==5
        out_e1(u:tend+1,i)=oute1(u:tend+1,i)+PSP1_e_final(1:tend+1-u+1);
        oute1=out_e1;
    elseif i==6
        out_e1(u:tend+1,i)=oute1(u:tend+1,i)+PSP1_e_final(1:tend+1-u+1);
        oute1=out_e1;
    end
end
end
end

```

```

elseif i==7
    out_e1(u:tend+1,i)=out_e1(u:tend+1,i)+PSP1_e_final(1:tend+1-u+1);
    out_e1=out_e1;
else
    out_e1(u:tend+1,i)=out_e1(u:tend+1,i)+0.85*PSP1_e_final(1:tend+1-u+1);
    out_e1=out_e1;
end
end
for k=1:population_MN_E
    for j=1:length(project_Ia_aff_MN_E(:,1))
        if i==project_Ia_aff_MN_E(j,k)
            OUT_MN_E(u,k)=OUT_MNE(u,k)+out_e1(u,i);
            OUT_MNE=OUT_MN_E;
        end
    end
end
for k=1:population_Ia_In_E
    for j=1:length(project_Ia_aff_Ia_In_E(:,1))
        if i==project_Ia_aff_Ia_In_E(j,k)
            OUT_Ia_In_E(u,k)=OUT_Ia_InE(u,k)+out_e1(u,i);
            OUT_Ia_InE=OUT_Ia_In_E;
        end
    end
end
end
end

outMNF=OUT_MN_F+OUT_RC_F_MN_F+rec_inh_E_to_F;
outMNE=OUT_MN_E+OUT_RC_E_MN_E+rec_inh_F_to_E;

%%%%%%%%%%%%%%%%%%%%%%%%%%%%%%%%%%%%%%%%%%%%%%%%%%%%%%%%%%%%%%%%%%%%%%%%

% recurrent inhibition / recurrent facilitation:
PSP_RC_F_total=OUT_MN_F_RC_F+OUT_RC_E_RC_F;
PSP_RC_E_total=OUT_MN_E_RC_E+OUT_RC_F_RC_E;

if (u-d5_f>=1)
    v=u-d5_f;
    for k=1:population_MN_F
        if (outMNF(v,k)>=vthr2_F)
            stim_f5(u,k)=vAP;
        else
            stim_f5(u,k)=0;
        end
        if stim_f5(u,k)>=vAP & stim_f5(u-1,k)==0
            for i=1:length(help_RC)
                stim_f5_neu(u+help_RC(i),k)=vAP;
            end
        end
        if u-21>=1
            if stim_f5(u,k)>=vAP & stim_f5(u-1,k)==0
                out_f5(1:u-21,k)=0+outf5(1:u-21,k);
                out_f5(u-20:min(u+870-20,tend+1),k)=RCFhigh;
                outf5=out_f5;
            end
        end
        for m=1:population_RC_F
            for j=1:nr_projections_MN_F_RC_F
                if k==project_MN_F_RC_F(j,m)
                    OUT_MN_F_RC_F(u,m)=OUT_MN_F_RCF(u,m)+out_f5(u,k);
                end
            end
        end
    end
end

```

```

        OUT_MN_F_RCF=OUT_MN_F_RC_F;
    end
end
end
end
end

if (u-d5_e>=1)
    v=u-d5_e;
    for k=1:population_MN_E
        if (outMNE(v,k)>=vthr2_E)
            stim_e5(u,k)=vAP;
        else
            stim_e5(u,k)=0;
        end
        if stim_e5(u,k)>=vAP & stim_e5(u-1,k)==0
            for i=1:length(help_RC)
                stim_e5_neu(u+help_RC(i),k)=vAP;
            end
        end
        if u-21>=1
            if stim_e5(u,k)>=vAP & stim_e5(u-1,k)==0
                out_e5(1:u-21,k)=0+oute5(1:u-21,k);
                out_e5(u-20:min(u+870-20,tend+1),k)=RCEhigh;
                oute5=out_e5;
            end
        end
        for m=1:population_RC_E
            for j=1:nr_projections_MN_E_RC_E
                if k==project_MN_E_RC_E(j,m)
                    OUT_MN_E_RC_E(u,m)=OUT_MN_E_RCE(u,m)+out_e5(u,k);
                    OUT_MN_E_RCE=OUT_MN_E_RC_E;
                end
            end
        end
    end
end
end
end

for k=1:population_RC_F
    if u-1>=1
        if PSP_RC_F_total(u-1,k)>RCFhigh*nr_projections_MN_F_RC_F*0.4 &
            stim_f5_neu(u,k)==vAP
            out_f6(1:u-1,k)=0+outf6(1:u-1,k);
            out_f6(u:tend+1,k)=outf6(u:tend+1,k)+PSP6_f(1:tend+1-u+1);
            outf6=out_f6;
        end
    end
    for m=1:population_MN_F
        for j=1:nr_projections_RC_F_MN_F
            if k==project_RC_F_MN_F(j,m)
                OUT_RC_F_MN_F(u,m)=OUT_RC_F_MNF(u,m)+out_f6(u,k);
                OUT_RC_F_MNF=OUT_RC_F_MN_F;
            end
        end
    end
    for m=1:population_RC_E
        for j=1:nr_projections_RC_F_RC_E
            if k==project_RC_F_RC_E(j,m)
                OUT_RC_F_RC_E(u,m)=OUT_RC_F_RCE(u,m)+out_f6(u,k);
            end
        end
    end
end

```



```

for i=1:population_Ia_In_F
    if tonic_background_Ia_In_F(u,i)>=vAP
        u;
        out_background_Ia_In_F(1:u-1,i)=0+out_background_Ia_InF(1:u-1,i);
        out_background_Ia_In_F(u:tend+1,i)=out_background_Ia_InF(u:tend+1,i)+PSP1_f(1:tend+1-
u+1);
        out_background_Ia_InF=out_background_Ia_In_F;
    end
end

% IPSP at MN_E
for i=1:population_Ia_In_F
    if u-1>=1
        if OUT_f_back_total(u-1,i)>=vthr3_F
            OUT_back_Ia_In_F(u,i)=vAP;
        end
    end
end

for i=1:population_Ia_In_F
    if OUT_back_Ia_In_F(u,i)>=vAP & OUT_back_Ia_In_F(u-1,i)==0
        u;
        out_f3a(1:u-1,i)=0+outf3a(1:u-1,i);
        out_f3a(u:tend+1,i)=outf3a(u:tend+1,i)+PSP3_f(1:tend+1-u+1);
    end
    for k=1:population_MN_E
        for j=1:length(project_Ia_In_F_MN_E(:,1))
            if i==project_Ia_In_F_MN_E(j,k)
                input_Ia_In_F_MN_E(u,k)=input_Ia_In_F_MNE(u,k)+out_f3a(u,i);
                input_Ia_In_F_MNE=input_Ia_In_F_MN_E;
            end
        end
    end
end
input_Ia_In_F_Ia_In_E_back=input_Ia_In_F_MN_E;

% extensor to flexor:

% PSP at Ia_In_E
for i=1:population_Ia_In_E
    if tonic_background_Ia_In_E(u,i)>=vAP
        u;
        out_background_Ia_In_E(1:u-1,i)=0+out_background_Ia_InE(1:u-1,i);
        out_background_Ia_In_E(u:tend+1,i)=out_background_Ia_InE(u:tend+1,i)+PSP1_e(1:tend+1-
u+1);
        out_background_Ia_InE=out_background_Ia_In_E;
    end
end

% IPSP at MN_F
for i=1:population_Ia_In_E
    if u-1>=1
        if OUT_e_back_total(u-1,i)>=vthr3_E
            OUT_back_Ia_In_E(u,i)=vAP;
        end
    end
end

for i=1:population_Ia_In_E

```

```

if OUT_back_Ia_In_E(u,i)>=vAP & OUT_back_Ia_In_E(u-1,i)==0
    u;
    out_e3a(1:u-1,i)=0+oute3a(1:u-1,i);
    out_e3a(u:tend+1,i)=oute3a(u:tend+1,i)+PSP3_e(1:tend+1-u+1);
end
for k=1:population_MN_F
    for j=1:length(project_Ia_In_E_MN_F(:,1))
        if i==project_Ia_In_E_MN_F(j,k)
            input_Ia_In_E_MN_F(u,k)=input_Ia_In_E_MNF(u,k)+out_e3a(u,i);
            input_Ia_In_E_MNF=input_Ia_In_E_MN_F;
        end
    end
end
end
input_Ia_In_E_Ia_In_F_back=input_Ia_In_E_MN_F;

% 'real' reciprocal inhibition

OUT_f3_total=
    OUT_Ia_In_F+input_Ia_In_E_Ia_In_F+OUT_RC_F_Ia_In_F+input_Ia_In_E_Ia_In_F_back;
OUT_e3_total=
    OUT_Ia_In_E+input_Ia_In_F_Ia_In_E+OUT_RC_E_Ia_In_E+input_Ia_In_F_Ia_In_E_back;

% IPSP at MN_E
if (u-d3_f>=1)
    v=u-d3_f;
    for i=1:population_Ia_In_F
        if OUT_f3_total(v,i)>=vthr_F
            out_f3(u,i)=vAP;
        end
    end
end

for i=1:population_Ia_In_F
    if out_f3(u,i)>=vAP & out_f3(u-1,i)==0
        out_f3b(1:u-1,i)=0+outf3b(1:u-1,i);
        out_f3b(u:tend+1,i)=outf3b(u:tend+1,i)+PSP3_f(1:tend+1-u+1);
    end
    for k=1:population_MN_E
        for j=1:length(project_Ia_In_F_MN_E(:,1))
            if i==project_Ia_In_F_MN_E(j,k)
                input_Ia_In_F_MN_E_2(u,k)=input_Ia_In_F_MNE_2(u,k)+out_f3b(u,i);
                input_Ia_In_F_MNE_2=input_Ia_In_F_MN_E_2;
            end
        end
    end
end
% mutual inhibition:
for k=1:population_Ia_In_E
    for j=1:length(project_Ia_In_F_Ia_In_E(:,1))
        if i==project_Ia_In_F_Ia_In_E(j,k)
            input_Ia_In_F_Ia_In_E(u,k)=input_Ia_In_F_Ia_In_E(u,k)+out_f3b(u,i);
            input_Ia_In_F_Ia_In_E=input_Ia_In_F_Ia_In_E;
        end
    end
end
end
rec_inh_F_to_E=input_Ia_In_F_MN_E+input_Ia_In_F_MN_E_2;

```

```

% IPSP at MN_F
if (u-d3_e>=1)
    v=u-d3_e;
    for i=1:population_Ia_In_E
        if OUT_e3_total(v,i)>=vthr_E
            out_e3(u,i)=vAP;
        end
    end
end

for i=1:population_Ia_In_E
    if out_e3(u,i)>=vAP & out_e3(u-1,i)==0
        out_e3b(1:u-1,i)=0+oute3b(1:u-1,i);
        out_e3b(u:tend+1,i)=oute3b(u:tend+1,i)+PSP3_e(1:tend+1-u+1);
    end
    for k=1:population_MN_F
        for j=1:length(project_Ia_In_E_MN_F(:,1))
            if i==project_Ia_In_E_MN_F(j,k)
                input_Ia_In_E_MN_F_2(u,k)=input_Ia_In_E_MNF_2(u,k)+out_e3b(u,i);
                input_Ia_In_E_MNF_2=input_Ia_In_E_MN_F_2;
            end
        end
    end
end
% mutual inhibition:
for k=1:population_Ia_In_F
    for j=1:length(project_Ia_In_E_Ia_In_F(:,1))
        if i==project_Ia_In_E_Ia_In_F(j,k)
            input_Ia_In_E_Ia_In_F(u,k)=input_Ia_In_E_Ia_In_F(u,k)+out_e3b(u,i);
            input_Ia_In_E_Ia_In_F=input_Ia_In_E_Ia_In_F;
        end
    end
end
end
end

rec_inh_E_to_F=input_Ia_In_E_MN_F+input_Ia_In_E_MN_F_2;

%%%%%%%%%%%%%%

figure
subplot(2,1,1)
hold on
plot(outMNF)
plot(VTHR)
hold off
subplot(2,1,2)
hold on
plot(outMNE)
plot(VTHR)
hold off

```

References

- Bashor DP (1998). A large-scale model of some spinal reflex circuits. *Biol Cybern* **78**, 147-157.
- Basmajian JV (1979). *Muscles Alive. Their functions revealed by electromyography*, 4th edn. Williams and Wilkins, Baltimore.
- Brown TG (1914). On the nature of the fundamental activity of the nervous centres; together with an analysis of the conditioning of rhythmic activity in progression, and a theory of the evolution of function in the nervous system. *J Physiol* **48**, 18-46.
- Brown TG (1911). The intrinsic factors in the act of progression in the mammal. *Proc R Soc London Ser B* **84**, 308-319.
- Brunel N & van Rossum MC (2007). Lapique's 1907 paper: from frogs to integrate-and-fire. *Biol Cybern* **97**, 337-339.
- Burke RE (2007). Sir Charles Sherrington's the integrative action of the nervous system: a centenary appreciation. *Brain* **130**, 887-894.
- Burke RE (1967). Composite Nature of the Monosynaptic Excitatory Postsynaptic Potential. *J Neurophysiol* **30**, 1114-1137.
- Burke D, Adams RW & Skuse NF (1989). The effects of voluntary contraction on the H reflex of human limb muscles. *Brain* **112**, 417-433.
- Coombs JS, Eccles JC & Fatt P (1955). Excitatory synaptic action in motoneurons. *J Physiol* **130**, 374-395.
- Crone C, Hultborn H, Jespersen B & Nielsen J (1987). Reciprocal Ia inhibition between ankle flexors and extensors in man. *J Physiol* **389**, 163-185.
- Crone C, Hultborn H & Jespersen B (1985). Reciprocal Ia inhibition from the peroneal nerve to soleus motoneurons with special reference to the size of the test reflex. *Exp Brain Res* **59**, 418-422.
- Crone C & Nielsen J (1994). Central control of disynaptic reciprocal inhibition in humans. *Acta Physiol Scand* **152**, 351-363.
- Curtis DR & Eccles JC (1959). The time course of excitatory and inhibitory synaptic actions. *J Physiol* **145**, 529-546.

Davidoff RA & Hackman JC (1984). Spinal Inhibition. In *Handbook of the Spinal Cord. Volumes 2 and 3: Anatomy and Physiology*, 1st edn, ed. Davidoff RA, pp. 385-460. Marcel Dekker, Inc. New York, USA, and Basel, Switzerland.

Dayan P & Abbott LF (2001a). Preface. In *Theoretical Neuroscience*, 1st edn, ed. Dayan P & Abbott LF, p.xiii, The MIT Press, Cambridge, USA.

Dayan P & Abbott LF (2001b). Neurons and Neural Circuits – Model Neurons I: Neuroelectronics. In *Theoretical Neuroscience*, 1st edn, ed. Dayan P & Abbott LF, pp. 151-194, The MIT Press, Cambridge, USA.

Dimitrijevic MR, Faganel J, Sharkey PC & Sherwood AM (1980). Study of sensation and muscle twitch responses to spinal cord stimulation. *Int Rehabil Med* **2**, 76-81.

Dimitrijevic MR, Gerasimenko Y & Pinter MM (1998). Evidence for a spinal central pattern generator in humans. *Ann N Y Acad Sci* **860**, 360-376.

Dimitrijevic MR & Nathan PW (1967). Studies of spasticity in man. 2. Analysis of stretch reflexes in spasticity. *Brain* **90**, 333-358.

Eccles JC, Eccles RM, Iggo A & Lundberg A (1961). Electrophysiological investigations on Renshaw cells. *J Physiol* **159**, 461-478.

Eccles JC, Fatt P & Landgren S (1956). Central pathway for direct inhibitory action of impulses in largest afferent nerve fibres to muscle. *J Neurophysiol* **19**, 75-98.

Eccles RM & Lundberg A (1958). The synaptic linkage of direct inhibition. *Acta physiol scand* **43**, 204-215.

Eccles RM & Lundberg A (1958). Integrative pattern of Ia synaptic actions on motoneurons of hip and knee muscles. *J Physiol* **144**, 271-298.

Eccles JC & Pritchard JJ (1937). The action potential of motoneurons. *J Physiol* **89** (Suppl), 43-45.

Ertekin C, Mungan B & Uludag B (1996). Sacral cord conduction time of the soleus H-reflex. *J Clin Neurophysiol* **13**, 77-83.

Gerasimenko YP, Bogacheva IN, Shcherbakova NA, Makarovskii AN (2001). Bioelectric activity of spinal cord in patients with vertebrospinal pathologies. *Bull Exp Biol Med* **132**, 1106-1109.

Gerasimenko YP, Makarovskii AN & Nikitin OA (2002). Control of locomotor activity in humans and animals in the absence of supraspinal influences. *Neurosci Behav Physiol* **32**, 417-423.

- Grillner S (1985). Neurobiological bases of rhythmic motor acts in vertebrates. *Science* **228**, 143-149.
- Grillner S, McClellan A & Perret C (1981). Entrainment of the spinal pattern generators for swimming by mechano-sensitive elements in the lamprey spinal cord in vitro. *Brain Res* **217**, 380-386.
- Hallett M, Berardelli A, Delwaide P, Freund HJ, Kimura J, Lüicking C, Rothwell JC & Shahani BT, Yanagisawa N (1994). Central EMG and tests of motor control. Report of an IFCN committee. *Electroencephalogr Clin Neurophysiol* **90**, 404-432.
- Halter J, Dolenc V, Dimitrijevic MR & Sharkey PC (1983). Neurophysiological assessment of electrode placement in the spinal cord. *Appl Neurophysiol* **46**, 124-128.
- Hodgkin AL & Huxley AF (1952). A quantitative description of membrane current and its application to conduction and excitation in nerve. *J Physiol* **117**, 500-544.
- Holsheimer J, Struijk JJ & Tas NR (1995). Effects of electrode geometry and combination on nerve fibre selectivity in spinal cord stimulation. *Med Biol Eng Comput* **33**, 676-682.
- Hultborn H (2001). State-dependent modulation of sensory feedback. *J Physiol* **533**, 5 - 13.
- Hultborn H (2006). Spinal reflexes, mechanisms and concepts: from Eccles to Lundberg and beyond. *Prog Neurobiol* **78**, 215-232.
- Hultborn H, Conway BA, Gossard JP, Brownstone R, Fedirchuk B, Schomburg ED, Enríquez-Denton M & Perreault MC (1998). How do we approach the locomotor network in the mammalian spinal cord? *Ann N Y Acad Sci* **860**, 70-82.
- Hultborn H, Jankowska E & Lindström S (1971a). Recurrent inhibition of interneurons monosynaptically activated from group Ia afferents. *J Physiol* **215**, 613-636.
- Hultborn H, Jankowska E, Lindström S & Roberts W (2001b). Neuronal pathway of the recurrent facilitation of motoneurons. *J Physiol* **218**, 495-514.
- Hultborn H & Pierrot-Deseilligny E (1979). Input-output relations in the pathway of recurrent inhibition to motoneurons in the cat. *J Physiol* **297**, 267-287.
- Hunt CC & Perl ER (1960). Spinal reflex mechanisms concerned with skeletal muscle. *Physiol Rev* **40**, 538-579.
- Jankowska E (1992). Interneuronal relay in spinal pathways from proprioceptors. *Prog Neurobiol* **38**, 335-378.

- Jankowska E (2001). Spinal interneuronal systems: identification, multifunctional character and reconfigurations in mammals. *J Physiol* **533**, 31-40.
- Jankowska E & Riddell JS (1995). Interneurones mediating presynaptic inhibition of group II muscle afferents in the cat spinal cord. *J Physiol* **483**, 461-471.
- Jankowska E & Roberts WJ (1972). An Electrophysiological demonstration of the axonal projection of single spinal interneurons in the cat. *J Physiol* **222**, 597-622.
- Jilge B, Minassian K, Rattay F & Dimitrijevic MR (2004). Frequency-dependent selection of alternative spinal pathways with common periodic sensory input. *Biol Cybern* **91**, 359-376.
- Jilge B, Minassian K, Rattay F, Pinter MM, Gerstenbrand F, Binder H & Dimitrijevic MR (2004). Initiating extension of the lower limbs in subjects with complete spinal cord injury by epidural lumbar cord stimulation. *Exp Brain Res* **154**, 308-326.
- Jolivet R, Roth A, Schuermann F, Gerstner W & Senn W (2008). Special issue on quantitative neuron modeling. *Biol Cybern* **99**, 237-239.
- Katz R & Pierrot-Deseilligny E (1998). Recurrent inhibition in humans. *Progress in Neurobiology* **57**, 325-355.
- Kern H, McKay WB, Dimitrijevic MM & Dimitrijevic MR (2005). Motor control in the human spinal cord and the repair of cord function. *Curr Pharm Des* **11**, 1429-1439.
- Lapicque L (1907). Recherches quantitatives sur l'excitation électrique des nerfs traitée comme une polarisation. *J Physiol Pathol Gen* **9**, 620-635.
- Lateva ZC & McGill KC (1999). Satellite potentials of motor unit action potentials in normal muscles: a new hypothesis for their origin. *Clin Neurophysiol* **110**, 1625-1633.
- Lehmkuhl D, Dimitrijevic MR & Renouf F (1984). Electrophysiological characteristics of lumbosacral evoked potentials in patients with established spinal cord injury. *Electroencephalogr Clin Neurophysiol* **59**, 142-155.
- Lloyd DPC (1943a). Reflex action in relation to pattern and peripheral source of afferent stimulation. *J Neurophysiol* **6**, 111-120.
- Lloyd DCP (1943b). Neuron patterns controlling transmission of ipsilateral hind limb reflexes in cat. *J Neurophysiol* **6**, 293-315.
- Lloyd DCP (1944). Functional organization of the spinal cord. *Physiol Rev* **24**, 1-17.
- MacGregor RI (1987). In *Neural and Brain Modelling*. Academic Press, New York.

Magladery JW, Porter WE, Park AM & Teasdall RD (1951). Electrophysiological studies of nerve and reflex activity in normal man. IV. The two-neurone reflex and identification of certain action potentials from spinal roots and cord. *Bull Johns Hopkins Hosp* **88**, 499-519.

Maynard FM Jr, Bracken MB, Creasey G, Ditunno JF Jr, Donovan WH, Ducker TB, Garber SL, Marino RJ, Stover SL, Tator CH, Waters RL, Wilberger JE, Young W (1997). International Standards for Neurological and Functional Classification of Spinal Cord Injury. American Spinal Injury Association. *Spinal Cord* **35**, 266-274.

Marque P, Nicolas G, Simonetta-Moreau M, Pierrot-Deseilligny E & Marchand-Pauvert V (2005). Group II excitations from plantar foot muscles to human leg and thigh motoneurons. *Exp Brain Res* **161**, 486-501.

McCrea DA (2001). Spinal circuitry of sensorimotor control of locomotion. *J Physiol* **533**, 41-50.

McCrea DA & Rybak IA (2008). Organization of mammalian locomotor rhythm and pattern generation. *Brain Res Rev* **57**, 134-146.

McCrea DM (1992). Can sense be made of spinal interneuron circuits? *Behav Brain Sci* **15**, 633-643.

Mendell LM & Henneman E (1971). Terminals of single Ia fibers: location, density, and distribution within a pool of 300 homonymous motoneurons. *J Neurophysiol* **34**, 171-187.

Minassian K, Rattay F, Pinter MM, Murg M, Binder H, Sherwood A & Dimitrijevic MR (2001). Effective spinal cord stimulation (SCS) train for evoking stepping locomotor movement of paralyzed human lower limbs due to SCI elicits a late response additionally to the early monosynaptic response. *Soc Neurosci Abstr* **27**, Program No. 935.12.

Minassian K, Gilge B, Rattay F, Pinter MM, Binder H, Gerstenbrand F & Dimitrijevic MR (2004). Stepping-like movements in humans with complete spinal cord injury induced by epidural stimulation of the lumbar cord: electromyographic study of compound muscle action potentials. *Spinal Cord* **42**, 401-416.

Minassian K, Persy I, Rattay F, Dimitrijevic MR, Hofer C & Kern H (2007a). Posterior root-muscle reflexes elicited by transcutaneous stimulation of the human lumbosacral cord. *Muscle Nerve* **35**, 327-336.

Minassian K, Persy I, Rattay F, Pinter MM, Kern H & Dimitrijevic MR (2007b). Human lumbar cord circuitries can be activated by extrinsic tonic input to generate locomotor-like activity. *Hum Mov Sci* **26**, 275-295.

Murg M, Binder H & Dimitrijevic MR (2000). Epidural electric stimulation of posterior structures of the human lumbar spinal cord: 1. muscle twitches - a functional method to define the site of stimulation. *Spinal Cord* **38**, 394-402.

Nielsen J, Kagamihara Y, Crone C & Hultborn H (1992). Central facilitation of Ia inhibition during tonic ankle dorsiflexion revealed after blockade of peripheral feedback. *Exp Brain Res* **88**, 651-656.

Pearson K & Gordon J (2000). Spinal Reflexes. In *Principles of Neural Science*, 4th edn, ed. Kandel ER, Schwartz JH, Jessell TM, pp. 713-736. McGraw-Hill, New York.

Persy I, Minassian K, Rattay F, Binder H & Dimitrijevic MR (2005). Motor output of the human lumbar networks depends on coded stimulation of the posterior roots in complete spinal cord injured individuals. Program No. 753.9. Abstract Viewer/Itinerary Planer. Washington, DC: Society for Neuroscience.

Pierrot-Deseilligny E & Burke D (2005a). Monosynaptic Ia excitation and post-activation depression. In *The Circuitry of the Human Spinal Cord: Its role in motor control and movement disorders*, 1st edn, ed. Pierrot-Deseilligny E & Burke D, pp. 63-112. Cambridge Univ. Press, New York, USA.

Pierrot-Deseilligny E & Burke D (2005b). Group II pathways. In *The Circuitry of the Human Spinal Cord: Its role in motor control and movement disorders*, 1st edn, ed. Pierrot-Deseilligny E & Burke D, pp. 288-336. Cambridge Univ. Press, New York, USA.

Pierrot-Deseilligny E & Burke D (2005c). Reciprocal Ia inhibition. In *The Circuitry of the Human Spinal Cord: Its role in motor control and movement disorders*, 1st edn, ed. Pierrot-Deseilligny E & Burke D, pp. 197-243. Cambridge Univ. Press, New York, USA.

Pinter MM, Gerstenbrand F & Dimitrijevic MR (2000). Epidural electrical stimulation of posterior structures of the human lumbosacral cord: 3. Control Of spasticity. *Spinal Cord* **38**, 524-531.

Pompeiano O (1984). Recurrent Inhibition. In *Handbook of the Spinal Cord. Volumes 2 and 3: Anatomy and Physiology*, 1st edn, ed. Davidoff RA, pp. 461-558. Marcel Dekker, Inc. New York, USA, and Basel, Switzerland.

Rall W (1967). Distinguishing Theoretical Synaptic Potentials Computed for Different Soma-Dendritic Distributions of Synaptic Input. *J Neurophysiol* **30**, 1138-1168.

Rall W, Burke RE, Smith TG, Nelson PG & Frank K (1967). Dendritic Location of Synapses and Possible Mechanisms for the Monosynaptic EPSP in Motoneurons. *J Neurophysiol* **30**, 1169-1193.

Rattay F (1999). The basic mechanism for the electrical stimulation of the nervous system. *Neuroscience* **89**, 335-346.

Rattay F (1998). Analysis of the electrical excitation of CNS neurons. *IEEE Trans Biomed Eng* **45**, 766-772.

Rattay F (1990). The space clamp experiment of Hodgkin and Huxley – non-propagating action potentials. In *Electrical Nerve Stimulation. Theory, Experiments, and Applications*. pp. 52-72. Springer Wien-New York.

Rattay F (1987). Ways to approximate current-distance relations for electrically stimulated fibers. *J Theor Biol* **125**, 339-349.

Rattay F, Minassian K & Dimitrijevic MR (2000). Epidural electrical stimulation of posterior structures of the human lumbosacral cord: 2. quantitative analysis by computer modeling. *Spinal Cord* **38**, 473-489.

Renshaw B (1940). Activity in the simplest spinal reflex pathways. *J Neurophysiol* **3**, 373-387.

Rogério RL & Kohn AF (2008). Simulation system of spinal cord motor nuclei and associated nerves and muscles, in a Web-based architecture. *J Comput Neurosci* **25**, 520-542.

Rybak IA, Stecina K, Shevtova NA & McCrea DA (2006). Modelling spinal circuitry involved in locomotor pattern generation: insights from the effects of afferent stimulation. *J Physiol* **577**, 641-658.

Sherwood AM, McKay WB & Dimitrijevic MR (1996). Motor control after spinal cord injury: assessment using surface EMG. *Muscle Nerve* **19**, 966-979.

Schieppati M (1987). The Hoffmann reflex: a means of assessing spinal reflex excitability and its descending control in man. *Prog Neurobiol* **28**, 345-376.

Stuart DG (2002). Reflection on spinal reflexes. *Adv Exp Biol Med* **508**, 249-257.

Struijk JJ, Holsheimer J & Boom HB (1993). Excitation of dorsal root fibers in spinal cord stimulation: a theoretical study. *IEEE Trans Biomed Eng* **40**, 632-639.

Sypert GW & Munson JB (1984). Excitatory Synapses. In *Handbook of the Spinal Cord. Volumes 2 and 3: Anatomy and Physiology*, 1st edn, ed. Davidoff RA, pp. 315-384. Marcel Dekker, Inc. New York, USA, and Basel, Switzerland.

Trappenberg TP (2007a). Neurons and conductance-based models. In *Fundamentals of Computational Neuroscience*, 5th edn, ed. Trappenberg TP, pp. 13-37. Oxford Univ. Press Inc., New York, USA.

Trappenberg TP (2007b). Spiking neurons and response variability. In *Fundamentals of Computational Neuroscience*, 5th edn, ed. Trappenberg TP, pp. 38-55. Oxford Univ. Press Inc., New York, USA.

Uchiyama T, Johansson H & Windhorst U (2003). A model of the feline medial gastrocnemius motoneurone-muscle system subjected to recurrent inhibition. *Biol Cybern* **89**, 139-151.

Uchiyama T & Widhorst U (2007). Effects of spinal recurrent inhibition on motoneuron short-term synchronization. *Biol Cybern* **96**, 561-575.

Westmoreland BF, Benarroch EE, Daube JR, Reagan TJ & Sandok BA (1994). The Spinal Level. In *Medical Neurosciences – An approach to Anatomy, Pathology, and Physiology by Systems and Levels*, 3rd edn, ed. Westmoreland BF, pp. 374-402. Lippincott Williams and Wilkins, Philadelphia, USA.

Willis WD (2006). John Eccles' studies of spinal cord presynaptic inhibition. *Prog Neurobiol* **78**, 189-214.

Willis WD & Coggeshall RE (1978). Peripheral Nerves, Sensory Receptors, and Spinal Roots. In *Sensory Mechanisms of the Spinal Cord*, 1st edn, ed. Willis WD, Coggeshall RE, pp. 9- 52. New York: Plenum Press.

Curriculum Vitae

Personal Data

Name Dipl.-Ing. Ursula Hofstätter
Date of Birth January 06, 1982
Place of Birth Vienna, Austria
Nationality Austria

Education

Since July 2006

PhD studies at the Vienna University of Technology, Vienna, Austria

October 2000 – November 2005

Studies in Technical Mathematics at the Vienna University of Technology,
Vienna, Austria

1992 – 2000

Secondary School: Gymnasium Maria Regina, Vienna, Austria

Graduation in June 2000

Internships

August 2003

Internship at the Raiffeisen Zentralbank Österreich AG (RZB), Legal and
Compliance Department, Vienna, Austria

August 2001

Internship at the Bank Austria Creditanstalt AG, Vienna, Austria

Employment Record

Since May 2008

Research associate at the Vienna University of Technology, Institute of Analysis
and Scientific Computing, Vienna, Austria

Since January 2008

Research associate at the Medical University of Vienna, Center for Biomedical Engineering and Physics, Vienna, Austria

October 2006 – December 2007

Research associate at the Ludwig Boltzmann Institute of Electrical Stimulation and Physical Rehabilitation, Vienna, Austria

February 2004 – October 2006

Assistant at the Raiffeisen Zentralbank Österreich AG (RZB), Legal and Compliance Department/Capital Market Services, Vienna, Austria

Awards

Junior Investigator Fellowship Award, The New York Academy of Sciences, New York, USA

Memberships

The New York Academy of Sciences

The Society for Neurosciences

List of scientific publications

Hofstoetter US, Minassian K, Hofer C, Mayr W, Rattay F & Dimitrijevic MR (2008). Modification of reflex responses to lumbar posterior root stimulation by motor tasks in healthy subjects. *Artif Organs* **32**, 644-648.

Rattay F & Hofstoetter U (2006). Der Einfluss verrauschter Sprachsignale auf das evozierte Feuerungsverhalten elektrisch stimulierter Nervenfasern. *Österr. Ges. Neurowissenschaften-Newsletter* **21**, 6.

Proceedings

Hofstoetter US, Ladenbauer J, Minassian K, Dimitrijevic MR & Rattay F (2008). Motor task-induced modifications of multiple spinal cord reflexes. Proceedings of the Junior Scientist Conference 2008, Vienna University of Technology, Vienna, Austria.

Ladenbauer J, Hofstoetter US, Minassian K, Dimitrijevic MR & Rattay F (2008). Activation of Neural Networks in the Human Spinal Cord with Implanted and Surface Electrodes: Conclusions from Finite Element Simulations. Proceedings of the Junior Scientist Conference 2008, Vienna University of Technology, Vienna, Austria.

W. Mayr, C. Hofer, K. Minassian, U. Hofstoetter, H. Kern, M. Bijak, E. Unger, F. Rattay & MR Dimitrijevic (2008). Modulation of stimulation frequency of afferents of the spinal cord from the same site and intensity can induce a variety of movements. Proceedings of the 13th Annual International FES Society Conference IFESS 2008 – from movement to mind, Freiburg, Germany.

Hofstoetter U, Minassian K, Persy I, Hofer C, Rattay F, Dimitrijevic M & Kern H (2007). Modification of monosynaptic responses to transcutaneous lumbar posterior root stimulation in multiple lower limb muscles by suprasegmental motor tasks in healthy subjects. Proceedings of the 9th Vienna International Workshop on Functional Electrical Stimulation. 179-182.

Minassian K, Hofstoetter U, Hofer C, Vogelauer M, Persy I, Rattay F, Dimitrijevic M & Kern H (2007). Stimulation of human lumbar posterior root afferents with surface electrodes. Proceedings of the 9th Vienna International Workshop on Functional Electrical Stimulation, Vienna, Austria. 255-258

Persy I, Kern H, Minassian K, Hofstoetter U, Hofer C, Rattay F & Dimitrijevic M (2007). Externally controlled coded trains of input to the human lumbar cord can elicit a variety of input related functional and non-functional movements. Proceedings of the 9th Vienna International Workshop on Functional Electrical Stimulation, Vienna, Austria. 259-262

Abstracts

Hofstoetter U, Minassian K, Mayr W, Rattay F & Dimitrijevic MR (2009). Posterior root-muscle reflexes: characteristics during resting- and locomotor-state of the human lumbar cord. *vfwf-Universitaetsvorlesung 2009*, Medical University of Vienna, Vienna, Austria.

Hofstoetter U, Minassian K, Mayr W, Rattay F & Dimitrijevic MR (2008). Posterior root-muscle reflexes: characteristics during resting- and locomotor-state of the human lumbar cord. Program No. 375.1. Abstract Viewer/Itinerary Planner. Washington 2008: Society for Neuroscience.

Minassian K, Hofstoetter U, Persy I, Dimitrijevic MR, Rattay F & Kern H (2007). Transcutaneous stimulation of human lumbar posterior roots. (abstract) *Artif Organs* **31**, A20-21.

Hofstoetter U, Minassian K, Persy I, Kern H, Hofer C, Rattay F & Dimitrijevic MR (2007). Modification of multisegmental motor nuclei outputs of the lumbar cord by suprasegmental motor tasks. (abstract) *Artif Organs* **31**, A21.

Persy I, Minassian K, Hofstoetter U, Hofer C, Rattay F, Kern H & Dimitrijevic MR (2007). Externally controlled “coded” trains of input stimuli to the human lumbar cord can elicit a variety of input-related functional and non-functional movements. (abstract) *Artif Organs* **31**, A21.

Contributions to International Conferences

Lectures

2008 K. Minassian, U. Hofstoetter, H. Kern, M.R. Dimitrijevic. Facilitation of functional standing and walking in wheel chair-bound spinal cord injured people by spinal cord stimulation: Study of neurocontrol and biomechanical output. Wings for Life International Projects 2006 - 2007 Meeting, Salzburg, Austria.

K. Minassian, U. Hofstoetter. Outline of Protocol for Assessment of Lumbar Neuronal Circuitry. Program for demonstration workshops in the following days. Summer School for the Biological Treatment of Chronic Spinal Cord Injury, Vienna, Austria.

K. Minassian, U. Hofstoetter, F. Rattay. "Spinal Cord Stimulation." BEST Summer School "Stimulate Your Nerves", Vienna, Austria.

F. Rattay, K. Minassian, U Hofstoetter, J. Ladenbauer, MR. Dimitrijevic: "New results in electrical nerve and muscle stimulation." Workshop, ETH Zurich, Zurich, Switzerland.

W. Mayr, C. Hofer, K. Minassian, U. Hofstoetter, H. Kern, M. Bijak, E. Unger, F. Rattay and MR Dimitrijevic. Modulation of stimulation frequency of afferents of the spinal cord from the same site and intensity can induce a variety of movements. IFESS 2008 – from movement to mind, 13th Annual International FES Society Conference, Freiburg, Germany.

K. Minassian, U. Hofstoetter. "Outline of Protocol for Assessment of Lumbar Neuronal Circuitry. Program for demonstration workshops in the following days." Summer School for the Biological Treatment of Chronic Spinal Cord Injury, Vienna, Austria.

2007 U. Hofstoetter, K. Minassian, I. Persy, C. Hofer, F. Rattay, MR. Dimitrijevic, H. Kern. "Monosynaptic responses to transcutaneous spinal cord stimulation and their modification by suprasegmental motor tasks". 9th Vienna International Workshop on Functional Electrical Stimulation, Vienna, Austria.

Poster contributions

2009 Hofstoetter U, Minassian K, Rattay F, Mayr W, Dimitrijevic MR. Effects of motor tasks on human lumbar cord reflex activity. Program No. 80.14. Neuroscience Meeting Planner. Chicago, IL: Society for Neuroscience, 2009.

- Minassian K, Hofstoetter US, Rattay F, Mayr W, Dimitrijevic MR. Posterior root-muscle reflexes and the H reflex in humans: Electrophysiological comparison. Program No. 658.12. Neuroscience Meeting Planner. Chicago, IL: Society for Neuroscience, 2009.
- Hofstoetter U, Minassian K, Mayr W, Rattay F, Dimitrijevic MR. Posterior root-muscle reflexes: characteristics during resting- and locomotor-state of the human lumbar cord. *yfwf-Universitaetsvorlesung 2009*, Medical University of Vienna, Vienna, Austria.
- 2008 Hofstoetter U, Minassian K, Mayr W, Rattay F, Dimitrijevic MR. Posterior root-muscle reflexes: characteristics during resting- and locomotor-state of the human lumbar cord. Program No. 375.1. Abstract Viewer/Itinerary Planner. Washington 2008: Society for Neuroscience.
- Hofstoetter US, Ladenbauer J, Minassian K, Dimitrijevic MR and Rattay F. Motor task-induced modifications of multiple spinal cord reflexes. Junior Scientist Conference 2008, Vienna, Austria.
- Ladenbauer J, Hofstoetter US, Minassian K, Dimitrijevic MR and Rattay F. Activation of Neural Networks in the Human Spinal Cord with Implanted and Surface Electrodes: Conclusions from Finite Element Simulations. Junior Scientist Conference 2008, Vienna, Austria.
- 2007 Dimitrijevic MR, Persy I, Hofstoetter U, Minassian K Rattay F, Hofer C, Kern H (2007). Externally controlled "coded" trains of input stimuli to the human lumbar cord can elicit a variety of input-related functional and non-functional movements. Program No. 288.5/MM7. Abstract Viewer/Itinerary Planner. San Diego: Society for Neuroscience.
- Minassian K, Hofstoetter U, Hofer C, Vogelauer M, Persy I, Rattay F, Dimitrijevic M, Kern H (2007). Stimulation of human lumbar posterior root afferents with surface electrodes. 9th Vienna International Workshop on Functional Electrical Stimulation, Vienna, Austria.
- Persy I, Kern H, Minassian K, Hofstoetter U, Hofer C, Rattay F, Dimitrijevic M (2007). Externally controlled coded trains of input to the human lumbar cord can elicit a variety of input related functional and non-functional movements. 9th Vienna International Workshop on Functional Electrical Stimulation, Vienna, Austria.

Other contributions

- 2008 Coordinator of the Summer School for the Biological Treatment of Chronic Spinal Cord Injury, Vienna, Austria.

Demonstration workshops for assessment of human spinal cord functions (2008).
Summer School for the Biological Treatment of Chronic Spinal Cord Injury,
Vienna, Austria.